BIOCHEMICAL AND BIOPHYSICAL CHARACTERIZATION OF A CLASS II ALPHA MANNOSIDASE FROM *LENS CULINARIS* (LENTIL) AND *CANAVALIA ENSIFORMIS* (JACK BEAN)

Thesis submitted to University Of Pune

For the degree of

DOCTOR OF PHILOSOPHY

IN

BIOTECHNOLOGY

By

AVINASH KUMAR

Under the guidance of

DR. SUSHAMA M. GAIKWAD

DIVISION OF BIOCHEMICAL SCIENCES

NATIONAL CHEMICAL LABORATORY

PUNE - 411 008 (INDIA)

AUGUST 2011

Dedicated to

My Parents, Family

And

Hemlata

CONTENTS

ACKNOWLEDGEMENTS

I take this opportunity to gratefully acknowledge my research guide ***Dr. Sushama M. Gaikwad*** *for her invaluable guidance, unending support and keen interest during the course of this investigation. She has given me the freedom to think and work and I shall cherish my learning experience under her. Although this eulogy is insufficient, I preserve an everlasting gratitude for her.*

I am grateful to ***Late Dr. M. I. Khan*** *for his valuable suggestions and help in learning many techniques. I am also grateful to* ***Dr. C. G. Suresh*** *and* ***Dr. S. S. Deshmukh*** *for their valuable suggestions during the course of investigation.*

I would also like to extend my sincere thanks to: ***Dr. B. M. Khan****, Plant Tissue Culture, NCL, for permission to use FPLC instrument,* ***Dr. (Mrs.) Vyjayanthi A. Kumar****, Organic Chemistry Division, NCL, for permission to use CD facility,* ***Dr. Suresh Bhat****, Polymer and Advanced Materials Division, NCL, for help in DLS facility,* ***Prof. Musti J. Swamy****, School of Chemistry, University of Hyderabad, for help in using the DSC facility and* ***Dr. Sushma Sabharwal****, Biochemistry section, Department of Chemistry, University of Pune, for being the external examiner all throughout my work.*

I express my deep feelings and love for my lab seniors ***Dr. Shashidhara, Dr. Feroz, Dr. Anil, Dr. Atul, Dr. Siddharth, Dr. Nagaraj, Dr. Sajid, Dr. Jay Prakash Singh, Late Rohtas, Dr. Sreekanth and my lab mates Asad, Shabab, Shadab, Ashutosh, Santosh (bond), Vaibhav, Ravi, Prasad, Sana, Ankita, Poorva and Vidyut*** *for their help, cooperation and maintaining pleasant and healthy atmosphere throughout my doctorate course.*

I would like to take this opportunity to express my love and thank my lab mates ***Ansary, Madhurima, Imran, Sonali, Ganesh and Sayli*** *for their good company and pleasant atmosphere in the lab and for countless things they have done for me and for always being there with me whenever I needed them.*

I would like to mention a special thanks to my friends ***Dr. Sajid, Ansary, Imran, Madhurima and Mujahid*** *for a wonderful time inside and outside the lab and for always being there for my support.*

I would also like to express my deep felt gratitude to my friends ***Dr. Arun, Dr. Sameer, Dr. Noor, Dr. Abhilash, Dr. Ruby, Santhosh, Rishi, Somesh, Prashant, Parth, Sumita, Neha, Poonam, Shakeel, Ambrish, Reetika, Dr. Santosh, Dr. Chetan, Dr. Fazal, Pushkar, Snehal mam, Manisha, Dr. Uma, Dr. Poorva, Nishant (Rambo), Urvashi, Vishnu, Gyan Prakash, Deepali, Harish, Trupti, Pallavi, Dr. Sarvesh, Prabhash, Yashwant and Manasi*** *for help, support and charming company.*

I would like to express my love and gratitude to ***Aparna****, for being a good friend, her everlasting zeal and enthusiasm and her kind help in some of the work presented here in the thesis.*

I also would like to thank ***Scientists and staff of Biochemical Sciences Division, NCL,*** *for helping me directly or indirectly during course of my stay in the division.*

I would like to take this opportunity to extend my sincere thanks to my special friend and my soul mate, ***Hemlata,*** *who has been a constant source of inspiration for me during my struggle through the thick and thins of my PhD work. This work would not have been possible without her constant support and sacrifice.*

I find no words for my best friend, ***Alok,*** *for his constant encouragement, belief and wonderful time in the room and outside in making my stay a pleasant one.*

I also extend my thanks to my childhood friends, ***Saumitra, Shubhradeep and Sujit*** *for their constant encouragement, belief and support throughout my work.*

I am really grateful to my friends ***Farhat, Priyanka, Rakhi, Avani, Divya, Aashita di, Rekha and Gourav*** *for their help and encouragement.*

I am also thankful to my friends ***Chandan*** *and* ***Monalisa*** *for their constant encouragement, help and support.*

My heartfelt gratitude goes to my friends ***Rachana, Sowjanya, Siddharth, Satish, Anukampa, Shova, Amarnath, Avishek and Garima*** *for their never ending support and belief.*

I am really grateful to ***Prof. S.C. Lakhotia, Prof. Rajiva Raman, Prof. Mercy Raman, Prof. J.K, Roy, Dr. Madhu Tapadia and Dr. Monisha Banerjee*** *for their consistent encouragement.*

My sincere thanks are also due to ***Brahma Nand uncleji,*** *and* ***Anita auntyji*** *for their constant encouragement and support.*

I am also grateful to ***Gautam (Babu)*** *uncle and* ***Siju uncle*** *for their constant support and encouragement.*

My special thanks to ***More uncleji, auntyji, Parikshit, Didi and Anshula*** *for providing a home like atmosphere during my stay in Pune.*

I find no words ***for my parents, my brother, Buaji, Fufaji, Guddu bhaiya, Seema bhabhi, Pappu bhaiya, Devisha bhabhi, Minu didi, Manish jijaji, Akshada, Bhavya, Nanaji, Naniji, Mamaji, Mamiji, Mausaji, Mausiji, Rahul, Roopa and Rishabh*** *who have been a constant inspiration for me during the thick and thins of my PhD work and this work would not have been possible without their constant support and sacrifices.*

Finally, I thank ***Heads, Division of Biochemical Sciences*** *and the* ***Director, National Chemical Laboratory*** *for permitting me to submit this work in the form of the thesis and* ***University Grants Commission, India,*** *for financial assistance.*

Avinash

राष्ट्रीय रासायनिक प्रयोगशाला
(वैज्ञानिक तथा औद्योगिक अनुसंधान परिषद)
डॉ. होमी भाभा रोड, पुणे - 411 008. भारत
NATIONAL CHEMICAL LABORATORY
(Council of Scientific & Industrial Research)
Dr. Homi Bhabha Road, Pune - 411008. India

CERTIFICATE

Certified that the work incorporated in the thesis entitled **"Biochemical and Biophysical Characterization of a Class II alpha mannosidase from *Lens culinaris* (Lentil) and *Canavalia ensiformis* (Jack Bean)"** submitted by Mr. **Avinash Kumar** was carried out under my supervision. Such materials that have been obtained from other sources have been duly acknowledged in the thesis.

Dr. Sushama M. Gaikwad
Research Guide

Communications Channels ☎ +91 20 25902000 +91 20 25893300 +91 20 25893400 Fax +91 20 25902601 (Director) +91 20 25902660 (Admin.) +91 20 25902639 (Business Development) URL : www.ncl-india.org

DECLARATION OF THE CANDIDATE

I declare that the thesis entitled **"Biochemical and Biophysical Characterization of a Class II alpha mannosidase from *Lens culinaris* (Lentil) and *Canavalia ensiformis* (Jack Bean)"** submitted by me for the degree of Doctor of Philosophy is the record of work carried out by me during the period from **20th July, 2006 to 26th May, 2011** under the guidance of **Dr. Sushama M. Gaikwad** and has not formed the basis for the award of any degree, diploma, associateship, fellowship, titles in this or any other University or other institute of Higher learning. I further declare that the material obtained from other sources has been duly acknowledged in the thesis.

Signature of the candidate

Date: . . . . . **Avinash Kumar**

LIST OF ABBREVIATIONS USED

ANS	1-anilino-8-naphthalenesulfonate
°C	degree celsius
CD	circular dichroism
Da	dalton
DMJ	1-deoxymannonojirimycin
DTNB	2, 2'-dithiobisnitrobenzoic acid
ER	endoplasmic reticulum
ERMI	endoplasmic reticulum α -mannosidase I
FPLC	fast performance liquid chromatography
Gal	galactose
GdnHCl	guanidium hydrochloride
Glc	glucose
GlcI	α -glucosidase I
GlcII	α -glucosidase II
GlcNAc	*N*-acethylglucosamine
GlcNAcTI	*N*-acetylglucosamine transferase I
GlcNAcTV	*N*-acetylglucosamine transferase V
GMI	golgi α -mannosidase I
GMII	golgi α -mannosidase II
GMIII	golgi α -mannosidase III
GMX	golgi α -mannosidase IIx
HPLC	high pressure liquid chromatography
IC_{50}	concentration of an inhibitor required for 50% inhibition of the enzyme
IUPAC	international union of pure and applied chemistry
Jbα-man	Jack Bean α-mannosidase
K	kelvin
K_a	association constant
k_{cat}	catalytic Efficiency
K_d	dissociation constant
kDa	kilo dalton
K_i	inhibition constant
kJ	kilo joules
K_m	Michaelis-Menten constant
K_s	static quenching constant
K_{sv}	Stern-Volmer (dynamic) quenching constant
LAM 1	Lentil α-mannosidase 1
LAM 2	Lentil α-mannosidase 2
Man	mannose
4-MeUmbαMan	4-methyl umbelliferyl α-D-mannopyranoside
MRE	mean residue ellipticity
$NaBH_4$	sodium borohydride
NBS	N-bromo succinimide
NRMSD	normalized root mean square deviation
PAGE	polyacrylamide gel electrophoresis
pK_a	acid dissociation constant
PNPαMan	para nitro phenyl α-D-mannopyranoside
rpm	revolutions per minute
SDS	sodium dodecyl sulphate

Swn	swainsonine
Trp	tryptophan
Tyr	tyrosine
UV	ultra violet
V, V_{max}	rate of an enzyme-catalyzed reaction, maximum reaction rate

ABSTRACT

Glycosidases have proved to be useful tools for probing structural features of cell surface glycoconjugates. α-Mannosidase (α-D-mannoside mannohydrolase, EC 3.2.1.24) plays a very important role in the mannose-trimming reaction during the biosynthesis of glycoproteins of higher eukaryotes, and a deficiency of this enzyme leads to mannosidosis, a lethal disease in human and cattle. α-mannosidase is also intimately involved in the quality control, a process that facilitates proper folding of newly formed polypeptide chains leading to retention and/or degradation of malfolded proteins in the Endoplasmic Reticulum (ER). There has been widespread interest in α-mannosidase in recent years, in particular, mammalian Golgi mannosidase-II involved in glycoprotein biosynthesis and is currently an important therapeutic target for the development of anticancer agents.

Investigation was carried out to characterize α-mannosidase from *Canavalia ensiformis* (Jack Bean), Jbα-man, to determine its structure-function relationship. Also, two α-mannosidase from *Lens culinaris* (Lentil), LAM 1 and 2, were purified and characterized to study its biochemical and biophysical characteristics. The thesis is divided into five chapters.

Chapter 1: Introduction

This part comprises a literature survey of protein folding, molten globule, glycosidases and α-mannosidases with reference to the classification, isolation, purification, properties and applications.

Chapter 2: Biochemical and Biophysical characterization of a Class II α-mannosidase from *Canavalia ensiformis* (Jack Bean)

Investigation of the catalytic and structural transitions of Jack bean α-mannosidase (Jbα-man) under particular denaturing conditions was performed. The enzyme shows maximum activity at pH 5.0 and 45 °C. In the pH range of 1.0 to 10.0, the enzyme was maximally stable at pH 5.0 for 1 h at 28 °C. The stability declined fast in the pH range of 1.0-3.0 and 8.0-10.0. However, Jbα-man incubated in the pH range of 11.0-12.0, showed 1.3 times higher activity which was also more stable as compared to that at pH 5.0. The free amino group was found to be present at or near the active site which

probably was involved in the stability and activation mechanism in the extreme alkaline pH range. The active site is constituted by the association of two unidentical subunits which are connected by disulfide linkages. Jbα-man, the metalloenzyme, has Zn^{2+} ions tightly bound to it and chelation of the metal ion reduces the thermal stability of the protein. E_a of Jbα-man with pNPαman as a substrate was 31.9 kJ mol^{-1} and with 4-MeUmbαman was 26.7 kJ mol^{-1}. The strong binding of the class II α-mannosidase inhibitor, Swainsonine (K_i = 52.9 nM), to the enzyme was found to be entropy driven.

Chapter 3: Unfolding studies of a Class II α-mannosidase from *Canavalia ensiformis* (Jack Bean)

The relevance of partially ordered states of proteins (such as the molten globule state) in cellular processes is beginning to be understood. We examined the conformational transitions in a multimeric and high molecular weight class II α-mannosidase from *Canavalia ensiformis* (Jack Bean) (Jbα-man) utilizing intrinsic fluorescence, solute quenching, hydrophobic dye binding, size exclusion chromatography and circular dichroism (CD) spectroscopy for the protein in presence of Guanidine hydrochloride (GdnHCl). The decomposition analysis of the protein spectra obtained during unfolding showed progressive appearance of class S, I, II and III trp. The parameter A and spectral center of mass showed multi state unfolding of the protein and phase diagram analysis revealed formation of an intermediate of Jbα-man in the vicinity of 1 M GdnHCl. The intermediate exhibited compact secondary and distorted tertiary structure with exposed hydrophobic amino acids on the surface, indicating the molten-globule nature. The dissociation, partial unfolding and aggregation of Jbα-man occurred simultaneously during chemical denaturation. The molten-globule possessed slightly higher hydrodynamic radius, perturbance in the structure up to 60 °C and stability of the structure up to 80 °C unlike the native jack bean α-mannosidase. The modes of chemical and thermal denaturation of the native protein were different. The solute quenching parameters confirmed the altered confirmation of the intermediate. Time resolved fluorescence studies showed two different lifetimes for both native and denatured protein. Quenching of the fluorescence of the denatured protein by acrylamide involved both static (K_s=7.39 M^{-1}) and collisional (K_{sv}=3.12 M^{-1}) components. Taken together, our results constitute one of the early reports of formation of GdnHCl induced molten globule in a class II α-mannosidase.

Chapter 4: Purification and characterization of two Class II α-mannosidases from *Lens culinaris* (Lentil)

Two class II α-mannosidases from *Lens culinaris* (Lentil), slightly differing in the electrophoretic mobility, were purified to homogeneity by alkaline native polyacrylamide gel electrophoresis (PAGE). Both the enzymes are glycoproteins with a carbohydrate content of about 10 %. The pH and temperature optima of the enzymes were 5.0 and 55 °C, respectively. At pH 5.0 the enzyme was stable for 30 min at 55 °C. The K_m and V_{max} of p-nitrophenyl-α-D-mannopyranoside for both the enzymes was about 4 mM and of 4-methylumbelliferryl-α-D-mannopyranoside was 15 μM. The K_i of Swainsonine for both the enzymes was about 5 nM. The enzyme was strongly inhibited by 2 mM Hg^{2+}, Cu^{2+}, Co^{2+} and 1 % SDS and partially inhibited by 100 mM mannose. The steady state fluorescence spectra of both the enzymes showed λ_{max} as 341 nm indicating trp to be in slightly hydrophobic environment and the far UV CD spectra with mimima around 212 nm showed that both the enzymes are predominantly β-sheet proteins. Owing to the similarity in properties and structure of both the enzymes, our results constitute one of the reports of existence of class II α-mannosidases as isozymes.

Chapter 5: Discussion and conclusion

In this chapter the properties of α-mannosidase from *Canavalia ensiformis,* Jbα-man and *Lens culinaris*, LAM 1 and 2 are compared with other mannosidases with respect to unfolding characteristics, inhibition constants, active site characterization, tryptophan environment and other biophysical properties.

LIST OF PUBLICATIONS:

- **Avinash Kumar** and Sushama M. Gaikwad, (2010) Multistate unfolding of α-mannosidase from *Canavalia ensiformis* (Jack Bean): Evidence for the thermostable molten globule, *Biochem Biophys Res Commun* 403, 391-397

- **Avinash Kumar** and Sushama M. Gaikwad, Jack bean α-mannosidase (Jbα-man): Tolerance to alkali, chelating and reducing agents and energetics of catalysis and inhibition. (Under Review)

- R. K. Sreejith, C. G. Suresh, Siddharth H. Bhosale, Varsha Bhavnani, **Avinash Kumar**, Sushama M. Gaikwad, Jayanta K. Pal, Conformational transitions of the catalytic domain of heme-regulated eukaryotic initiation factor 2α kinase, a key translational regulatory molecule. (Under Review)

- **Avinash Kumar** and Sushama M. Gaikwad, Purification and biochemical characterization of two class II α-mannosidases from *Lens culinaris* (Lentil) (Manuscript under preparation)

LIST OF PRESENTATIONS:

- Presented poster titled "**α-mannosidase from *Lens culinaris* (Lentil) seeds**" in the 77th Annual meeting of the Society of Biological Chemists, India held at IIT Chennai, India in December 2008.

- Presented poster titled "**Biochemical Characterization of Two α-mannosidases from Lentil (*Lens culinaris)* seeds**" in the 78th Annual meeting of the Society of Biological Chemists, India held at NCCS, Pune, India in November 2009.

- Presented poster titled "**Folding-Unfolding studies of α-mannosidase from *Aspergillus fischeri* (NCIM 508)**" in the Symposium on Recent Trends in Biophysics held at Banaras Hindu University (BHU), Varanasi, India in February 2010.

- Presented poster titled "**Guanidine hydrochloride (GdnHCl) mediated conformational transitions of a class II α-mannosidase from *Canavalia ensiformis* (Jack Bean) (Jbα-man)"** in the 79th Annual meeting of the Society of Biological Chemists, India held at IISc, Bangalore, India in December 2010.

CHAPTER 1

INTRODUCTION

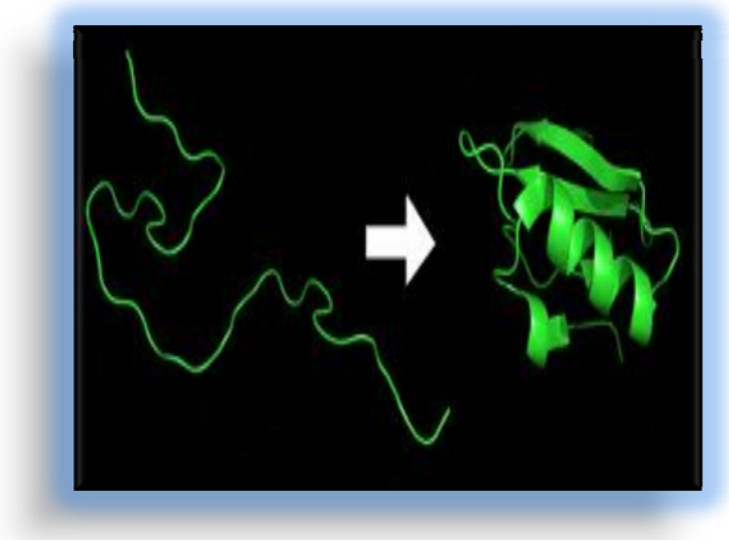

Glycosylation being one of the most widespread post translational modifications of proteins is yet poorly understood. Every cell in nature is coated with a dense layer of carbohydrates at its surface. Decorating intra- and extracellular proteins with large carbohydrate chains is a costly endeavor for a cell to undertake, yet it is seen in ubiquity, indicating that it has great significance. Carbohydrates comprise significant amount of the mass in biological systems, yet were long considered to be useful in little more than energy storage. The landmark discovery that the molecular determinant of blood type was a carbohydrate began the notion that sugars played a functional role in biological systems (1). Research in recent decades has highlighted many detailed and important functions of these molecules.

Carbohydrates and their derivatives play major roles in the activity of the immune system, fertilization, cell growth, pathogenesis, blood clotting, inflammation and interactions and adhesions (2, 3). Lectins are carbohydrate-binding proteins able to recognize glycoproteins and/or glycolipids and can consequently mediate many specific biological functions such as immune defense (mannose binding protein) and cell-cell adhesion (selectins) (4-6).

Most of the soluble and membrane-bound proteins synthesized in the ER are glycosylated.

Protein N-glycosylation occurs primarily in the endoplasmic reticulum (ER) and Golgi apparatus, and involves a series of discrete catalytic steps. A diverse series of enzymes, known as glycosidases, have evolved to carry out the complex steps of this pathway.

Glycosidases

Glycosidases play important roles in biological systems ranging from the degradation of polysaccharides to the manipulation of the structures of glycoconjugates at the surface of proteins. They are involved in biological processes such as the digestion, the biosynthesis of glycoproteins and the catabolism of glycoconjugates (7). The glycosidic bond, between two glucosyl residues in cellulose or starch is one of the most stable

linkages with a half-life for spontaneous hydrolysis being in the range of 5 million years. But hydrolysis carried out by enzyme is accomplished with rate constants up to $1000s^{-1}$, which make these enzymes some of the most efficient catalysts (8). Classification of glycoside hydrolases, or glycosidases, based on amino acid sequences was first performed in the early 1990's (9). It was determined that the 301 known glycoside hydrolases sequences could be grouped into 35 families. The substrate specificities and reaction mechanisms of the classified enzymes corresponded to their family placement. Currently, the carbohydrate-active enzyme database (CAZy; www.cazy.org) has classified thousands of glycoside hydrolases into more than one hundred families (10). The member enzymes of a given family come from a wide variety of organisms, but retain similarity in the types of reactions catalyzed, and the mechanism employed. This indicates that, despite the increase in sequence data, the classification scheme remains robust, as it has been validated by biochemical means.

Mechanism for enzymatic hydrolysis of glycosides

Basic mechanisms of the hydrolysis of interglycosidic bonds were proposed in 1953 by Koshland (11). Indeed, hydrolysis of the glycosidic bond can occur with one of two possible stereochemical outcomes: inversion or retention of anomeric configuration (12-14). Both mechanisms involve oxocarbenium-ion like transition states and a pair of carboxylic acids in the active site of the enzyme. With inverting β-glycosidases, as described by Koshland, hydrolysis proceeds via a single step mechanism in which the sugar anomeric centre is attacked by a water molecule that acts as a nucleophile (Fig. 1.1).

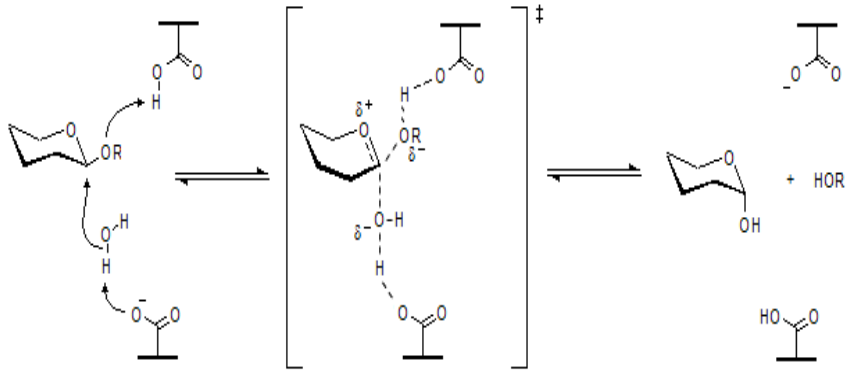

Fig 1.1: *General mechanism of inverting β-glycosidases.*

This reaction is catalysed by two carboxylic acid moieties both present in the active site. Deprotonation of the water molecule by the carboxylate enhances its nucleophilicity and allows it to attack the anomeric position. The glycosidic bond is cleaved and releases the alcohol which results in the inversion of the anomeric centre of the cleaved sugar. In contrast, retaining β-glycosidases proceed via a double-step mechanism (Fig. 1.2).

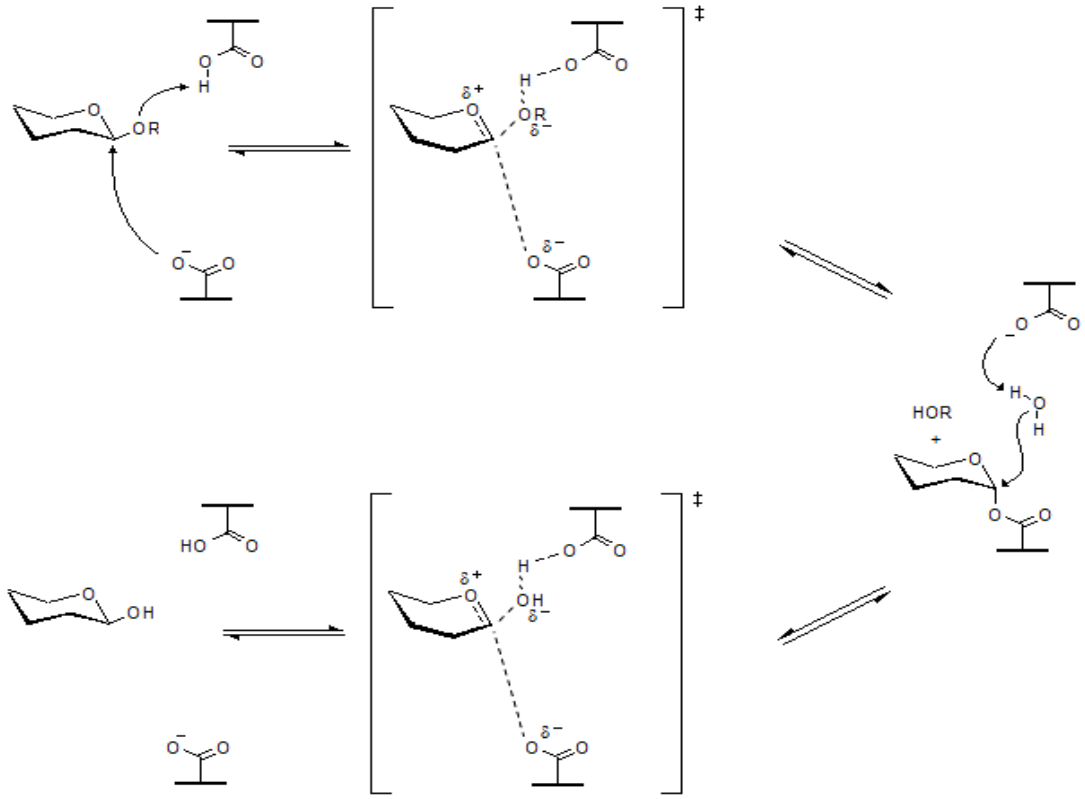

Fig 1.2: *General mechanism of retaining β-glycosidases.*

The first carboxylate attacks the anomeric position and cleaves the glycosidic bond with release of an alcohol. A water molecule then attacks the remaining sugar which is bound to the first carboxylic acid. This step is catalysed by the second carboxylic acid which deprotonates the water molecule so enhancing its nucleophilicity. The reaction affords the cleaved sugar without inversion of the anomeric center (15). Retaining and inverting β-glycosidases differ mainly by the distance separating the two carboxylic groups of the active site. This distance is around 5 Å in retaining enzymes and around

10 Å in inverting enzymes. The greater span found in inverters is necessary to accommodate the nucleophilic water molecule. The hydrolysis processes have been more thoroughly studied for β-glycosidases. Nevertheless, it has been reported that α-glycosidases act through a similar pathway to β-glycosidases (16). The mechanisms have been evidenced by the isolation of α-linked intermediates (17).

However, subtle differences, between α- and β-glycosidases seem to exist in the oxocarbenium ion character of the transition state (12).

For β-glycosidases, the interactions involving the nucleophilic carboxyl oxygens, the anomeric center and the alcohol at C (2) position support delocalization of the positive charge on the anomeric carbon (Fig. 1.3 B). On the other hand, for α-glycosidases, these interactions occur between the carboxyl oxygen, the endocyclic oxygen and the anomeric center resulting in the delocalization of the positive charge on the anomeric oxygen (Fig. 1.3 A) (18).

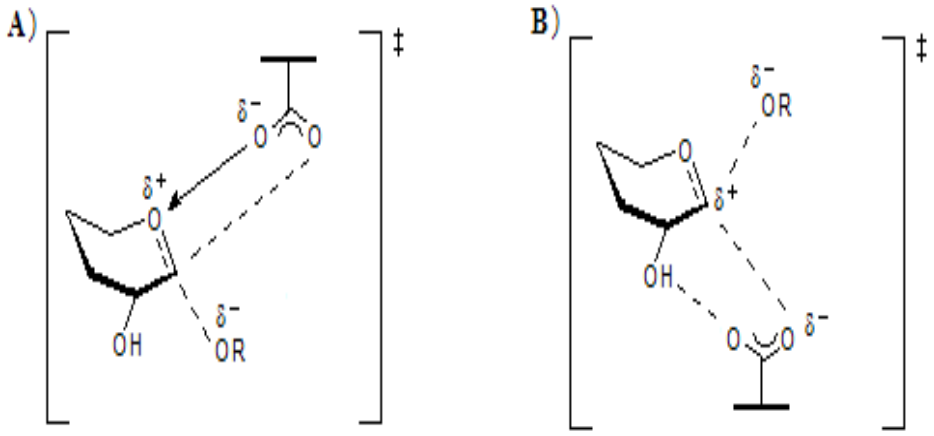

***Fig. 1.3**: Comparison of the transition states for **A)** α- and **B)** β- retaining glycosidases.*

Mannosidase

Mannosidases are Glycohydrolases involved in the processing of mannose containing glycans in vivo. They are involved in the maturation and degradation of glycoprotein-linked oligosaccharides. Use of natural substrates for specificity determination,

antibodies from subcellular localization, specific enzymic inhibitors and mutant cell lines, has revealed the presence of different α-mannosidase isoenzymes. This suggests that α-mannosidases have multiple functions in glycoprotein metabolism (19).

Types

1. Alpha-Mannosidase (α-D-mannoside mannohydrolase): are involved in hydrolysis of terminal α-D-mannose residues in α-D-mannosides.
   EC 3.2.1.24

2. Beta-Mannosidase (mannanase, mannase, β-mannoside mannohydrolase): are involved in the hydrolysis of terminal non-reducing β-D-mannose residues in β-D-mannosides.
   EC 3.2.1.25

Classification of α-Mannosidase

There are two classes of processing α-mannosidase based on their distinctive substrate specificity, responses to inhibitors, cation requirements, protein molecular weights, subcellular localization, enzyme mechanisms and characteristic regions of conserved amino acid sequences (19-21). There is significant correlation of biochemical and physiological roles of the various member genes for each of these two classes. Processing mannosidases are located in both the ER and Golgi of mammalian cells. The differential activity of Class II α-mannosidase towards artificial substrates has important practical ramifications. Because Class II enzymes are readily assayed with aryl mannosides, they are almost always employed for the initial screening of new potential inhibitors. Class I enzymes are not as easily assayed, so good inhibitors of these may be missed or incompletely characterized (19)

Table 1.1: *Classification of α-mannosidases.*

Sl. No.	Properties	Class I α-Mannosidase	Class II α-Mannosidase
1	Substrate Specificity	α-1,2 mannoside linkages	α-1,2 α-1,3 and α-1,6 mannoside linkages
2	Artificial substrates (aryl mannosides)	Inactive	Active
3	Ca^{2+}	Required for activity	Not required for activity
4	Inhibition	1-deoxymannojirimycin (dMNJ) and Kifunensine (KF)	Swainsonine and 1,4-dideoxy-1,4-imino-D-mannitol (DIM)
5	Cleavage of glycosidic linkage	By Inversion of configuration of the released mannose (22, 23)	By Retention of configuration of released mannose (24)
6	Glycohydrolase Family	47	38

Class I α-mannosidases

Trimming of α1,2-linked mannose residues to form $Man_5GlcNAc_2$ in mammalian cells was originally attributed to a Golgi enzyme called α-mannosidase I (25) but it is now clear that, in addition to the ER enzymes, there are at least two Golgi α1,2-mannosidases in mammalian cells which are involved in this process, called Class IA and IB. Partial amino acid sequence information derived from purified enzymes was used for TR-PCR to isolate human (26), murine (27), and porcine (28) cDNAs encoding enzymes designated as α-mannosidase IA. Regions of conserved sequence were used to isolate murine and human Golgi α-mannosidase IB cDNAs by RT-PCR (29).

Mammalian α-mannosidase IA and IB are type II Ca^{2+}-dependent transmembrane enzymes. Their N-terminal transmembrane domain is flanked by a variable cytoplasmic

domain of about 10-35 amino acids and a `stem region' that is not required for enzyme activity and is followed by a large C-terminal catalytic domain. These class-I α-mannosidases are inhibited by 1-deoxymannojirimycin and related compounds, but not by swainsonine. Although their N-terminal regions may differ, their catalytic domains have been conserved through eukaryotic evolution. Within the same species the catalytic domains of α-mannosidases IA and IB are about 65% identical in amino acid sequence while they are around 90% identical between mammalian species for each α-mannosidase IA and IB. The mammalian α-mannosidases exhibit about 35% amino acid identity with non-mammalian α1,2-mannosidases, including the yeast ER processing α-mannosidase.

Mammalian α-mannosidases IA and IB are derived from distinct genes. The murine and human α1,2-mannosidase IB genes span 60-80 kb of the genome, and consist of 13 exons with identical intron-exon structures (30, 31).

The multiple Class I α-mannosidases found in *A. nidulans* (32) and *O. novo-ulmi* (Accession#: AF12945) also appear to have arisen from recent duplication events, in that these proteins are more similar to each other than to either of the mammalian Class I α-mannosidases. This is significant, because it suggests that the Class I α-mannosidase gene families in both lineages have independently undergone expansion and evolution through gene duplication and divergence.

Class II α-mannosidases

The second family of mannosidases, the Class II α-mannosidases is more diverse in their biochemical properties and physiological functions (19). The majority of class II α-mannosidase enzymes that have been characterized catalyze the degradation of Asn-linked oligosaccharides. This group of enzymes consists of three subfamilies of genes (Classes IIA, IIB and IIC) with distinct cellular functions. Enzymes of this class also have a wider range of cellular compartmentalization and can be localized to the cytosol and lysosomes in addition to the Golgi complex (33). The Class IIA subfamily is

involved in N-glycan synthesis in the Golgi, while the Class IIB and Class IIC are involved in N-glycan breakdown, removal and recycling in the cytoplasm, lysosome and vacuole. The first subfamily of Class II genes (Class IIA) are responsible for removal of α-1,3- and α-1,6-linked mannose residues from N-glycans during their synthesis (Fig. 1.4), a process which occurs in the higher eukaryotes, but does not occur in lower eukaryotes, such as fungi.

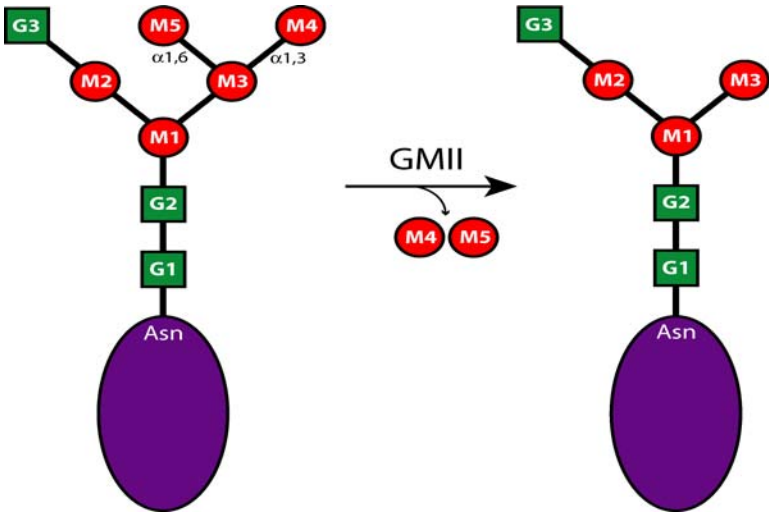

Fig. 1.4: *Mechanism of catalysis of Golgi α-mannosidase II.*

The second subfamily (Class IIB) is found in higher eukaryotes. These enzymes are involved in N-glycan degradation in the lysosome. The third subfamily (Class IIC) contains a more heterogeneous set of enzymes, with a diversity of functions and cellular localizations. Members of this family are found in higher and lower eukaryotes and are likely involved in many aspects of N-glycan degradation and recycling. Sequence analysis clearly resolves the various inter-relationships of these proteins (34).

The Class IIC subfamily has very low sequence similarity to the other two subfamilies. Phylogenetic analysis of the sequences shows that the Class IIA and Class IIB subfamilies have diverged more recently than the Class IIC subfamily. A likely scenario is that a single common ancestor was duplicated after the divergence of lower eukaryotes, such as fungi, from the higher eukaryotes. The lower eukaryotes thus only

contain the orthologue of the common ancestor. Subsequent duplication in the higher eukaryotes led to the formation of the three subfamilies of Class II genes found in higher eukaryotes. These gene sequences diverged and evolved more specialized functions, such as the more complex N-glycan pathways (Class IIA), and more efficient degradation pathways (Class IIB).

It is intriguing that the two classes of α-mannosidases have such similar and overlapping functions. The Class I genes and the Class IIA genes have complementary functions in the N-glycans synthesis pathway of higher eukaryotes. The other Class II genes have broad substrate specificities and are able to cleave α-1, 2 (as well as α-1,3, and α-1,6) mannose linkages, a property it shares with the Class I genes. The Class I and Class II genes show no sequence similarity and appear to have originated independently and represent a classic case of convergent evolution (35).

Class III α-mannosidases

α-Mannosidases that can provide an alternative route independent of α-mannosidase II for the synthesis of complex N-glycans have been described in mammals like rat brain that lacks α-mannosidase II activity (36), in rat liver (37-39) and in several tissues of the α-mannosidase II knockout mice (40). These enzymes can produce Man_3-$GlcNAc_2$ without the prior action of GlcNAc transferase I. The rat brain α-mannosidase cleaves $Man_{4-9}GlcNAc$ to $Man_3GlcNAc$ and is resistant to swainsonine and 1-deoxymannojirimycin.

Unlike α-mannosidase II, it does not utilize p-nitrophenyl α-mannopyranoside. A Co^{2+}-dependent α-mannosidase that can trim $Man_{4-9}GlcNAc$ to $Man_3GlcNAc$ has been purified from rat liver (37-39). This enzyme was immunolocalized to the ER, Golgi and endosomes of rat liver. A Co^{2+}-dependent enzyme activity that trims $Man_5GlcNAc_2$ to $Man_3GlcNAc_2$ was found in tissues of the α-mannosidase II knock-out mice and called α-mannosidase III (40). The α-mannosidase from lepidopteran insect cell line, Sf9 (41) is an integral membrane glycoprotein with type II topology.

Table 1.2: *Comparison of Class I, II and III α-mannosidase*

Class	Sub-class	Source	Function	Metal ion requirement	Inhibitor
I	A	Lower and higher eukaryotes	Glycoprotein breakdown by cleavage of α-1,2 linkage	Ca^{2+}	1-deoxymannojirimycin
	B	Lower and higher eukaryotes	Glycoprotein breakdown by cleavage of α-1,2 linkage	Ca^{2+}	1-deoxymannojirimycin
II	A	Higher eukaryotes	Glycoprotein synthesis	Not required with some exceptions as Jbα-man etc.	Swainsonine
	B	Higher eukaryotes	Glycoprotein breakdown by cleavage of α-1,2, α-1,3 and α-1,6 linkage		Swainsonine
	C	Lower and higher eukaryotes	Glycoprotein breakdown by cleavage of α-1,2, α-1,3 and α-1,6 linkage		Swainsonine
III		Higher eukaryotes	Glycoprotein synthesis, does not utilize pNPαMan	Co^{2+}	1-deoxymannojirimycin and Swainsonine

Unlike other class III α-mannosidases, it can hydrolyze p-nitrophenyl α-D-mannopyranoside, and it is inhibited by swainsonine. This enzyme is actually different from Golgi II α-mannosidase as its activity is stimulated by cobalt and it can hydrolyze various substrates containing terminal mannose residues but not $GlcNAcMan_5GlcNAc_2$. So this enzyme also has been designated as Sf9 α-mannosidase III (Sf9ManIII) and its functions in an alternate N-glycan processing pathway in Sf9 cells (42).

The relationship between these various enzymes that can form $Man_3GlcNAc_2$ is not known, but they may be related to each other since they are all stabilized by Co^{2+}, as are the cytosolic enzymes. Additional work is required to establish the role of these enzymes in the processing pathway and their relationship to each other and to the product of the α-mannosidase IIx gene (43).

Endo α-mannosidase

There is an alternative pathway for trimming glucose residues from the oligosaccharide precursor. A specific endo α-mannosidase purified from Golgi membrane fractions was discovered in Spiro's laboratory (21, 44). This enzyme is the only processing glycosidase that cleaves an internal glycosidic linkage, producing $Man_8GlcNAc_2$ isomer A from $Glc_{1-3}Man_9GlcNAc_2$. The endo α-mannosidase prefers monoglucosylated oligosaccharides as substrates, but it can cleave $Glc_{1-3}Man_{4-9}GlcNAc$ to yield $Man_{3-8}GlcNAc$ and $Glc_{1-3}Man$ in vitro. In contrast to α-glucosidases I and II, its activity is enhanced with glucosylated oligosaccharide substrates lacking mannose residues on adjacent branches of the oligosaccharide. Some evidence demonstrating endo α-mannosidase activity in vivo in the absence of a α-glucosidase blockade has been obtained (45), but the importance of the endo-mannosidase in glycoprotein maturation is cell-specific (46).

The enzyme has no divalent ion requirement, has a neutral pH optimum and is specifically inhibited by the disaccharides Glcα1,3-(1-deoxy)mannojirimycin and

Glcα1,3-(1,2-dideoxy)mannose (47). It has been purified by ligand affinity chromatography from rat liver Golgi membranes along with calreticulin (48). A rat liver endo α-mannosidase cDNA has been isolated (49). It encodes a 52 kDa protein with distinct levels of tissue-specific expression. There is no related protein found in the data base, consistent with the observation that its appearance is a relatively late event during eukaryotic evolution (50).

Inhibitors of class II α-mannosidases and their biological activities

Mannostatin A

Mannostatin A was discovered by Aoyagi and collaborators in 1989 and so named because of their highly potent inhibition of α-mannosidase activity. It was isolated from the soil microorganism *Streptoverticillum verticillus* during screening of culture broths for mannosidase inhibitors (51). Inhibition by mannostatin A of α-mannosidases prepared from epididymes of adult rats has been shown to be competitive. When tested on various glycosidases, Mannostatin A was inactive toward β-glucosidase, α- and β-galactosidase, β-mannosidase but was a potent inhibitor of jack bean α-mannosidase. Mannostatin A also proved to be an effective competitive inhibitor of the glycoprotein-processing enzyme α-mannosidase II but was inactive toward α-mannosidase I (52, 53).

Swainsonine

Discovery

Swainsonine, a polyhydroxylated indolizidine alkaloid (Fig. 1.5), discovered in 1978 by Dorling *et al.*, (54) displayed reversible inhibition of class II α-mannosidases (lysosomal and Golgi α-mannosidases). Swainsonine was first isolated in Australia from the plant *Swainsona canescens* (55), which was toxic to livestock. Swainsonine has then been identified as the toxic principle of locoism, a syndrome developed by animals ingesting the locoweed infested species *Astragalus* and *Oxytropis* species (56), and more recently in the poisonous plant *Ipomea carnea* (57), and the fungus *Rhizoctonia leguminocola* (58).

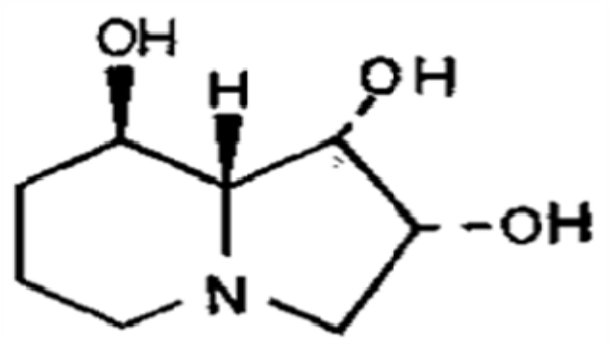

Swainsonine

***Fig. 1.5**: Structure of Swainsonine.*

History

The clinical signs of locoism include nervousness, aggression, hyperactivity, increasing mis co-ordination, head tremors, loss of weight, reproductive alterations, weakness and death. These symptoms are attributed to lysosomal storage disease which is characterized by cytoplasmic vacuolation of cells of the central nervous system.

However, purified Swainsonine alone is now known not to be neurotoxic, but loco syndrome may be caused by ingestion of a combination of alkaloids found in *Swainsona canescens* or *Astragalus* (59). Dorling *et al.*, recognized that the lysosomal storage disorder induced in animals grazing *Swainsona* species was biochemically and morphologically similar to the rare genetic mannosidosis that occurs in humans. This affection is characterized by accumulation in cells and excretion in urine of mannose-rich oligosaccharides, resulting from a deficiency of lysosomal α-mannosidase (60). It has been found that Swainsonine concentrates and accumulates in lysosomes of normal human fibroblasts and human lymphoblasts in culture, since it is almost fully ionized within the acidic environment of this organelle (61, 62).

***Table 1.3**: Swainsonine inhibition.*

IC_{50} (nM)	Enzyme
50-100	α-mannosidase (jack bean)
70	α-mannosidase (human liver lysosomal)
20	α-mannosidase (rat lysosomal)
40	α-mannosidase (human lysosomal)
No inhibition	Golgi mannosidase I (rat liver)
200	Golgi mannosidase II (rat liver)
160	α-mannosidase (rat liver lysosomal)

Such accumulation produces the inhibition of the intracellular lysosomal α-mannosidase which induces incomplete catabolism of the carbohydrate moiety of glycoproteins and storage of the remaining proteins which finally leads to disease as a consequence. It is assumed that this mode of action also occurs *in vivo*. Actually, Swainsonine provides a valuable tool for the study of human mannosidosis despite the fact it also inhibits Golgi α-mannosidase II (63, 64).

Specificity

Swainsonine was the first compound able to alter glycoprotein processing. It displayed inhibitory ability toward jack bean α-mannosidase, rat liver Golgi α-mannosidase II but was without effect on Golgi α-mannosidase I (65-67). In addition, Swainsonine did not inhibit ER α-mannosidase or the soluble α-mannosidases of rat liver (68). The selectivity of Swainsonine toward α-mannosidases was established against other glycosidases such as α-glucosidase, β-galactosidase and β-glucoronidase and lysosomal β-mannosidases (61). The pKa of Swainsonine was determined to be 7.4 which mean that Swainsonine would be fully ionized at pH 4.0 (69). Molecular modelling has shown that the relative positions of the cationic ammonium center and the three hydroxyl groups mimic an intermediate cationic structure of the hydrolysis mediated by

α-mannosidases II and thus accounts for the apparent specificity of Swainsonine for α-mannosidases II (62).

Application

The use of glycosidase inhibitors has recently appeared as a promising approach to treat cancers (70). Transferases, α-glucosidases and α-mannosidases are the most relevant targets in the field of cancer for the development of cellular glycosidase inhibitors. Using Swainsonine, Humphries *et. al.*, tested the hypothesis that specific glycans structures are required for pulmonary colonization by tumor cells (71). Furthermore, the addition of Swainsonine (2.5 μg/ml) to the drinking water of the mice further reduced the incidence of lung colonization by B16-F10 melanoma cells (72). Since all cellular glycoproteins which normally express complex-type oligosaccharides are affected by Swainsonine treatment, investigations were carried out to determine whether the effects of Swainsonine on cellular proliferation could be widespread amongst non-transformed tissues in the body. These studies showed that the effects of this compound would appear to be cell specific, since it does not equally affect the processing of all glycoproteins (73). Moreover, the systemic administration of high doses of Swainsonine to sheep induces mannosidosis (74, 75). However, no evidence of an over toxic reaction was observed when Swainsonine was administrated orally to rodents (76). So it was considered that the mannosidosis induced by Swainsonine could be species- or tissue specific phenomena (77).

Applications of class II α-mannosidase

Study of the biological function of glycoprotein glycans is rapidly emerging as a field of cell biology. α-Mannosidase (α-D-mannoside mannohydrolase, E.C. 3.2.1.24) is known to play an important role in the processing of mannose containing glycans *in vivo,* because a deficiency of the enzyme results in the lethal disease called mannosidosis, a hereditary disease reported in humans (78) and cattle (79).

- α-Mannosidases have been employed in the analysis of mannose containing glycans (e.g. high mannose-type sugar chains of glycoproteins) and glycolipids containing α linked mannoside residues (80).
- To elucidate the biological role and structures of the carbohydrate moieties of the mannoproteins, a highly specific α-mannosidase active on the polymannose component is required. Almond α-mannosidase as well as jack bean α-mannosidase have been used for analysis of sugar chain structures (81).
- The new invention provides means and strategies for treating the lysosomal storage disorder α-mannosidosis by enzyme replacement therapy. In particular, the reduction of stored neutral mannose-rich oligosaccharides takes place in cells within the central nervous system. Accordingly, the lysosomal α-mannosidase are used for the preparation of a medicament for reducing the intracellular levels of neutral mannose-rich oligosaccharides in cells within one or more regions of the central nervous system (82).
- Golgi α-mannosidase II is a target for inhibition of growth and metastasis of cancer cells. Golgi α-mannosidase inhibitor Swainsonine acts as anti-cancer agent (83).
- And also, α-mannosidase inhibitors and their analogs were utilized to design potential anti-HIV agents (84).
- In plants, increased levels of mannosidase have been reported during the seed germination and fruit ripening (85). Jagadeesh *et al.*, reported the increase in the activity of α-mannosidase in tomato during fruit ripening observed in the study is significant in the context of involvement of this enzyme in deglycosylation of glycoproteins resulting in release of free *N*-glycans. Free *N*-glycans (and hence *N*-glycoproteins) have a role in fruit ripening in tomato, where tunicamycin application to mature green fruit prevented both ripening and softening of the fruit (86).

Plant class II α-mannosidases

Several reports on α-mannosidases from plant sources are available and jack bean α-mannosidase is the most studied among for all of its characteristics.

Jack bean α-Mannosidase

An α-mannosidase which is able to hydrolyze a naturally occurring α-mannoside, yeast mannan, and several synthetic α-D-mannosides was isolated from jack bean meal. This enzyme was used to explore the linkage of mannose in several glycoproteins. α-mannosidase was purified approximately 500-fold from jack bean meal (87). This enzyme was able to hydrolyze α-1,6, α-1,2, and α-1,3-linked oligomannosides. Approximately 5% of the total mannose present in the yeast mannan was set free by α-mannosidase after prolonged incubation. The fact that no sugars other than mannose were detected in the mannan digests indicates that this enzyme is not a polysaccharidase (endoenzyme) in nature. The enzyme hydrolyzes mannobiose, mannotriose, and mannotetraose derived from yeast mannan.

Metal ion requirement and inhibition:

α-Mannosidase from jack-bean meal is stabilized by Zn^{2+} addition during the purification. At pH values below neutrality, the enzyme undergoes reversible spontaneous inactivation. The enzyme is also subject to irreversible inactivation, which is prevented by the addition of albumin or by Zn^{2+}. Other cations, such as Co^{2+}, Cd^{2+} and Cu^{2+}, accelerate inactivation; an excess of Zn^{2+} again exerts a protective action, and so does EDTA in suitable concentration. It is postulated that α-mannosidase is a dissociable Zn^{2+}-protein complex in which Zn^{2+} is essential for enzyme activity (88). The jack-bean α-mannosidase seems to exist naturally as a zinc-protein complex and may be considered as a metalloenzyme (89).

Other studies:

Jack bean α-mannosidase had wide acceptor specificity and could transfer mannosyl residues to various acceptors such as D-fructose, L-arabinose, maltose, lactose, and sucrose (90). The enzyme is a retaining Glycohydrolase. It was shown to be mechanistically similar to the lysosomal enzyme and would provide a useful model

system in mechanistic studies and inhibitor design (91). Two new mechanism-based inhibitors, 5-fluoro-α-D-mannosyl fluoride and 5-fluoro-β-L-gulosyl fluoride, which function by the steady state trapping of such an intermediate, were synthesized and tested. Both show high affinity and the latter has been used to label the active site nucleophile. Comparative liquid chromatographic/mass spectrometric analysis of peptic digests of labeled and unlabeled enzyme samples confirmed the unique presence of this peptide of m/z 1180.5 in the labeled sample. They have shown presence of Aspartic acid residue at active site, contained within the peptide sequence Gly-Trp-Gln-Ile-Asp-Pro-Phe-Gly-His-Ser, which showed excellent sequence similarity with regions in mammalian lysosomal and Golgi α-mannosidase sequences, family 38 class II α-mannosidases in which the Asp in the above sequence is totally conserved (92). Mechanism of inhibition of enzyme by swainsonine is also reported (93).

***Erythrina indica* α-mannosidase**

α-mannosidase from *Erythrina indica* seeds (94) is a Zn^{2+} dependent glycoprotein with 8.6% carbohydrate. The enzyme has energy of activation of the enzyme was found to be 23 kJ mol^{-1}. N-terminal sequence was deduced to be Asp, Thr, Gln, Glu, and Asn. Treatment of the enzyme with N-bromo succinimide (NBS) led to total loss of enzyme activity and modification of a single tryptophan residue led to inactivation. The enzyme exhibited immunological identity with α-mannosidase from *Canavalia ensiformis* but not with the same enzyme from Glycine max and *Cicer arietinum*. Incubation of *E. indica* seed lectin with α-mannosidase resulted in 35% increase in its activity. Lectin induced activation of α-mannosidase could be completely abolished in presence of lactose, a sugar specific for lectin (95).

Mung Bean α-mannosidase

α-mannosidase II from mung bean seedlings was purified to homogeneity by a combination of techniques comprising DEAE-cellulose, hydroxyapatite chromatography, gel filtration chromatography, lectin affinity chromatography and preparative gel electrophoresis. The purified protein did not show any metal ion

requirement and had pH optima of 6.0. The purified enzyme exhibited a single band on SDS-PAGE that migrated with the M_r 125 K standard. The enzyme preferred to remove the α1, 6-linked mannose first but 40% of the times removed the α1, 3-linked mannose first. It was strongly inhibited by swainsonine, less strongly by 1, 4-dideoxy-1, 4-imino-D-mannitol and not inhibited by 1-deoxymannojirimycin. (96).

Tomato α-mannosidase

Tomato (*Lycopersicon esculentum*) was found to contain two isoforms of class II α-mannosidase, isoform I and II, which were purified by ion exchange and gel filtration chromatography showing 6 and 24% of the total activity, respectively. Both the enzymes had pH optima of 4.5 and were thermally stable at 65 °C for up to 15 min. The K_m values for pNPαman were 1.11 and 1.05 mM, respectively. Purified isoform II had a SDS M_r of ca. 38,000 (97).

***Capsicum annuum* α-mannosidase**

A class II α-mannosidase showing increase in activity with increase in softening in *Capsicum annuum*, was purified to homogeneity by ammonium sulphate fractionation, ion-exchange chromatography and gel filtration chromatography. The purified enzyme had a native and SDS M_r of 43,000 and 23,000 respectively. The optimal pH was 5.7, the optimal temperature was 50 °C and the enzyme was thermally stable up to 60 °C for 15 min. The K_m for pNPαman was 0.7 mM. 0.1mM Cu^{2+} and Fe^{2+} inhibited the enzyme activity by nearly 95% (98).

Rice α-mannosidase

α-mannosidase from dry rice seeds was purified to homogeneity. Optimum pH and K_m for pNPαman were pH 4.3-4.5 and 1.04 mM, respectively. The enzyme digested mannobioses and Zn^{2+} ion was required for activity whereas EDTA and swainsonine inhibited the activity by 80% and 96% respectively (99).

***Gingko biloba* α-mannosidase**

An α-mannosidase from developing *Gingko biloba* seeds was purified to apparent homogeneity having a native molecular weight of 340 kDa and subunit molecular weight of 120 kDa. The enzyme activity was enhanced by the addition of Co^{2+} but the addition of Zn^{2+}, Ca^{2+} or EDTA did not show any significant effect. The enzyme prefers the oligomannose type free *N*-glycans bearing only one GlcNAc residue as substrate (100). It was also found that the substrate specificity of this enzyme was significantly regulated by Co^{2+} ions (101). Structural analysis of the products also showed clearly that the enzyme can produce truncated high-mannose type *N*-glycans, found in developing or growing plant cells, suggesting that the enzyme might be involved in the degradation of high-mannose type free *N*-glycans (101).

***Phaseolus vulgaris* α-mannosidase**

Two enzymes, α-mannosidase I and II, with pI of 5.1 and 6.1 respectively were purified to electrophoretic homogeneity by ammonium sulphate fractionation, DEAE-Sephadex ion-exchange chromatography, G-200 gel filtration chromatography and isoelectric focusing. Most of the activity was present as α-mannosidase I. This enzyme was purified extensively and its molecular weight was determined to be 194 kDa. The enzyme activity was shown to depend on zinc and the pH optimum and K_m value was determined for pNPαman. α-mannosidase II was only partially purified and some of its properties were studied in order to compare the two enzymes (102). An alternate immunoadsorbent affinity purification of the two enzyme forms was established (103). Both the enzymes have molecular weights about 210- 220 kDa and contain approximately 2 mol zinc / mol protein. Both are glycoproteins with 8.3% and 16.5% neutral sugar content, respectively. α-mannosidase II showed greater thermo stability than α-mannosidase I. Both the proteins appear to be composed of two non-covalently bound subunits of molecular weight of about 110 kDa (104).

Almond α-mannosidase

Almond α-mannosidase was purified by separation on columns of DEAE-Sephadex A50 and hydroxyapatite. Its optimum pH was about 3.8 and was shown to be stable in the pH range of 6 to 8. Its activity was stable up to 60 °C and was found to be more thermo stable than jack bean α-mannosidase (105).

Babaco α-mannosidase

An α-mannosidase from the latex of Babaco was purified to electrophoretic homogeneity. The molecular mass was determined to be in the range of 260-280 kDa and pI in the range of 5.85-6.55, suggesting different glycosylated isoforms. The optimal temperature was determined to be in the range of 50 – 60 °C and the optimal pH was found to be 4.5. The K_m value for pNPαman was found to be 1.25 mM (106).

Table 1.4: *Summary of plant class II α-mannosidases*

Source	Mol.Wt. (kDa)	Subunit Mol. Wt. (kDa)	Optimum pH	Optimum Temp. (°C)	K_m (mM)	Metal ion requirement	Metal ion inhibitor	Reference
Jack bean	230	66 and 49	5.0	45	-	Zn^{2+}	Cu^{2+}, Co^{2+} and Cd^{2+}	88,89
Mung bean	-	125	6.0	-	-	-	-	96
Tomato	-	38	4.5	65	1.08	-	-	97
Capsicum	43	23	5.7	50	0.7	-	Cu^{2+} and Fe^{2+}	98
Rice	-	-	4.3-4.5	-	1.04	Zn^{2+}		99
Gingko biloba	340	120	-	-	-	Co^{2+}	Ca^{2+}	100,101
Phaseolus vulgaris	194	110	4.6	-	1.6	Zn^{2+}	-	102

Source	Mol.Wt. (kDa)	Subunit Mol. Wt. (kDa)	Optimum pH	Optimum Temp. (°C)	K_m (mM)	Metal ion requirement	Metal ion inhibitor	Reference
Almond	-	-	3.8	60	-	-	-	105
Babaco	260-280	-	4.5	50-60	1.25	-	-	106
Erythrina indica	-	-	-	-	-	Zn^{2+}	-	95

Microbial class II α-Mannosidases

Microbial class II α-mannosidases are used in the analysis of glycopeptides and the developmental regulation of lysosomal enzymes.

The reports on production of class II α-mannosidases from bacteria include *Bacillus sp.* (107) *Acinetobacter* (108), *Arthrobacter* (109), *Flavobacterium dormitator* (110), and *Cellulomonas* (111), *Arcanobacterium haemolyticum* (112) alkalophilic bacterium *Bacillus halodurans* (113) and *Escherichia coli* (114). Protozoans are also known to produce α-mannosidase which is involved in the processing of high mannose oligosaccharides present in the processed proteins. Avila *et al.*, reported presence of 12 acid hydrolases including α-mannosidase from *Trypanosoma cruzi* (115) and characterization of neutral α-mannosidase from *Trypanosoma cruzi* (116) and *Trypanosoma rangeli* (117) has also been reported. *Aspergilli are the* major producers, viz., *Aspergillus niger* (118, 119), *Aspergillus saitoi* (120, 121), *Aspergillus oryzae* (122, 123), *Aspergillus* sp. (124) , *Aspergillus nidulans*, *Aspergillus flavus* (125) and reports concerning α-mannosidase from *Penicillium citrinum* (126), *Aspergillus fumigates* (127) and *Dictyostellium discoideum* (128) *Phellinus abietis* (129), *Trichoderma reesei* (130), *Neurospora crassa* (131) *are* also available. Among the yeasts, *Saccharomyces cerevisiae* (132) and *Candida albicans* (133) α-mannosidases are well studied.

Animal class II α-mannosidases

Animal sources of α-mannosidase include humans, rat, bovine (134) and pig (135) which form very important source for the study of the enzyme widely. Apart from these, α-mannosidase has also been reported from monkey brain (136), murine (137), lepidopteran insect, *Drosophila melanogaster* (138), Japanese Quail oviduct (139), calf liver (140), hen oviduct (141) etc.

In humans, cattle, cat and guinea pig, lack of lysosomal α-mannosidase activity causes the autosomal recessive disease called α-mannosidosis. Lysosomal α-mannosidase is a major exoglycosidase in the glycoprotein degradation pathway. Recently, great progress has been made in studying the enzyme and its deficiency. This includes cloning of the gene encoding the enzyme, characterization of mutations related to the disease, establishment of valuable animal models, and encouraging results from bone marrow transplantation experiments (142).

Crystal structure of class II α-mannosidases

Not many three-dimensional structures of class II α-mannosidases are known. Those known are of *Drosophila* Golgi α-mannosidase II (143) and *Streptococcus Pyogenes* α-mannosidase II (144). The most extensively studied of these enzymes is the *Drosophila* GH38 α-mannosidase II, which has been shown to be a retaining α-mannosidase that targets both α-1,3 and α-1,6 mannosyl linkages, an activity that enables the enzyme to process $GlcNAcMan_5GlcNAc_2$ hybrid *N*-glycans to $GlcNAcMan_3GlcNAc_2$. The crystal structure of Drosophila Golgi α-mannosidase II in the absence (Fig. 1.6 A) and presence (Fig 1.6 B) of the anti-cancer agent swainsonine reveals a novel protein fold with an active site zinc intricately involved both in the substrate specificity of the enzyme and directly in the catalytic mechanism.

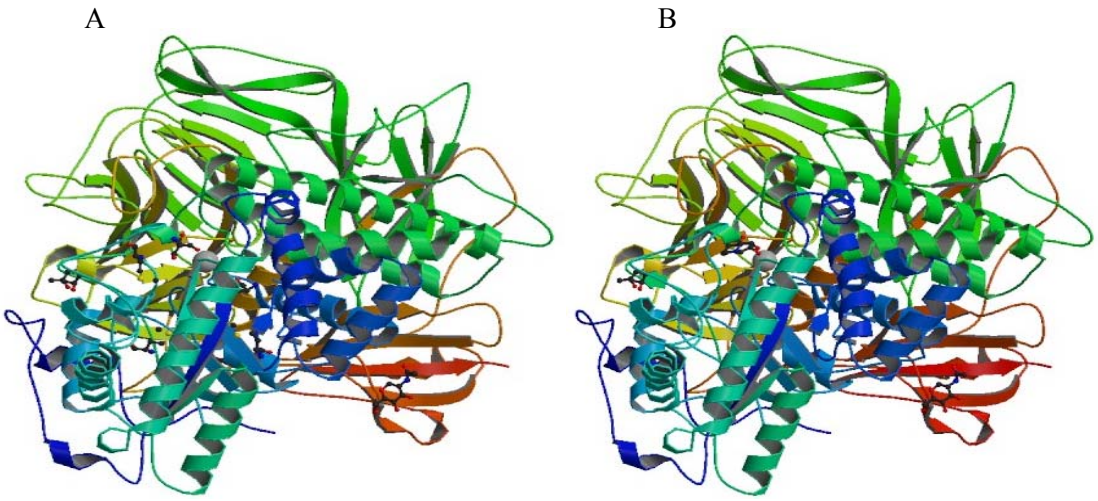

Fig 1.6: *Crystal structure of Drosophila Golgi α-mannosidase in absence (A) and presence (B) of swainsonine.*

Streptococcus pyogenes (M1 GAS SF370) GH38 enzyme (Spy1604; hereafter SpGH38) is an alpha-mannosidase with specificity for alpha-1, 3 mannosidic linkages. The 3D X-ray structure of SpGH38 (Fig. 1.7), obtained in native form at 1.9 Å resolution, reveals a canonical GH38 five-domain structure in which the catalytic "-1" subsite shows high similarity with the *Drosophila* enzyme, including the catalytic Zn^{2+} ion. In contrast, the "leaving group" subsites of SpGH38 display considerable differences to the higher eukaryotic GH38s; features that contribute to their apparent specificity.

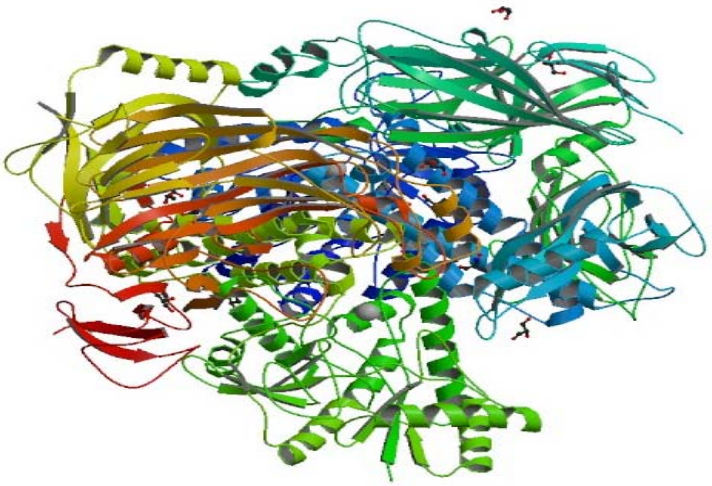

Fig 1.7: *Crystal structure of Streptococcus α-mannosidase.*

Protein Folding

The process by which a linear polypeptide chain transforms into three-dimensional functional structure is known as protein folding (Fig. 1.8). Defining mechanism governing folding remains a central point in biophysics and molecular biology. Each amino acid in the chain can be thought of having certain 'gross' chemical features. These may be hydrophobic, hydrophilic or electrically charged. These amino acids interact with each other and their surroundings in the cell to produce a well-defined, three dimensional shape of the folded protein known as the native state. Protein folding is a topic of fundamental interest since it concerns the mechanisms by which linear information of genetic message is transformed into three dimensional and functional structure of protein (145).

To be biologically active, all proteins must adopt specific folded three-dimensional structures. Yet the genetic information for the protein specifies only the primary structure, the linear sequence of amino acids in the polypeptide backbone. Most purified proteins can spontaneously refold in vitro after being completely unfolded, so the three-dimensional structure must be determined by the primary structure. How this occurs has come to be known as 'the protein folding problem' (146).

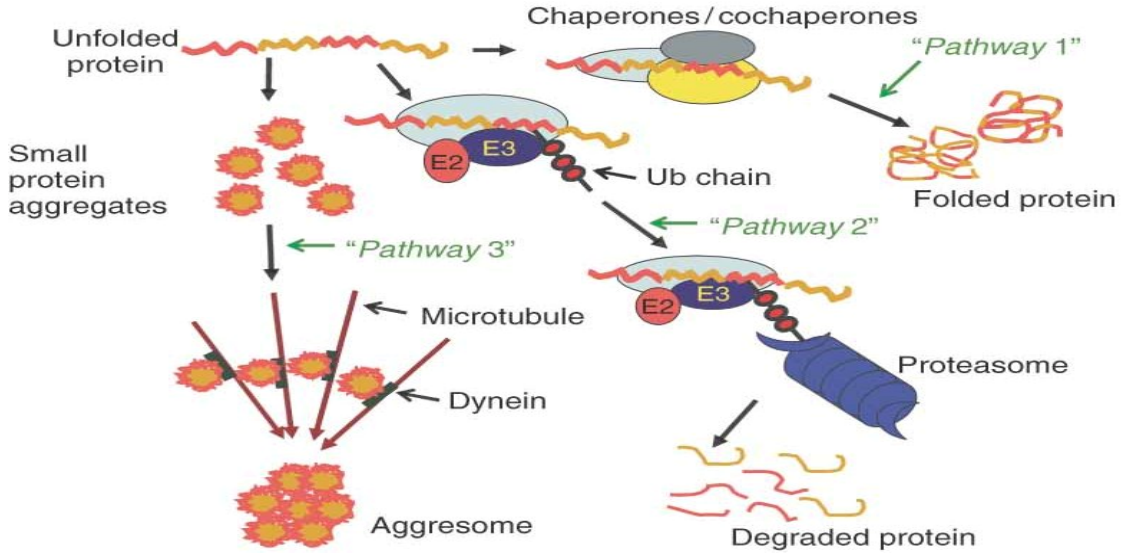

Fig. 1.8: *The in vivo protein folding pathway.*

The protein folding problem comprises three different related questions:

- By what kinetic process or pathway does the protein adopt its native and biologically-active folded conformation?
- What is the physical basis of the stability of folded conformations?
- Why does the amino acid sequence determine one particular folding process and resultant three-dimensional structure, instead of some other?

The stable conformational states of proteins

Different protein conformations differ only in the angle of rotation about the bonds of the backbone and amino acid side chains, except that they may also differ in covalent disulphide bonds, which are unique. Proteins with non-homologous amino acid sequences usually have different conformations. In contrast, homologous proteins invariably have essentially the same folded conformation, even if their amino acid similarities are minimal (147, 148). How much alteration is necessary before a protein no longer folds to its normal conformation, either remaining unfolded or adopting a new conformation, is not certain. Proteins have been, found to be surprisingly adaptive to mutations that would be expected to be disruptive, but the hydrophobic core seems to be the most critical aspect for stability of the normal folded state (149-151). Folded proteins demonstrate varying degrees of flexibility (152), which are of direct relevance to protein folding, in that it reflects the free energy constraints on unfolding and refolding (146).

The ideal unfolded protein is the random coil, in which the rotation angle about each bond of the backbone and side-chains is independent of that of bonds distant in the sequence, and where all conformations have comparable free energies, except when atoms of the polypeptide chain come into too close proximity. Unfolded states produced under different unfolding conditions, which often have different physical properties, are indistinguishable thermodynamically, so they are probably different sub-sets of the truly random spectrum of non-native conformations (153-155). Most importantly, unfolded proteins do not generally contain co-operative folded structures.

A variety of proteins have been observed under certain conditions to exist in stable conformations that are neither fully folded nor fully unfolded. These conformations have sufficient similarities to suggest that they are different manifestations of a third stable conformational state (156, 157). The most common properties are:

- The overall dimensions of the polypeptide chain are much less than those of a random coil and only marginally greater than those of the fully folded state.
- The average content of secondary structure is similar to that of the folded state.
- The interior side-chains are in homogeneous surroundings, in contrast to the asymmetric environments they have in the fully folded state.
- Many interior amide groups exchange hydrogen atoms with the solvent more rapidly than in the folded state, but more slowly than in the fully unfolded state.
- Interconversions with the fully unfolded state are rapid and non co-operative, but slow and co-operative with the fully folded state. (146).

Existence of folding pathways has been suggested, on which protein molecule passes through well-defined partially structured intermediates (145, 158, 159).

Protein folding intermediates:

A number of equilibrium and kinetic studies have led to structural characterization of folding/unfolding intermediates, which is a prerequisite to solve the folding problem. Partially folded states are characterized at equilibrium under mildly denaturing conditions, such as by altering pH, addition of salts and alcohols, chemical denaturants such as urea and guanidine hydrochloride or by changing temperature and pressure. Equilibrium intermediates characterized in different proteins were found to be related to kinetic folding intermediate transiently populated in early phase of folding reaction. This partially folded state was termed ‘molten globule’ since it had shape with loosely collapsed hydrophobic core (157).

Table 1.5: *Experimental Techniques used to monitor protein folding.*

Techniques	**Information about folding process**
Protein engineering	Role of individual amino acids in stability
Laser scattering	Radius of gyration
Gel filtration chromatography	Radius of gyration
DSC	Thermodynamics of folding process
Fluorescence spectroscopy	
a. Intrinsic	Environment and orientation of Trp
b. Polarization and anisotropy	Dynamics of fluorophore
c. FRET	Distance between two point in a protein
d. Quenching	Accessibility and environment of fluorophore
e. REES	Difference between environment fluorophore
f. Stopped flow	Time scale of fluorescence changes
g. Ligand binding	Formation of native structure at active site
Circular Dichroism (CD)	
a. Far-UV	Secondary structure
b. Near-UV	Tertiary structure
c. Stopped flow	Time for secondary and tertiary structure formation
Hydrogen exchange	
a. Native state exchange	Detection of metastable state
b. NMR	Rate of formation of backbone hydrogen bonds and protection form exchange of amino acid side chains
Real time NMR	Environment of protein side chain
Dynamic NMR	Detect equilibrium species
Laser temperature jump	Trigger folding /unfolding at nano seconds

Molten globule is a compact intermediate with high content of native-like secondary structure but fluctuating tertiary structure (156, 160). It contains accessible hydrophobic surfaces which bind a hydrophobic dye, 1-anilinonaphthalene sulfonate (ANS). The absence of near UV circular dichroism spectrum shows that in this intermediate aromatic resides can rotate in a symmetrical environment. Sub-millisecond kinetic methods have improved resolution time of kinetic studies allowing detection of early events of folding. More recently, techniques such as hydrogen exchange NMR, solution

X-ray scattering, protein engineering and site-directed mutagenesis have provided detailed picture of molten globules of many proteins. The latest experimental techniques, which are used to characterize protein folding intermediates, have been described in Table 1.5. Also, theoretical approaches based on computer simulations to understand folding process have been developed.

The ultimate objective of such studies is to define complete energy landscape for the folding reaction and to understand in detail how this is defined by the sequence. Various studies have shown that molten globule (MG) state has heterogeneous structure in which one portion of molecule is more organized and native like while other portions being less organized (161). How much native-like structure is present depends on protein species and solution conditions and a remarkable diversity in molten-globule structure of different proteins has been observed (162, 163). Thus, it will be useful to describe MG state and other partially folded states of different globular proteins so that we can see the features in common as well as differences among the different proteins.

Molten Globules

Molten globules are thought to be general intermediates in protein folding and unfolding**.** Soon after the term 'molten globule' was coined by Kuwajima in 1989, the identification and characterization of molten globules as intermediates in protein folding and unfolding picked up the pace. Examples of the classical molten globule state of some proteins are described here:

α-lactalbumin

In 1995 Wu and colleagues (164) tried to clarify whether molten globule state of α-lactalbumin resembles an expanded native-like protein or a non-specific collapsed polypeptide. They showed that the molten globule properties of α-lactalbumin are largely confined to one of its two domains. The α-helical domain forms a helical structure with a native-like tertiary fold, while the β-sheet domain is largely unstructured. They thus concluded that molten globules possess a native-like backbone

topology, but this topology does not necessarily encompass the entire polypeptide chain. Their studies also indicated that molten globules provide an approximate solution to, and considerable simplification of the protein folding problem.

Photoactive yellow protein (PYP)

Biological signalling generally involves the activation of a receptor protein by an external stimulus followed by interactions between the activated receptor and its downstream signal transducer. The relay of signals generally occurs by highly specific interactions between fully folded proteins. However, there are results indicating that many regulatory proteins are intrinsically unstructured, providing a serious challenge to the nature of structure-function relationships in signalling. In a study on the structural changes that occur upon activation of the blue light receptor photoactive yellow protein (PYP) Lee and colleagues (165) found that activation greatly reduces the tertiary structure of PYP but leaves the level secondary structure largely unperturbed. In addition, activated PYP exposes previously buried hydrophobic patches and allows significant solvent penetration into the core of the protein. These traits are the distinguishing hallmarks of molten globule states. Their results showed that receptor activation by light converts PYP to a molten globule and indicated stimulus-induced unfolding to a partially unstructured molten globule as a novel theme in signalling.

Apolipoprotein E

The unfolding of Apolipoprotein E (apo E), one of the culprits in Alzheimer's disease, was carried out by Morrow *et al.* (166) and they found that the amino-terminal domain of apoE4 is less susceptible to chemical and thermal denaturation than the apoE3 and apoE2. The urea denaturation curves of the 22-kDa amino-terminal domains of the apoE isoforms at pH 7.4 and 4.0 showed that at pH 7.4, apoE3 and apoE4 revealed an apparent two-state denaturation. At pH 4.0 apoE4 and apoE3 displayed the same order of denaturation but with distinct plateaus, suggesting the presence of a stable folding intermediate. In contrast, apoE2 proved the most stable and lacked the distinct plateau observed with the other two isoforms and could be fitted to a two-state unfolding

model. The structure of the apoE4 folding intermediate at pH 4.0 in 3.75 M urea was characterized and found to be a single molecule with the characteristics of a molten globule. They proposed a model of the apoE4 molten globule in which the four-helix bundle of the amino-terminal domain is partially opened, generating a slightly elongated structure and exposing the hydrophobic core. Molten globules have been implicated in both normal and abnormal physiological function, so the differential ability of the apoE isoforms to form a molten globule may contribute to the isoform-specific effects of apoE in disease.

Clusterin

Clusterin is a heterodimeric glycoprotein, most abundantly secreted by cultured rat Sertoli cells. Clusterin has been shown to bind to a variety of molecules with high affinity including lipids, peptides, and proteins and the hydrophobic probe 1-anilino-8-naphthalenesulfonate (ANS). Given this variety of ligands, Clusterin must have specific structural features that provide the protein with its promiscuous binding activity. Using sequence analyses, Bailey and colleagues (167) showed that Clusterin likely contains three long regions of natively disordered or molten globule-like structures containing putative amphipathic α-helices. These disordered regions were found to be highly sensitive to trypsin digestion, indicating a flexible nature. Clusterin bound ANS in a manner that was very similar to that of molten globular proteins. Furthermore, they also found that, when bound to ANS, at least one cleavage site within the protease-sensitive disordered regions of Clusterin was protected from trypsin digestion. They proposed that natively disordered regions with amphipathic helices form a dynamic, molten globule like binding site and provide Clusterin the ability to bind to a variety of molecules.

p53

It is not currently known in what state (folded, unfolded or alternatively folded) client proteins interact with the chaperone Hsp90. Park *et al.* (168) showed that one client, the p53 DNA-binding domain, undergoes a structural change in the presence of Hsp90 to

adopt a molten globule–like state. Addition of one- and two-domain constructs of Hsp90, as well as the full-length three-domain protein, to isotopically labeled p53 led to reduction in NMR signal intensity throughout p53, particularly in its central β-sheet. This reduction seems to be associated with a change of structure of p53 without formation of a distinct complex with Hsp90. Fluorescence and hydrogen-exchange measurements supported a loosening of the structure of p53 in the presence of Hsp90 and its domains. They proposed that Hsp90 interacts with p53 by multiple transient interactions, forming a dynamic heterogeneous manifold of conformational states that resembles a molten globule.

p53 is a transcription factor that maintains genome integrity, and its function is lost in 50% of human cancers. The majority of p53 mutations are clustered within the core domain. Bom and colleagues (169) investigated the effects of low pH on the structure of the wild-type (wt) p53 core domain (p53C) and the R248Q mutant. At low pH, the tryptophan residue is partially exposed to the solvent, suggesting a fluctuating tertiary structure. On the other hand, the secondary structure increases, as determined by circular dichroism. Binding of the probe bis-ANS (bis-8-anilinonaphthalene-1-sulfonate) indicated that there is an increase in the exposure of hydrophobic pockets for both wt and mutant p53C at low pH. This behavior is accompanied by a lack of cooperativity under urea denaturation and decreased stability under pressure when p53C is in acidic pH. Together, these results indicated that p53C acquired a partially unfolded conformation (molten-globule state) at low pH (5.0). The hydrodynamic properties of this conformation are intermediate between the native and denatured conformation. ^{1}H-^{15}N HSQC NMR spectroscopy confirms that the protein has a typical molten-globule structure at acidic pH when compared with pH 7.2. Human breast cells in culture (MCF-7) transfected with p53-GFP revealed localization of p53 in acidic vesicles, suggesting that the low pH conformation is present in the cell. Low pH stress also tends to favor high levels of p53 in the cells. Taken together, these data suggested that p53 may play physiological or pathological roles in acidic microenvironments.

Horse cytochrome c

To understand the stabilization, folding, and functional mechanisms of proteins, it is very important to understand the structural and thermodynamic properties of the molten globule state. In a very recent study, the global structure of the acid molten globule state, which Nakamura *et al.* (170) called MG1, of horse cytochrome *c* at low pH and high salt concentrations was evaluated by solution X-ray scattering (SXS), dynamic light scattering, and circular dichroism measurements. MG1 was globular and slightly (3%) larger than the native state, N. Calorimetric methods, such as differential scanning calorimetry and isothermal acid-titration calorimetry, were used to evaluate the thermodynamic parameters in the transitions of N to MG1 and MG1 to denatured state D of horse cytochrome *c*. The heat capacity change, ΔC_p, in the N-to-MG1 transition was determined to be 2.56 kJ K^{-1} mol^{-1}, indicating the increase in the level of hydration in the MG1 state. Moreover, the intermediate state on the thermal N-to-D transition of horse cytochrome *c* at pH 4 under low-salt conditions showed the same structural and thermodynamic properties of the MG1 state in both SXS and calorimetric measurements. The Gibbs free energy changes (ΔG) for the N-to-MG1 and N-to-D transitions at 15 °C were 10.9 and 42.2 kJ mol^{-1}, respectively.

Taka-amylase A (TAA)

The thermostability properties of taka-amylase A (TAA) were investigated by chemically modifying carboxyl groups on the surface of the enzyme with AMEs. The modified taka-amylase A (TAA_{MOD}) exhibited a 200% improvement in starch-hydrolyzing productivity at 60°C. By studying the kinetic, thermodynamic and biophysical properties, Siddiqui *et al.* (171) found that TAA_{MOD} had formed a thermostable, MG state, in which the unfolding of the tertiary structure preceded that of the secondary structure by at least 20°C. The X-ray crystal structure of TAA_{MOD} revealed no new permanent interactions (electrostatic or other) resulting from the modification. By deriving thermodynamic activation parameters of TAA_{MOD}, the authors concluded that thermostabilisation have been caused by a decrease in the entropy of the transition state, rather than being enthalpically driven. Far-UV CD shows

that the origin of decreased entropy may have arisen from a higher helical content of TAA_{MOD}. This study provides new insight into the intriguing properties of an MG state resulting from the chemical modification of TAA.

Pea lectin (PSL)

Pea lectin (PSL) is a dimeric protein in which each subunit comprises two intertwined, post-translationally processed polypeptide chains - a long β-fragment and a short α-fragment. Using guanidine hydrochloride-induced denaturation, Sen and Mandal (172) have investigated and characterized the species obtained in the unfolding equilibrium of PSL. During unfolding, the fragment chains become separated, and the unfolding pattern reveals a β-fragment as intermediate that has the molten globule characteristics. As examined by ANS binding, the fragment intermediate showed ~ 20 fold increase in ANS fluorescence, and a large increase in ANS lifetime (12.8 ns). The tryptophan environment of the molten globule β-fragment probed by selective modification with N-bromosuccinimide (NBS), showed that two tryptophans, possibly Trp 53 and Trp 152 are oxidized while the other Trp 128 remains resistant to oxidation. These results seem to indicate that the larger fragment chain of PSL can independently behave as a monomeric or single domain protein that undergoes unfolding through intermediate state(s), and may provide important insight into the folding problem of oligomeric proteins in general and lectins in particular.

Wheat germ lipase

Wheat germ lipase is a cereal lipase which is a monomeric protein. In a study in 2010, Ahmad *et al.* (173) sought to structurally characterize this protein along with equilibrium unfolding in solution. Conformational changes occurring in the protein with varying pH, were monitored by circular dichroism (CD) spectroscopy, fluorescence emission spectroscopy, binding of ANS and dynamic light scattering (DLS). Their study showed that acid denaturation of lipase lead to characterization of multiple monomeric intermediates. Native protein at pH 7.0 showed far-UV spectrum indicating mixed structure with both α and β type of characteristics. Activity of lipase

was found to fall on either sides of pH 7.0–8.0. Acid-unfolded state was characterized at pH 4.0 with residual secondary structure, disrupted tertiary spectrum and red-shifted fluorescence spectrum with decreased intensity. Further decrease in pH lead to formation of secondary structure and acid-induced molten globule state was found to be stabilized at pH 1.4, with exposed tryptophan residues and hydrophobic patches. Notably, interesting finding of this study was characterization of acid-induced state at pH 0.8 with higher secondary structure content than native lipase, regain in tertiary spectrum and induction of compact conformation. Although enzymatically inactive, acid-induced state at pH 0.8 was found to be structurally more stable than native lipase. Little work has been done to understand the folding profiles of multi-domain proteins at alkaline conditions. Sen and colleagues (174) have found the formation of a molten globule-like state in bovine serum albumin at pH 11.2 with the help of spectroscopic techniques. Interestingly, this state has features similar to the acid-denatured state of human serum albumin at pH 2.0. This state has also shown significant increase in ANS binding in comparison to the native state. At pH 13.0, the protein seems to acquire a state very close to 6 M guanidinium hydrochloride denatured one. But, reversibility study showed that it can regain nearly 40% of its native secondary structure. On the contrary, tertiary contacts were disrupted irreversibly.

New experimental results showed that either gain or loss of close packing can be observed as a discrete step in protein folding or unfolding reactions. This finding poses a significant challenge to the conventional two-state model of protein folding. Results of interest involve dry molten globule (DMG) intermediates, an expanded form of the protein that lacks appreciable solvent. When an unfolding protein expands to the DMG state, side chains unlock and gain conformational entropy, while liquid-like van der Waals interactions persist. Four unrelated proteins are now known to form DMGs as the first step of unfolding, suggesting that such an intermediate may well be commonplace in both folding and unfolding. Data from the literature showed that peptide amide protons are protected in the DMG, indicating that backbone structure is intact despite loss of side-chain close packing. Other complementary evidence showed

that secondary structure formation provides a major source of compaction during folding (175). The conventional two-state folding model breaks down when there are DMG intermediates, a realization that has major implications for future experimental work on the mechanism of protein folding.

Role of Molten Globule in protein folding

The detection and characterization of the intermediate states between the Unfolded and the Native states must basically be a right approach to the elucidation of the folding mechanism. The detection of the molten globule indicates that the protein folding takes place in a hierarchical manner, reflecting the hierarchy of the three-dimensional structure of natural proteins. To firmly establish such a molecular mechanism of folding, the folding kinetics of the molten globule from the fully unfolded state needs to be measured directly and study the relationship between the rate and the backbone topology (176).

Importance of protein folding

Of all the molecules found in living organisms, proteins are the most important. They are used to support the skeleton, control senses, move muscles, digest food, defence against infections and process emotions. The importance of protein folding has been recognized for many years. Almost a half-century ago, Linus Pauling discovered two quite simple, regular arrangements of amino acids, the α-helix and the β-sheet that are found in almost every protein. And in the early 1960s, Christian Anfinsen showed that the proteins actually tie themselves: If proteins become unfolded, they fold back into proper shape of their own accord; no shaper or folder is needed. Indeed, we now know that Anfinsen's conclusions needed expansion: Sometimes a protein will fold into a wrong shape. And some proteins, aptly named chaperones, keep their target proteins from getting off the right folding path. These two small but important additions to Anfinsen's theory hold the keys to protein folding diseases (177, 178).

Molecular chaperones

Almost three decades after Christian Anfinsen had won the Nobel Prize for demonstrating that protein folding is governed solely by the protein itself, other scientists discovered that some proteins have helped in the process. This help consists of proteins called chaperones (or chaperonins) that are associated with the target protein during part of its folding process. However, once folding is complete (or even before) the chaperone will leave its current protein molecule and go on to support the folding of another. Proper folding of some proteins appears to call for not just one chaperone, but several. However, several lines of evidence suggest that chaperones' primary function may be to prevent aggregation (179, 180).

Protein Folding and Biotechnology:

An intense research is focused to understand the structural basis of protein folding and stability and mechanistic role of early folding intermediates. Finding a solution to protein folding problem has many practical applications.

- **Predicting structure of protein**

A thorough understanding of the physical principles that govern folding of globular proteins is required for rational efforts to predict the three-dimensional structure of proteins. The methodologies used can be divided into three general categories: comparative modeling, Fold recognition or threading and ab-initio methods. These methods involve the development of an energy function capable of identifying the most stable conformation of a protein and a scoring function for the evaluation of protein models.

- **Solving the protein aggregation problem**

Protein aggregation *in vivo* is widespread phenomenon that arises from early folding intermediates through kinetic competition between proper folding and misfolding. Wide range of human diseases results due to incorrect folding of proteins, thereby leading to deposition of aggregates or plaques. A list of some human diseases is

presented in Table 1.6 that has been found to be a ramification of altered protein conformation. Possible treatment of these diseases could exploit detailed knowledge of protein folding and the prevention of abnormal folding.

Table 1.6: *Some protein misfolding diseases.*

Diseases	Protein involved	Cause
Crueltzfeldt-jacob	Prion protein	Toxic folding /aggregation
Alzheimer's	Beta-amyloid	Toxic folding/aggregation
Cystic fibrosis	CFTR	Misfolding
Cancer	Protein 53 (transcription factor)	Misfolding
Familial amyloid polyneuropathy	Apolipoprotein	Aggregation
Parkinson's	Alpha-synuclein	Amyloid fibril formation
Huntington's	Huntington	Amyloid fibril formation
Familial visceral amyloidosis	Lysozyme	Aggregation
Cataract	Crystallins	Aggregation
Marfan syndrome	Fibrillin	Misfolding
Scurvy	Collagen	Misfolding
Osteigenesis imperfect	Type 1 procollagen	Misassembly
Amyotropic lateral sclerosis	Superoxide dismutase	Misfolding
Finish type familial amyloidosis	Gesolin	Amyloid fibril formation
Kelanddic cerebral angiopathy	Cystatin C	Amyloid fibril formation
Type II diabetes	Islet amyloid polypeptide	Amyloid fibril formation

- ***De novo* designing**

Important field of research dependent upon our understanding of protein folding is *de novo* protein designing for constructing completely new positions with determined function. Grado *et al*., (181) have reviewed the different methods for *de novo* protein design, which usually consist of choosing a function of protein followed by searching a proteins scaffold capable of supporting the reactive groups in desired geometry. It is then necessary to determine an amino acid sequence able to fold into an adequate and stable three-dimensional structure, done by either exploring genetic methods or by combinatorial and computational algorithms.

Success in functionally-active designed polypeptide has been obtained in the field of catalysis, metal ion and heme binding, and introduction of cofactors. The successful design of a four-helix bundle protein that binds four heme groups with high affinity has been reported. It is clear that *de novo* protein design represents a growing field of research that will be useful both in testing the principles of protein folding and in offering the perspectives to design new proteins with practical applications for pharmaceuticals and diagnostics.

Treating protein misfolding

The purpose of studying any human disease is to find ways to treat it. The story of protein folding has not yet led to treatments for the diseases involved, but this could happen within the next decade. The key is to find a small molecule, a drug that can either stabilize the normally folded structure or disrupt the pathway that leads to a misfolded protein. Although, many molecular biologists and protein chemists believe this will be quite difficult, others are more optimistic. It is difficult to pinpoint where the search for treatment currently stands, however. Treatments based on our growing knowledge and continued research of protein folding is on the way. When they arrive, the saga that began with Pauling's fundamental studies of protein structure and Anfinsen's investigation of what some call 'the second genetic code' will reach its practical fruition (179).

Present investigation

Literature survey of glycosylation and the novelty and importance of the class II α-mannosidases has been presented in this chapter. Our group at National Chemical Laboratory (Pune, India) is working in the area of carbohydrate-protein interactions, class II α-mannosidases and protein chemistry for last 25 years. Besides the physiological and therapeutic importance of the class II α-mannosidase, it also serves as an interesting model to study the conformation related function of the enzyme (182-184). We have already purified and structurally and functionally characterized the class II α-mannosidase from *Aspergillus fischeri* (182-188). In the present investigation we studied the structure-function relationship of the class II α-mannosidase from *Canavalia ensiformis* (Jack Bean). Jack bean α-mannosidase (Jbα-man) was studied for its conformational and functional transitions under the effect of pH, temperature, chelating agent, reducing agent and guanidine hydrochloride. The energetics of catalysis and thermodynamics of inhibition was also studied for Jbα-man. On the other hand, we purified two isozymes of class II α-mannosidase from *Lens culinaris* (Lentil) (LAM 1 and 2), which were characterized for their pH and temperature optima and stability, K_m, V_{max}, pK_a of amino acids involved at the active site, activation energy and inhibition with swainsonine. Steady state fluorescence spectra and far UV circular dichroism spectra for both the enzymes were also obtained. Solute quenching studies for both the enzymes with ionic quenchers were also performed.

References

1. Landsteiner, K. (1931) *Science* **73**, 403-409.
2. Alberts, B., Bray, D., Lewis, J., Raff, M., Roberts, K. and Watson, J.D. (1994) *Molecular Biology of the Cell*, 3rd edition, Garland Publishing.
3. Rudd, P.M., Elliott, T., Cresswell, P., Wilson, I.A. and Dwek, R.A. (2001) *Carbohydrate and Glycobiology* **291**, 2370-2376.
4. Dwek, R.A. (1996) *Chem Rev* **96**, 683-720.
5. Drickamer, K. and Taylor, M.E. (1993) *Annu Rev Cell Biol* **9**, 237-264.
6. Hart, G.W. (1992) *Curr Opin Cell Biol* **4**, 1017-1023.
7. de Melo, E.B., da Silveira Gomes, A. and Carvalho, I. (2006) *Tetrahedron* **62**, 10277-10302.
8. Wolfenden, R., Lu, X. and Young, G. (1998) *J Am Chem Soc* **120**, 6814-6815.
9. Henrissat, B. (1991) *Biochem J* **280**, 309-316.
10. Coutinho, P.M. and Henrissat, B. (1999) *in: Recent Advances in Carbohydrate Bioengineering*, The Royal Society of Chemistry, Cambridge, pp 3–12.
11. Koshland, D.E. (1953) *Biol Rev* **28**, 416-436.
12. Zechel, D.L. and Withers, S.G. (2000) *Acc Chem Res* **33**, 11-18.
13. Withers, S.G. (2001) *Carb Polymers* **44**, 325-327.
14. Sinnot, M.L. (1990) *Chem Rev* **90**, 1171-1202.
15. Vasella, A., Davies, G.J. and Böhm, M. (2002) *Curr Opin Chem Biol* **6**, 619-629.
16. McCarter, J.D. and Withers, S.G. (1996) *J Am Chem Soc* **118**, 241-242.
17. Uitdehaag, J.C.M., Mosi, R., Kalk, K.H., van der Veen, B.A., Dijkhuisen, L., Withers, S.G. and Dijkstra, B.W. (1999) *Nat Struct Biol* **6**, 432-436.

18. Heightman, T.D. and Vasella, A.T. (1999) *Angew Chem Int Ed Engl* **38**, 750-770.

19. Daniel, P.F., Winchester, B. and Warren, C.D. (1994) *Glycobiology* **4**, 551-556.

20. Moremen, K.W., Trimble, R.B. and Herscovics, A. (1994) *Glycobiology* **4**, 113-125.

21. Herscovics, A. (1999) *in: B.M. Pinto (Ed.), Comprehensive Natural Products Chemistry,* **3**, Elsevier, Amsterdam, pp.13-35.

22. Lipari, F., Gour-Salin, B.J. and Herscovics, A. (1995) *Biochem Biophys Res Commun* **209**, 322-336.

23. Lal, A., Pang, P., Kalelkar, S., Romero, P.A., Herscovics, A. and Moremen, K.W. (1998) *Glycobiology* **8**, 981-995.

24. Howard, S., Braun, C., McCarter, J., Moremen, K.W., Liao, Y.F. and Withers, S.G. (1997) *Biochem Biophys Res Commun* **238**, 896-898.

25. Kornfeld, R. and Kornfeld, S. (1985) *Annu Rev Biochem* **54**, 631-664.

26. Bause, E., Bieberich, E., Rolfs, A., Volker, C. and Schmidt, B. (1993) *Eur J Biochem* **217**, 535-540.

27. Lal, A., Schutzbach, J.S., Forsee, W.T., Neame, P.J. and Moremen, K.W. (1994) *J Biol Chem* **269**, 9872-9981.

28. Bieberich, E., Treml, K., Volker, C., Rolfs, A., Kalz-Fuller, B. and Bause, E. (1997) *Eur J Biochem* **246**, 681-689.

29. Camirand, A., Heysen, A., Grondin, B. and Herscovics, A. (1991) *J Biol Chem* **266**, 15120-15127.

30. Tremblay, L.O., Campbell Dyke, N. and Herscovics, A. (1998) *Glycobiology* **8**, 585-595.

31. Campbell Dyke, N., Athanassiadis, A. and Herscovics, A. (1997) *Genomics* **41**, 155-159.

32. Eades, C.J. and Hintz, W.E. (2000) *Gene* **255**, 25-34.

33. Gonzalez, D.S. and Jordan, I.K. (2000) *Mol Biol Evol* **17**, 292-300.

34. Eades, C.J., Gilbert, A.M., Goodman, C.D. and Hintz, W.E. (1998) *Glycobiology* **8**, 17-33.

35. Eades, C.J. and Hintz, W.E. (2000) *Biotechnol Bioprocess Eng* **5**, 227-233.

36. Tulsiani, D.R. and Touster, O. (1985) *J Biol Chem* **260**, 13081-13087.

37. Bonay, P. and Hughes, R.C. (1991) *Eur J Biochem* **197**, 229-238.

38. Monis, E., Bonay, P. and Hughes, R.C. (1987) *Eur J Biochem* **168**, 287-294.

39. Bonay, P., Roth, J. and Hughes, R.C. (1992) *Eur J Biochem* **205**, 399-407.

40. Chui, D. et al. (1997) *Cell* **90**, 157-167.

41. Jarvis, D.L., Bohlmeyer, D.A., Liao, Y.F., Lomax, K.K., Merkle, R.K., Weinkauf, C. and Moremen, K.W. (1997) *Glycobiology* **7**, 113-127.

42. Kawar, Z., Karaveg, K., Moremen, K.W. and Jarvis, D.L. (2001) *J Biol Chem* **276**, 16335-163340.

43. Herscovics, A. (1999) *Biochim Biophys Acta* **1473**, 96-107.

44. Spiro, R.G. (1994) *in: J. Rothblatt, P. Novick, T. Stevens (Eds.), Guidebook to the Secretory Pathway*, Sambrook and Tooze Publication, Oxford University Press, Oxford, pp. 188-189.

45. Weng, S. and Spiro, R.G. (1996) *Glycobiology* **6**, 861-868.

46. Karaivanova, V.K., Luan, P. and Spiro, R.G. (1998) *Glycobiology* **8**, 725-730.

47. Hiraizumi, S., Spohr, U. and Spiro, R.G. (1993) *J Biol Chem* **268**, 9927-9935.

48. Spiro, R.G., Zhu, Q., Bhoyroo, V. and Soling, H.D. (1996) *J Biol Chem* **271**, 11588-94.

49. Spiro, M.J., Bhoyroo, V.D. and Spiro, R.G. (1997) *J Biol Chem* **272**, 29356-29363.

50. Dairaku, K. and Spiro, R.G. (1997) *Glycobiology* **7**, 579-586.

51. Aoyagi, T., Yamamoto, T., Kojiri, K., Morishima, H., Nagai, M., Hamada, M., Takeuchi, T. and Umezawa, H. (1989) *J Antibiot (Tokyo)* **42**, 883-889.

52. Tropea, J.E., Kaushal, G.P., Pastuszak, I., Mitchell, M., Aoyagi, T., Molyneux, R.J. and Elbein, A.D. (1990) *Biochemistry* **29**, 10062-10069.

53. Berecibar, A., Grandjean, C. and Siriwardena, A. (1999) *Chem Rev* **99**, 799-844.

54. Dorling, P.R., Huxtable, C.R. and Vogel, P. (1978) *Neuropathol Appl Neurobiol* **4**, 285-295.

55. Colegate, S.M., Dorling, P.R. and Huxtable, C.R. (1979) *Aust J Chem* **32**, 2257-2264.

56. Molyneux, R.J. and James, L.F. (1982) *Science* **216**, 190-1901.

57. Haraguchi, M. et al. (2003) *J Agric Food Chem* **51**, 4995-5000.

58. Schneider, M.J., Ungemach, F.S., Broquist, H.P. and Haris, T.M. (1983) *Tetrahedron* **39**, 29-32.

59. Bowlin, T.L. and Sunkara, P.S. (1988) *Biochem Biophys Res Commun* **151**, 859-864.

60. Jolly, R.D., Winchester, B.G., Gehler, J., Dorling, P.R. and Dawson, G. (1981) *J Appl Biochem* **3**, 273-291.

61. Chotai, K., Jennings, C., Winchester, B. and Dorling, P. (1983) *J Cell Biochem* **21**, 107-117.

62. Ikeda, K., Kato, A., Adachi, I., Haraguchi, M. and Asano, N. (2003) *J Agric Food Chem* **51**, 7642-7646.

63. Cenci di Bello, I., Dorling, P. and Winchester, B. (1983) *Biochem J* **215**, 693-696.

64. Watson, A.A., Fleet, G.W.J., Asano, N., Molyneux, R. and Nash, R. (2001) *J Phytochemistry* **56**, 265-295.

65. Tulsiani, D.R., Harris, T.M. and Touster, O. (1982) *J Biol Chem* **257**, 7936-7939.

66. Tulsiani, D.R., Broquist, H.P., James, L.F. and Touster, O. (1988) *Arch Biochem Biophys* **264**, 607-617.

67. Cenci di Bello, I., Fleet, G., Namgoong, S.K., Tadano, K. and Winchester, B. (1989) *Biochem J* **259**, 855-861.

68. Bischoff, J. and Kornfeld, R. (1986) *J Biol Chem* **261**, 4758-4765.

69. Dorling, P.R., Huxtable, C.R. and Colegate, S.M. (1980) *Biochem J* **191**, 649-651.

70. Humphries, M.J. and Olden, K. (1989) *Pharmac Ther* **44**, 85-105.

71. Humphries, M.J., Matsumoto, K., White, S.L. and Olden, K. (1986) *Proc Natl Acad Sci U S A* **83**, 1752-1756.

72. Dennis, J.W. (1986) *Cancer Res* **46**, 5131-5136.

73. Spearman, M.A., Damen, J.E., Kolodka, T., Greenberg, A.H., Jamieson, J.C. and Wright, J.A. (1991) *Cancer Letters* **57**, 7-13.

74. Huxtable, C.R. and Dorling, P.R. (1982) *Am J Pathol* **107**, 124-126.

75. Huxtable, C.R., Dorling, P.R. and Walkley, S.U. (1982) *Acta Neuropathol* **58**, 27-33.

76. Huxtable, C.R. and Dorling, P.R. (1985) *Acta Neuropathol* **68**, 68-73.

77. Tulsiani, D.R. and Touster, O. (1987) *J Biol Chem* **262**, 6506-6514.

78. Ockerman, P.A. (1967) *Acta Paediatr Scand*, Suppl 177:35-6.

79. Burditt, L.J., Phillips, N.C., Robinson, D., Winchester, B.G., Van-de-Water, N.S. and Jolly, R.D. (1978) *Biochem J* **175**, 1013-1022.

80. Bischoff, J., Liscum, L. and Kornfeld, R. (1986) *J Biol Chem* **261**, 4766-4774.

81. Misaki, R., Fujiyama, K., Yokoyama, H., Ido, Y., Miyauchi, K., Yoshida, T. and Seki, T. (2003) *Journal of Bioscience and Bioengineering* **96**, 187-192.

82. http://www.freepatentsonline.com/WO2005094874.html.

83. van den Elsen, J.M., Kuntz, D.A. and Rose, D.R. (2001) *EMBO J* **20**, 3008-3017.

84. Winkler, D.A. and Holan, G. (1989) *J Med Chem* **32**, 2084-2089.

85. Agrawal, K.M.L. and Bahl, O.P. (1968) *J Biol Chem* **243**, 103-111.

86. Jagadeesh, B.H., Prabha, T.N. and Srinivasan, K. (2004) *Plant Science* **166**, 1451-1459.

87. Li, Y.T. (1967) *J Biol Chem* **242**, 5474-80.

88. Snaith, S.M. and Levvy, G.A. (1968) *Biochem J* **110**, 663-70.

89. Snaith, S.M. (1975) *Biochem J* **147**, 83-90.

90. Hara, K., Fujita, K., Nakano, H., Kuwahara, N., Tanimoto, T., Hashimoto, H., Koizumi, K. and Kitahata, S. (1994) *Biosci Biotechnol Biochem* **58**, 60-3.

91. Howard, S., Braun, C., McCarter, J., Moremen, K.W., Liao, Y.F. and Withers, S.G. (1997) *Biochem Biophys Res Commun* **238**, 896-8.

92. Howard, S., He, S. and Withers, S.G. (1998) *J Biol Chem* **273**, 2067-72.

93. Kang, M.S. and Elbein, A.D. (1983) *Plant Physiol* **71**, 551-554.

94. Kestwal, R.M. and Bhide, S.V. (2005) *Indian J Biochem Biophys* **42**, 159-160.

95. Kestwal, R.M., Konozy, E.H., Hsiao, C.D., Roque-Barreira, M.C. and Bhide, S.V. (2007) *Biochim Biophys Acta* **1770**, 24-8.

96. Kaushal, G.P., Szumilo, T., Pastuszak, I. and Elbein, A.D. (1990) *Biochemistry* **29**, 2168-2176.

97. Suvarnalatha G. and Prabha T.N. (1999) *Phytochemistry* **50**, 1111-1115.

98. Priya Sethu K.M. and Prabha T.N. (1997) *Phytochemistry* **44**, 383-387.

99. Kishimoto T., Hori H., Takano D., Nakano Y. Watanabe M. and Mitsui T. (2001) *Physiol. Plant.* **112**, 15-24.

100. Woo K.K., Miyazaki M., Hara S., Kimura M. and Kimura Y. (2004) *Biosci. Biotechnol. Biochem.* **68**, 2547-2556.

101. Woo K.K. and Kimura Y. (2005) *Biosci. Biotechnol. Biochem.* **69**, 1111-1119.

102. Paus E. and Christensen T.B. (1972) *Eur. J. Biochem.* **25**, 308-314.

103. Paus E. (1976) *FEBS Lett.* **72**, 39-42.

104. Paus E. (1977) *Eur. J. Biochem.* **73**, 155-161.

105. Misaki R., Fujiyama K., Yokoyama H., Ido Y., Miyauchi K., Yoshida T. and Seki T. (2003) *J. Biosci. Bioengg.* **96**, 187-192.

106. Blom H., Reyes F. and Carlsson J. (2008) *J. Agric. Food Chem.* **56**, 10872-10878.

107. Nankai, H., Hashimoto, W. and Murata, K. (2002) *Appl Environ Microbiol* **68**, 2731-2736.

108. Kathoda, S., Sawaya, Y., Asatsuma, K., Suzuki, F. and Hayashibe, M. (1977) *Agric Biol Chem* **41**, 331-337.

109. Jones, G.H. and Ballou, C.E. (1969) *J Biol Chem* **244**, 1043-1051.

110. Yamamoto, S. and Nagasaki, S. (1975) *Agric Biol Chem* **39**, 1981-1989.

111. Takegawa, K., Miki, S., Jikibara, T. and Iwahara, S. (1989) *Biochim Biophys Acta* **991**, 431-437.

112. Carlson, P. and Kontiainen, S. (1994) *J Clin Microbiol* **32**, 854-855.

113. Takami, H. et al. (2000) *Nucleic Acids Res* **28**, 4317-4331.

114. Sampaio, M.M., Chevance, F., Dippel, R., Eppler, T., Schlegel, A., Boos, W., Lu, Y.J. and Rock, C.O. (2004) *J Biol Chem* **279**, 5537-5548.

115. Avila, J.L., Casanova, M.A., Avila, A. and Bretaña, A. (1979) *J Protozool* **26,** 304-311.

116. Bonay, P. and Fresno, M. (1999) *Glycobiology* **9**, 423-433.

117. Nok, A.J., Shuaibu, M.N., Kanbara, H. and Yanagi, T. (2000) *Parasitol Res* **86**, 923-928.

118. Swaminathan, N., Matta, K.L., Donoso, L.A. and Bahl, O.P. (1972) *J Biol Chem* **247**, 1775-1779.

119. Matta, K.L. and Bahl, O.P. (1972) *J Biol Chem* **247**, 1780-1787.

120. Amano, J. and Kobata, A. (1986) *J Biochem* **99**, 1645-1654.

121. Ichishima, E., Arai, M., Shigematsu, Y., Kumagai, H. and Sumida-Tanaka, R. (1981) *Biochim Biophys Acta* **658**, 45-53.

122. Yamamoto, K., Hitomi, J., Kobatake, K. and Yamaguchi, H. (1982) *J Biochem* **91**, 1971-1979.

123. Akao, T. et al. (2006) *Biosci Biotechnol Biochem* **70**, 471-479.

124. Keskar, S.S., Gaikwad, S.M., Khire, J.M. and Khan, M.I. (1993) *Biotechnol Lett* **15**, 685-690.

125. Augustin, J. and Sikl, D. (1978) *Folia Microbiol (Praha)* **23**, 349-350.

126. Yoshida, T., Inoue, T. and Ichishima, E. (1993) *Biochem J* **290 (Pt 2)**, 349-354.

127. Li, Y., Fang, W., Zhang, L., Ouyang, H., Zhou, H., Luo, Y. and Jin, C. (2009) *Glycobiology* **19**, 624-32.

128. Schatzle, J., Bush, J. and Cardelli, J. (1992) *J Biol Chem* **267**, 4000-4007.

129. Zouchova, Z., Kocourek, J. and Musilek, V. (1977) *Folia Microbiol (Praha)* **22**, 61-65.

130. Petergem, V.F., Contreas, H., Contreas, R., Beeumen, V.J. (2001) *J Mol Biol* **312**, 157-165.

131. Vaughn, L.E. and Davis, R.H. (1981) *Mol Cell Biol* **1**, 797-806.

132. Jelinek-Kelly, S., Akiyama, T., Saunier, B., Tkacz, J.S. and Herscovics, A. (1985) *J Biol Chem* **260**, 2253-2257.

133. Ana Bertha, V.R., Rozalia, B.O. and Arturo, F.C. (1993) *FEMS Microbial Lett* **106**, 321-325.

134. Heikinheimo, P. et al. (2003) *J Mol Biol* **327**, 631-44.

135. Bause, E., Breuer, W., Schweden, J., Roeser, R. and Geyer, R. (1992) *Eur J Biochem* **208**, 451-7.

136. Mathur, R., Alvares, K. and Balasubramanian, A.S. (1984) *Biochem Biophys Res Commun* **123**, 1185-93.

137. Merkle, R.K., Zhang, Y., Ruest, P.J., Lal, A., Liao, Y.F. and Moremen, K.W. (1997) *Biochim Biophys Acta* **1336**, 132-46.

138. Numao, S., Kuntz, D.A., Withers, S.G. and Rose, D.R. (2003) *J Biol Chem* **278**, 48074-48083.

139. Oku, H., Hase, S. and Ikenaka, T. (1991) *J Biochem* **110**, 29-34.

140. Schweden, J., Legler, G. and Bause, E. (1986) *Eur J Biochem* **157**, 563-570.

141. Yamashiro, K., Itoh, H., Yamagishi, M., Natsuka, S., Mega, T. and Hase, S. (1997) *J Biochem* **122**, 1174-81.

142. Sun, H. and Wolfe, J.H. (2001) *Exp Mol Med* **33**, 1-7.

143. Van den Elsen, J.M., Kuntz, D.A. and Rose, D.R. (2001) *EMBO J* **20:** 3008-3017.

144. Suits, M.D.L., Zhu, Y., Taylor, E.J., Zechel, D.L., Gilbert, H.J., Davies, G.J. (2010) *Plos One* **5:** E9006-e9006.

145. Oas, T.G. and Kim, P.S. (1988) *Nature* **336**, 42-48.

146. Creighton, T.E. (1990) *Biochem J* **270**, 1-16.

147. Bajaj, M. & Blundell, T. (1984) *Annu Rev Biophys Bioeng* **13**, 453-492.

148. Chothia, C. & Lesk, A. M. (1986) *EMBO J* **5**, 823-826.

149. Lim, W. A. & Sauer, R. T. (1989) *Nature* **339**, 31-36.

150. Kellis, J. T., Jr., Nyberg, K. & Fersht, A. R. (1989) *Biochemistry* **28**, 4914-4922.

151. Bowie, J. U., Reidhaar-Olson, J. F., Lim, W. A. & Sauer, R. T. (1990) *Science* **247**, 1306-1310.

152. McCammon, J. A. & Harvey, S. C. (1987) *Dynamics of Proteins and Nucleic Acids*, Cambridge University Press, London.

153. Griko, Yu, V., Privalov, P. L., Venyaminov, S., Yu. & Kutyshenko, V.P. (1988) *J Mol Biol* **202**, 127-138.

154. Privalov, P. L., Tiktopulo, E. I., Venyaminov, S. Yu., Griko, Yu. V., Makhatadze, G. I. & Khechinashvili, N. N. (1989) *J Mol Biol* **205**, 737-750.

155. Privalov, P. L. (1979) *Adv Protein Chem* **33**, 167-241.

156. Ptitsyn, 0. B. (1987) *J Protein Chem* **6**, 273-293.

157. Kuwajima, K. (1989) *Proteins: Struct Funct Genet* **6**, 87-103.

158. Feng, H., Zhou, Z. and Bai, Y. (2005) *Proc Natl Aca Sc, USA* **102**, 5026-5031.

159. Simmons, D.A. and Konermann, L. (2002) *Biochemistry* **41**, 1906-1914.

160. Dolgikh, D.A., Gilmanshin, R.I., Brazhnikov, E.V., Bychkova, V.E., Semisotnov, G.V., Venyaminov, S.Y. and Ptitsyn, O.B. (1981) *FEBS Lett* **136**, 311-315.

161. Arai, M., Kuwajima, K. (2000) *Adv Protein Chem* **53**, 209-271.

162. Haq, S.K., Rasheedi, S. and Khan, R.H. (2002) *Eur J Biochem* **269**, 47-52.

163. Privalov, P.L. (1996) *J Mol Biol* **258**, 707-725.

164. Wu, C.L., Peng, Z-Y. and Kim, P.S. (1995) *Nat Struct Biol* **2**, 281-286.

165. Lee, B-C., Croonquist, P.A., Sosnick, T.R. and Hoff, W.D. (2001) *J Biol Chem* **276**, 20821-20823.

166. Morrow, A.J., Hatters, D.M., Lu, B., Hochtl, P., Oberg, K.A., Rupp, B. and Weisgraber, K.H. (2002) *J Biol Chem* **277**, 50380-50385.

167. Bailey, R.W., Dunker, A.K., Brown, C.J., Garner, E.C. and Griswold, M.D. (2001) *Biochemistry* **40**, 11828-11840.

168. Park, S.J., Borin, B.N., Martinez-Yamout, M.A. and Dyson H.J. (2011). *Nat Struct Mol Biol* **11**: 537-541.

169. Bom, A.P.D.A., Freitas, M.S., Moreira, F.S., Ferraz, D., Sanches, D., Gomes, A.M.O., Valente, A.P., Cordeiro, Y. and Silva, J.L. (2010) *J Biol Chem* **285**: 2857-2866.

170. Nakamura, S., Seki, Y., Katoh, E., and Kidokoro, S-i. (2011) *Biochemistry* **50**: 3116-3126.

171. Siddiqui, K.S., Poljak, A., Francisci, D.D., Guerriero,G., Pilak, O., Burg, D., Raftery, M.J., Parkin, D.M., Trewhella, J. and Cavicchioli, R. (2010) *Protein Eng Des Sel* **23**: 769-780.

172. Sen, D. and Mandal, D. (2011) *Biochimie* **93**: 409-417.

173. Ahmad, E., Fatima, S., Khan, M.M. and Khan, R.H. (2010) *Biochimie* **92**: 885-893.

174. Sen, P., Ahmad, B. and Khan, R.H. (2010) *Eur Biophys J* **37**: 1303-1308.

175. Baldwin, R. L., Frieden, C. and Rose, G. D. (2010) *Proteins: Struct Funct Bioinfo* **78**: 2725–2737.

176. Kuwajima, K. (2002) *Proc Ind Natl Sc Aca* **68**, 333-340.

177. Thomasson, W.A.(1996) *FASEB J* **10**.

178. King, J. (1993) *Technology Review*, 58-61.

179. Taubes, G. (1996) *Science* **271**, 1493-1495.

180. Thomas, P.J., Qu, B.H. and Pedersen, P.L. (1995) *TIBS* **20**, 456-459.

181. DeGrado, W.F., Wasserman, Z.R. and Lear, J.D. (1989) *Science* **243**, 622-628.

182. Gaikwad, S.M., Keskar, S.S. and Khan, M.I. (1995) *Biochim Biophys Acta* **1250**, 144-8.

183. Keskar, S.S., Gaikwad, S.M., Khan, M.I.(1996) *Enz Micro Tech* **18**, 602-604.

184. Gaikwad, S.M., Khan, M.I. and Keskar, S.S. (1997) *Biotechnol Appl Biochem* **25**, 105-108.

185. Shashidhara, K.S. and Gaikwad, S.M. (2007) *J. Fluoresc.* **7**, 559-605.

186. Shashidhara, K.S. and Gaikwad, S.M. (2009) *Int. J. Biol. Macromol.* **44**, 112-115.

187. Shashidhara, K.S., Gaikwad, S.M., Khan, M.I., Bharadwaj, K.C. and Pandey, G. (2009) *Res. J. Biotech.*

188. Shashidhara, K.S. and Gaikwad, S.M. (2010) *J. Fluoresc.* **20**, 827-836.

CHAPTER 2

BIOCHEMICAL AND BIOPHYSICAL CHARACTERIZATION OF A CLASS II α- MANNOSIDASE FROM *CANAVALIA ENSIFORMIS* (JACK BEAN)

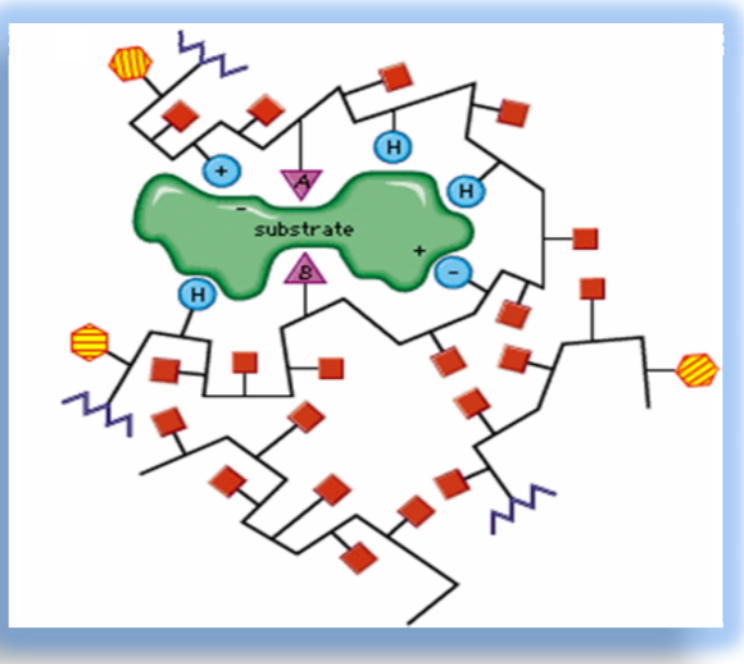

Avinash Kumar *and Sushama M. Gaikwad. Jack bean α-mannosidase (Jbα-man): Tolerance to alkali, chelating and reducing agents and energetics of catalysis and inhibition. (Under Review)*

Summary

Investigations of the catalytic and structural transitions of Jack bean α-mannosidase (Jbα-man) under particular conditions was performed. The enzyme shows maximum activity at pH 5.0 and 45 °C. In the pH range of 1.0 to 10.0, the enzyme was maximally stable at pH 5.0 for 1 h at 28 °C. The stability declined fast in the pH range of 1.0-3.0 and 8.0-10.0. However, Jbα-man incubated in the pH range of 11.0-12.0, showed 1.3 times higher activity which was also more stable as compared to that at pH 5.0. The free amino group was found to be present at or near the active site which probably was involved in the stability and activation mechanism in the extreme alkaline pH range. The active site is constituted by the association of two unidentical subunits which are connected by disulfide linkages. Jbα-man, the metalloenzyme, has Zn^{2+} ions tightly bound to it and chelation of the metal ion reduces the thermal stability of the protein. E_a of Jbα-man with pNPαman as a substrate was 31.9 kJ mol^{-1} and with 4-MeUmbαman was 26.7 kJ mol^{-1}. The strong binding of the class II α-mannosidase inhibitor, Swainsonine (K_i = 52.9 nM), to the enzyme was found to be entropy driven.

Introduction

α-mannosidase (α-mannoside mannohydrolase, E.C. 3.2.1.24), an exoglycosidase, catalyzes the hydrolysis of terminal non-reducing mannose residues in mannans during N-linked glycosylation, a posttranslational modification in eukaryotes. Based on the amino acid sequence analysis and some biochemical properties, α-mannosidases are grouped into glycosyl hydrolase family 38 which includes α1,2-, α1,3- and α1,6-mannosidases, commonly referred to as Class II α-mannosidases and glycosyl hydrolase family 47 which include α1,2- mannosidases commonly referred to as Class I α-mannosidases. Class I α-mannosidases are strongly inhibited by 1-deoxymannojirimycin while swainsonine is the strong inhibitor of class II enzymes (1). The deficiency of this enzyme in humans and cattle leads to a fatal disease called mannosidosis (2). The enzymes of this glycosylation pathway are potential targets for development of inhibitors such as swainsonine as anticancer agents (3) due to altered distribution of N-linked sugars on the cell surface of tumor cell lines (4). Conditions which perturb the stabilizing forces involved in holding together the three dimensional

structure of a protein affect the native conformation by changing its physical properties and biological activity.

Jbα-man is a high molecular weight metalloenzyme of 230 kDa existing naturally as zinc-protein complex (5). Purification and characterization of this enzyme from jack bean meal has already been reported by Snaith and Levvy (6). Its mechanism of inhibition with swainsonine (7) and identification of the catalytic nucleophile at the active site have also been carried out by Howard et al (8).

We have reported the existence and characterization of a molten globule upon denaturation of Jack bean α-mannosidase with Guanidine Hydrochloride (GdnHCl) (9). We have also studied the α-mannosidase from *Aspergillius fischeri* for its biochemical and biophysical transitions (10-13).

The present enzyme from plant source, *Canavalia ensiformis*, jack bean (Jbα-man) possesses several interesting properties, which were studied in detail to investigate the structure-function relationship.

Materials and methods

Materials

α-mannosidase from *Canavalia ensiformis* (Jack Bean) (Jbα-man), 1-anilino-8-naphthalenesulfonate (ANS), ethylenediaminetetraacetic acid (EDTA), Swainsonine, Citraconic anhydride, β-mercaptoethanol (β-ME) and 2,2'-dithiobisnitrobenzoic acid (DTNB) were purchased from Sigma Aldrich Ltd., USA. All other reagents and buffer compounds used were of analytical grade. For spectroscopic measurements, solutions were prepared in MilliQ water.

Preparation of Jbα-man

For studying the effect of pH, a stock solution of 1 mg ml-1 Jbα-man procured from Sigma Ltd. was prepared in milliQ water and dialyzed extensively. Enzyme samples were spun and clear supernatant was taken for spectroscopic measurement. Protein concentration was determined by the method of Lowry *et al*. before taking measurement.

Enzyme assay

The α-mannosidase activity was estimated by incubating 3 µg enzyme with 500 µM pNP-α-mannopyranoside (pNPαMan), in 50 mM CPB, pH 5.0 in a total volume of 0.5 ml at 45 °C for 15 min. The reaction was terminated by adding 1 ml of 1 M Na_2CO_3 and the p-nitro phenol released was determined from its absorbance at 405 nm. One unit (U) of enzyme activity was defined as the amount of enzyme required to liberate 1 µmol of p-nitro phenol per minute under the standard assay conditions. (Molar Extinction Coefficient of p-nitro phenol = 17.7×10^3 $M^{-1}cm^{-1}$).

For the other substrate, α-mannosidase (30 ng) was incubated with 10 µM 4-methylumbellideryl-α-mannopyranoside (4-MeUmbαMan) in 50 mM CPB of pH 5.0 in a total volume of 0.5 ml at 45 °C for 15 min. The reaction was terminated by adding 1 ml of 0.3 M Na_2CO_3. The fluorescence was measured in a Perkin Elmer LS 50B luminescence spectrometer using excitation wavelength of 360 nm and emission at 445 nm. One unit (U) of enzyme activity was defined as the amount of enzyme required to liberate 1 µmol of 4-methylumbelliferone per minute under standard assay conditions.

Fluorescence measurements

Steady-state fluorescence measurements were performed on Perkin Elmer LS 50B luminescence spectrometer at 28 °C. The protein solution of 100 µg/ml was excited at 295 nm and emission was recorded in the range of 310–400 nm. Slit widths of 7 nm each were set for excitation and emission monochromators and the spectra were recorded at 100 nm/min. To eliminate the background emission, the signal produced by buffer solution was subtracted.

Circular dichroism (CD) measurements

The CD spectra of the enzyme were recorded on a J-715 Spectropolarimeter (Jasco, Tokyo, Japan) at 28 °C in a quartz cuvette. Each CD spectrum was accumulated from five scans at 100 nm/min with a 1 nm slit width and a time constant of 1 s for a nominal resolution of 0.5 nm. Far UV CD spectra of the enzyme (125 μg/ml) were collected in the wavelength range of 200–250 nm using a cell of path length 0.1 cm for monitoring the secondary structure. All spectra were corrected for buffer contributions and observed values were converted to mean residue ellipticity (MRE) in deg cm^2 $dmol^{-1}$ defined as

$$MRE = M\theta_\lambda / 10dcr \quad (1)$$

Where, M is the molecular weight of the protein, θλ is CD in millidegree, d is the path length in cm, c is the protein concentration in mg/ ml and r is the average number of amino acid residues in the protein.

ANS binding studies

The intermediate states of denatured and native α-mannosidase incubated in 25 mM buffers of different pH (1-12) were analyzed by the hydrophobic dye (ANS) binding. The final ANS concentration used was 50 μM, excitation wavelength was 375 nm and total fluorescence emission was monitored between 400 and 550 nm. Reference spectrum of ANS in buffer was subtracted from the spectrum of the sample.

Effect of pH

Samples of α-mannosidase (100 μg/ml) were incubated in an appropriate buffer over the pH range of 1-12 for 4 h at 28 °C. The following buffers (25 mM) were used for these studies: Glycine-HCl for pH 1-3, acetate for pH 4-5, phosphate for pH 6-7, Tris-HCl for pH 8-9 and Glycine-NaOH for pH 10-12. pH of the reaction remained stable even after 4 h. Fluorescence measurements and ANS binding studies were performed as described above.

Samples of α-mannosidase (125 μg/ml) were incubated in 20mM concentration of the above mentioned buffers and were used for CD measurements as described above.

For stability studies, time course of effect of pH on α-mannosidase was carried out by incubating the enzyme (20 µg) in the above mentioned buffers for 6 h. Aliquots were removed after 30 min interval and assayed for activity under standard assay conditions. Activity at 0 min at pH 5.0 was taken as 100%.

Citraconylation

The α-mannosidase (3 µg) in 50mM Glycine-NaOH buffer, pH 11.0 was treated with 2, 5 and 10mM citraconic anhydride respectively, at 28 °C and assayed for the enzyme activity. The enzyme samples incubated under same conditions without citraconic anhydride served as control. Reactivation of the enzyme was checked by adjusting the pH of the treated sample to 5.0 and then assaying the enzyme activity.

Substrate protection studies

Substrate protection studies were carried out by mixing the enzyme (3 µg) with 500 µM pNPαMan before treatment with citraconic anhydride and then assaying the modified enzyme with proper controls.

Effect of temperature

Time course of the effect of temperature on α-mannosidase was carried out by incubating the enzyme (20 µg) in the temperature range of 35-70 °C for 2 h. Aliquots were removed after every 20 min interval and assayed for the enzyme activity under standard assay conditions. Activity at 0 min and at 25 °C was taken as 100%.

Differential Scanning Calorimetry (DSC)

DSC measurements were made on a MicroCal VP-DSC differential scanning calorimeter (MicroCal LLC, Northampton, MA, USA) equipped with two fixed cells, a reference cell and a sample cell. DSC experiments were carried out as a function of pH. Samples were dialyzed extensively against buffers of desired pH before recording the thermograms. Buffer and protein solutions were degassed before loading. All the data were analyzed by using the Origin DSC software provided by the manufacturer.

Effect of EDTA and β-mercaptoethanol

Jbα-man (20 μg) was treated with EDTA (10 mM) for 24 h. Aliquots were removed after 3, 5, 7 and 24 h, respectively and assayed for the enzyme activity. The enzyme sample incubated with 10 mM EDTA for 24 h was used for fluorescence and CD measurements as described above. The protein concentration used was 100 and 125 μg/ml, respectively. Reactivation and refolding was checked by incubating 24 h treated enzyme with 2mM Zn^{2+} ions for 30 min and then assaying the enzyme activity as well as performing the fluorescence and CD measurements.

For thermal stability studies, the protein sample (125 μg/ml) and the sample treated with EDTA (10 mM) were incubated at specified temperature for 10 min and then the CD measurements were performed as described above.

Similarly, Jbα-man treated with β-ME (5 mM) at pH 5, 7, 9 and 11 was checked for enzyme activity, fluorescence and CD measurements.

SDS-PAGE was run for both β-ME treated and untreated Jbα-man (20 μg) to determine whether the subunits are limked by the disulfide bonds and also the active quaternary structure of the enzyme.

Dynamic Light Scattering (DLS) studies

The protein solution (250 μg/ml) incubated at 28 °C and in presence of 5 mM β-ME and SDS incubated at 28 °C as well as boiled was subjected to particle size analysis at 28 °C on a Brookhaven 90 plus particle size analyzer.

Determination of free and total cysteine content

The enzyme sample (75 μg) was used for the determination of free and total cysteine content according to the method of Habeeb (14) using 5,5'-dithiobis-2-nitrobenzoic acid (DTNB) as the modifying reagent.

Substrate kinetics

K_m and V_{max} of α-mannosidase for both the substrates pNPαMan and 4-MeUmbαMan were determined by Michelis-Menten method at different temperatures ranging from 30 to 45 °C by varying the substrate concentrations. The activity of the enzyme was expressed as units/ mg/min. The K_{cat} was expressed as V_{max}/µmole of the enzyme/min. The activation energy, E_a for both the substrates was calculated from the slope of the plot of ln V_{max} vs 1000/T, as E_a = -slope x R (R, universal gas constant = 8.314 x 10^{-3} kJ/mol). ΔG was calculated by using the equation, $\Delta G = RT\ln K_d$ (here, the values of K_m were used for dissociation constant K_d).

Inhibition kinetics

α-mannosidase (3 µg) was incubated with inhibitor, swainsonine (20-300 nM) in 50 mM CPB of pH 5.0 and 250 µM as well as 500 µM pNPαMan in a total reaction volume of 0.5 ml in the temperature range of 30-45 °C for 15 min. The reaction was stopped by adding 1 ml of 1 M Na_2CO_3. Dixon plots (15) were used to determine the K_i. ΔH was calculated from the slope of the plot of ln K_a vs 1000/T. ΔG was calculated by using the equation, $\Delta G = -RT\ln K_a$ (here, the values of $1/K_i$ were used for binding constant K_a). ΔS was calculated by using the equation, $\Delta G = \Delta H - T\Delta S$.

Results and Discussion

Effect of pH

The Jbα-man showed maximum activity at pH 5.0 at 45°C. The stability of the enzyme was checked at different pH at 28 °C. It was found to be stable at pH 5.0 for 1 h and slowly lost the activity, up to 55%, during 6 h. The enzyme drastically lost the activity within 30 min of incubation in the pH range of 1.0 – 3.0 (Fig. 2.1A) and substantially at pH 7.0-10.0. Interestingly, the enzyme incubated at pH 11.0 and 12.0 showed 30% increase in the activity, compared to that incubated at pH 5.0. To study the active site geometry of the enzyme at pH 11.0 and 12.0, chemical modification of the enzyme was taken up.

Site specific modification of the enzyme at pH 11.0 by citraconic anhydride (inset Fig. 2.1B) led to the progressive inactivation of the enzyme with increasing concentration of the reagent and incubation time. The presence of single free amino group (Fig. 2.1B) at the active site was further confirmed by substrate protection and reactivation reaction at pH 5.0, showing about 85 % and 90 % regain in the activity, respectively. The K_m and V_{max} values of the citraconic anhydride modified enzyme were altered to 3.85 mM and 1.56 U/mg/min from 2.70 mM and 2.13 U/mg/min, respectively, indicating participation of the free amino group in stabilizing the catalytic geometry of the active site at pH 11.0 and 12.0. Thus, pseudo first order kinetics of the modification of the enzyme with citraconic anhydride, reactivation at pH 5.0, protection by substrate and favourable changes in the K_m and V_{max} values of the modified enzyme do indicate the presence of free amino group at or near the active site. This could be conferring the stability to the active site geometry of the enzyme. This conformation at pH 11.0 and 12.0 is stabilized in such a way that the enzyme can utilize even more substrate than after incubation at pH 5.0 leading to activation in that pH range.

Drastic loss in the secondary structure of Jbα-man, incubated in the pH range of 1.0 to 3.0 (Fig. 2.1C) was observed as shown in the far UV CD spectra. The total loss of activity in this pH range can be correlated with the collapse of the secondary structure.

The hydrophobic amino acids were also exposed to the surface in this pH range as the protein did bind ANS with increase in fluorescence intensity and blue shift in emission maximum, the effect being more pronounced at pH 1.0. The secondary structure of Jbα-man was almost intact in the alkaline conditions (pH 8-12) as shown in the far UV CD spectra (Fig. 1C). Nevertheless, the activation and unusual stability of Jbα-man in the pH range of 11.0 to 12.0 was probably due to the free amino group stabilizing the active site.

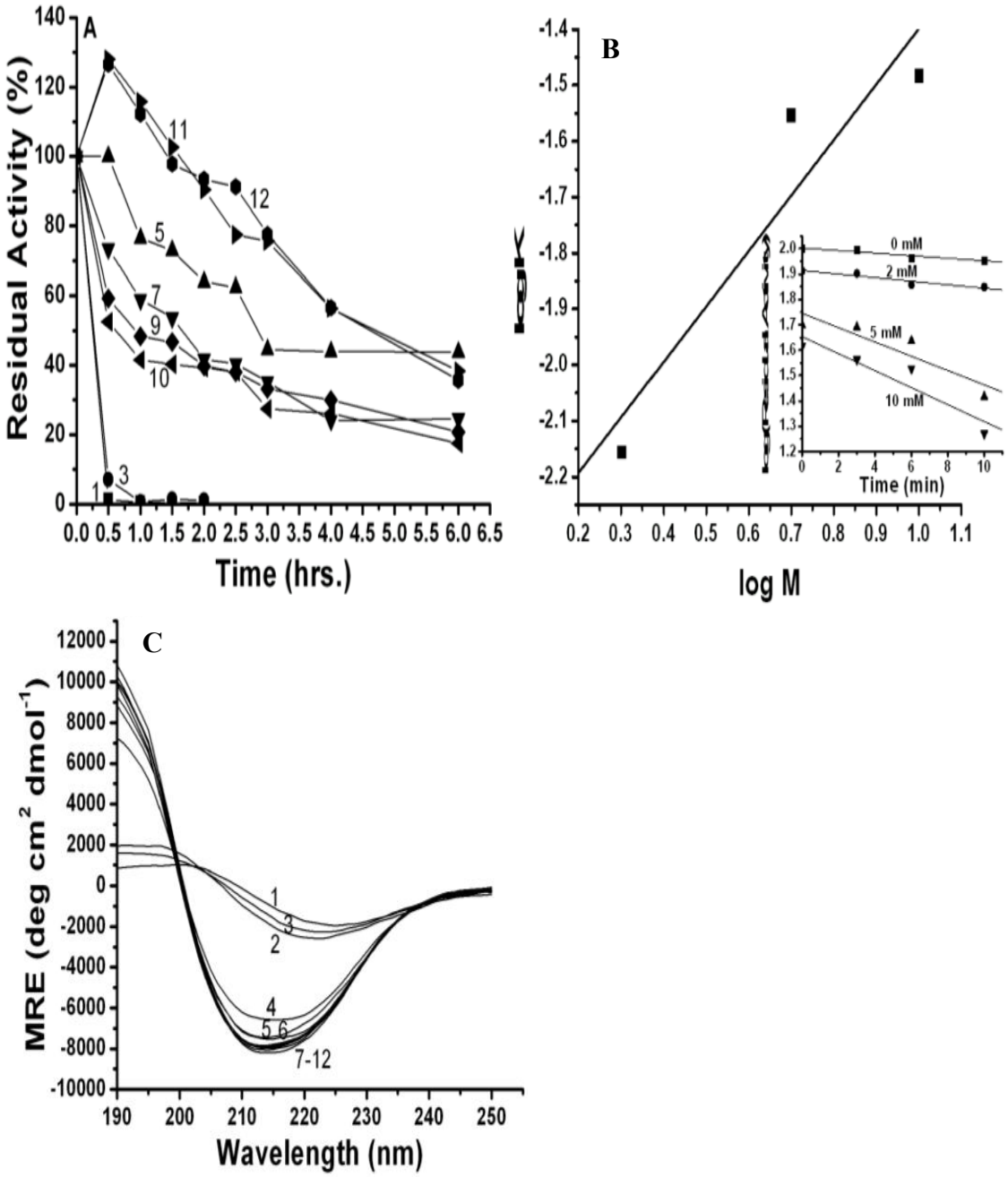

Fig. 2.1: Stability of Jbα-man at different pH. *(A)Jbα-man (20 µg) was incubated at different pH at 25 °C. The aliquots were removed and the assay was carried out. The numbers on the lines indicate the pH. (B) Determination of number of lysine residues at active site, inset: Citraconic anhydride modification of Jbα-man (3 µg) at 25 °C at pH 11.0. (B) Far UV CD spectra of Jbα-man (125 µg/ml) incubated at different pH at 25 °C for 4 h. The numbers on the lines indicate the pH.*

Effect of temperature

The thermal stability of Jbα-man was examined in the temperature range of 35-70 °C (Fig. 2.2A). The enzyme retained almost 50% activity after 2 h at 55 °C. At 55 °C and above, the inactivation of the enzyme within first 20 min was drastic and was slow later on up to 2 h. The Mean Residue Ellipticity (MRE) of the native enzyme at 219nm observed in the far UV CD spectra was decreased by 13% at 70 °C (Fig. 2.2B) indicating that it could be the perturbance in the active site and not the distortion of the β-sheet region which leads to inactivation of the enzyme at and above 55 °C.

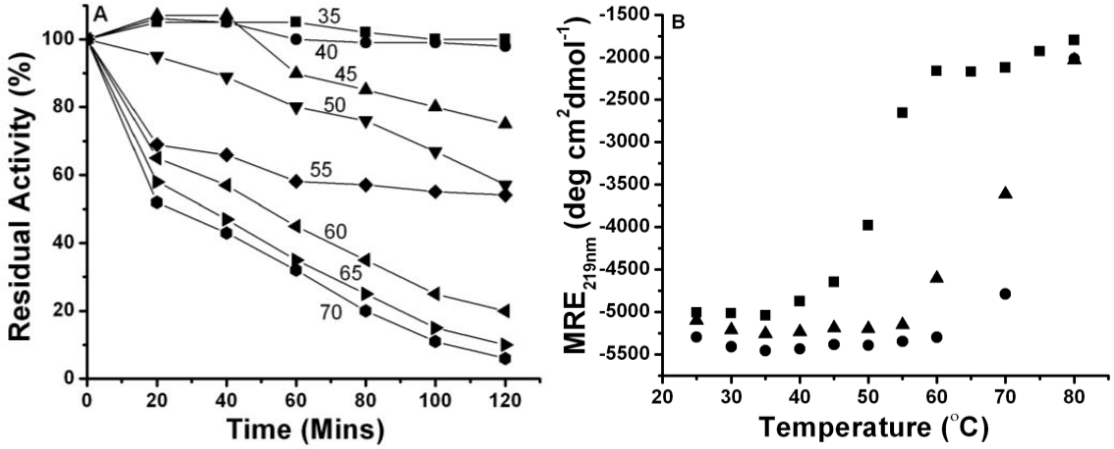

Fig. 2.2: Thermal stability of Jbα-man. *(A) Time course of thermal inactivation of Jbα-man (20 µg) incubated at 35-70 °C for 2 h. The aliquots were removed after specific time interval and assay was carried out. The numbers on the lines indicate the temperature in °C. (B) The MRE of Jbα-man (125 µg/ml) at 219 nm after 10 min incubation at temperatures from 25-80 °C: native enzyme (●), enzyme after 24 h incubation in absence (▲) and presence of 10 mM EDTA (■).*

with the fit of the single transition peak data to a non- two-state transition model is given (Fig. 2.3). Both two state method and non-two-state method use the Levenberg–Marquardt non-linear least square method. The two-state model gives calorimetric enthalpy (ΔH_c) change and the thermal mid-point of transition (T_m), whereas the non-two state model gives van't Hoff enthalpy (ΔH_v) in addition to calorimetric enthalpy and thermal mid-point of transition.

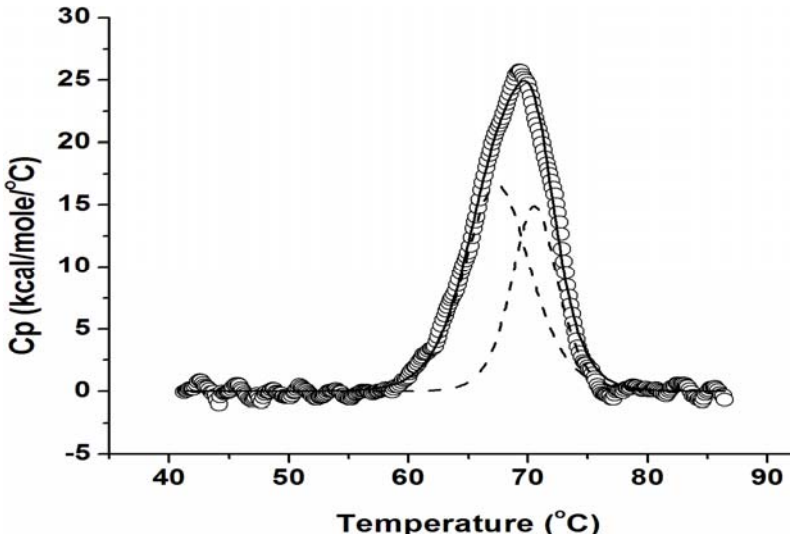

Fig 2.3: DSC thermogram of Jbα-man in 20 mM Glycine-NaOH at pH 11.0. *The scan rate was 30 K h^{-1}. The data points are shown as open circles, and the solid lines are the best fits of the DSC data to the non two state transition model. Protein concentration used was 0.0042 mM*

Table 2.1(A) shows the DSC data obtained for the thermal transition of Jbα-man at different pH (5.0-11.0). CD studies in this pH range (Fig. 2.1C) show that the secondary structure of Jbα-man are very similar, indicating that Jbα-man is stable over this wide range of pH. At pH 5.0, 7.0 and 9.0, the protein precipitated and so the calorimetric data could not be satisfactorily fit by a non-two-state, two-peak model. From the data presented in Table 2.1(A) it is seen that at pH 5.0 the T_m is 342.8 K, which slightly increases with pH up to pH 9.0. Up on treatment with the inhibitor, swainsonine at pH 5.0, the enzyme showed an increase in thermal stability as shown by the shift in T_m to 354.9 K.

At pH 11.0, the calorimetric data could be satisfactorily fit by a non-two-state, two-peak model. The T_{m1} and T_{m2} values were 340.4 and 343.5 K, respectively. The ratio of $\Delta H_{c1}/\Delta H_{v1}$ was 0.98 and the ratio of $\Delta H_{c2}/\Delta H_{v2}$ was 0.43, (Table 2.1(B)) indicating that the monomers start to unfold first followed by the unfolding of the complete oligomer.

Table 2.1(A): *Thermodynamic parameters from DSC measurements on the thermal transition of Jbα-man as a function of pH*

pH	T_m (K)
5	342.8
7	344.8
9	345.4
11	342.4
5+Swn*	354.9

**SWN - swainsonine*

Table 2.1(B): *Thermodynamic parameters from DSC measurements on the thermal transition of Jbα-man at pH11.0.*

pH	T_m	T_{m1} (K)	ΔH_{c1} (kJ mol^{-1})	ΔH_{v1} (kJ mol^{-1})	T_{m2} (K)	ΔH_{c2} (kJ mol^{-1})	ΔH_{v2} (kJ mol^{-1})	$\Delta H_{c1}/\Delta H_{v1}$	$\Delta H_{c2}/\Delta H_{v2}$
11	342.4	340.4	122.5	125.2	343.5	76.36	183.3	0.98	0.42

Effect of EDTA

Since, Jbα-man is a metalloenzyme (4), the role of Zn^{2+} ions in the catalysis and stabilization of the conformation of the protein was investigated using EDTA. The metal ion seemed to be tightly bound to the protein, as the enzyme retained 34 % activity in presence of 10 mM EDTA even after 24 h. Significant amount of activity (84 %) was regained by adding 2 mM Zn^{2+} ions to the reaction mixture. The conformational changes in the protein in presence of EDTA after 24 h as observed in fluorescence and CD spectroscopy were, 40% increase in the fluorescence intensity (Fig. 2.4A) indicating change in the microenvironment of trp and 15% loss in the negative ellipticity (Fig. 2.4B) indicating some loss in the secondary structure. Both the

changes were recovered after addition of 2 mM Zn^{2+} ions to the reaction mix (Fig. 2.4A and B).

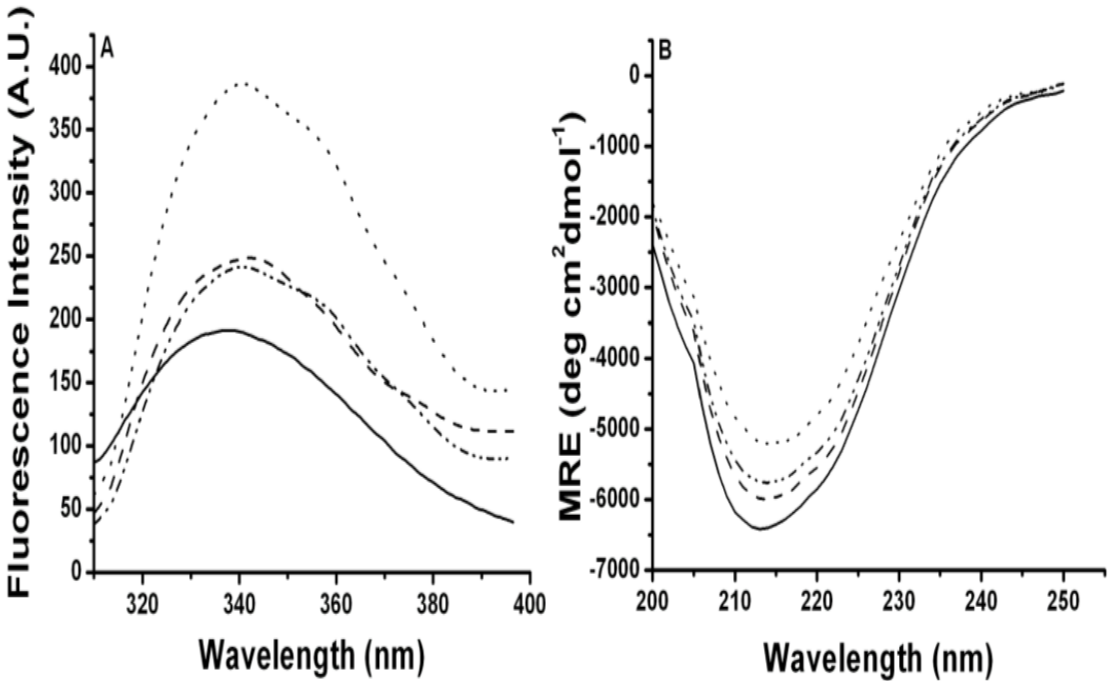

Fig. 2.4: Effect of EDTA on the conformation of Jbα-man. *(A) Fluorescence spectra of Jbα-man (100 µg/ml) and (B) far UV CD spectra of Jbα-man (125 µg/ml) incubated for 20 mins (—), 24 h (----), 24 h with 10 mM EDTA (....) and 24 h treated with 10 mM EDTA and reactivated with 2 mM Zn^{2+} ions (-..-).*

The EDTA treated enzyme was also checked for thermal stability in the temperature range of 25-80 °C. The metal chelated enzyme started losing the structure at 50 °C, while the native protein retained the structure up to 60 °C (Fig. 2.2B), indicating that the metal ion is important for properly folded structure of the enzyme.

Effect of β-mercaptoethanol

Jbα-man consists of three free cysteine residues in the native condition and showed eleven after reduction of the denatured protein as determined by DTNB modification. Four disulfide linkages could be deduced from the data, which can be inter subunit or some of them can be intra subunit linkages. Either all or few of these disulfide linkages

along with non-covalent interactions bring about the association of the unidentical subunits to constitute the active site of the enzyme.

Jbα-man was treated with 5 mM β-ME in duplicate. One of the samples was boiled for 10 min and the other was incubated at 28 °C for 10 min. Both the samples were subjected to SDS-PAGE, stained for activity using 4-MeUmbα-man and then for protein using the silver staining method. The sample incubated at room temperature showed a fluorescent band around 115 kDa indicating active enzyme (Fig. 2.5A). After protein staining one prominent band around 115 kDa and two faint bands around 66 and 49 kDa were observed (Fig. 2.5B). The boiled sample on the other hand showed two protein bands around 66 and 49 kDa (Fig. 2.5B). The enzyme not treated with β-ME showed only single band with fluorescence indicating activity (lane 1 Fig. 2.5B).

Thus, the active oligomer for Jbα-man is a dimer formed by association of unidentical monomers of 66 kDa and 49 kDa. The active site seems to be constituted by the association of the two unidentical subunits. Besides non-covalent interactions such as ionic and hydrophobic, this association also seems to contain disulfide linkages. The native Jbα-man as reported is a 230 kDa protein (6). Our studies indicate it to be a dimer of active dimers of 115 kDa which are formed by the association of the 66 and 49 kDa monomers through disulfide linkages in addition to the non covalent interactions. Under native conditions, there is little effect of the reducing agent. The disulfides are reduced and subunits are separated only after boiling the reaction mixture.

Both the samples were also subjected to DLS analysis. The sample treated with β-ME and SDS and incubated at 28 °C showed mean hydrodynamic diameter of 4.5 nm as compared to the native enzyme which showed mean hydrodynamic diameter of 22.9 nm. The sample treated with β-ME and SDS and boiled showed mean hydrodynamic diameter of 2.6 nm. The reduction in mean hydrodynamic diameter upon treatment with β-ME at 28 °C and further reduction in mean hydrodynamic diameter up on boiling again suggests that the native enzyme exists as a dimer of active dimers formed with

disulfide linked monomers and the disulfide bonds are reduced and subunits separated only after boiling.

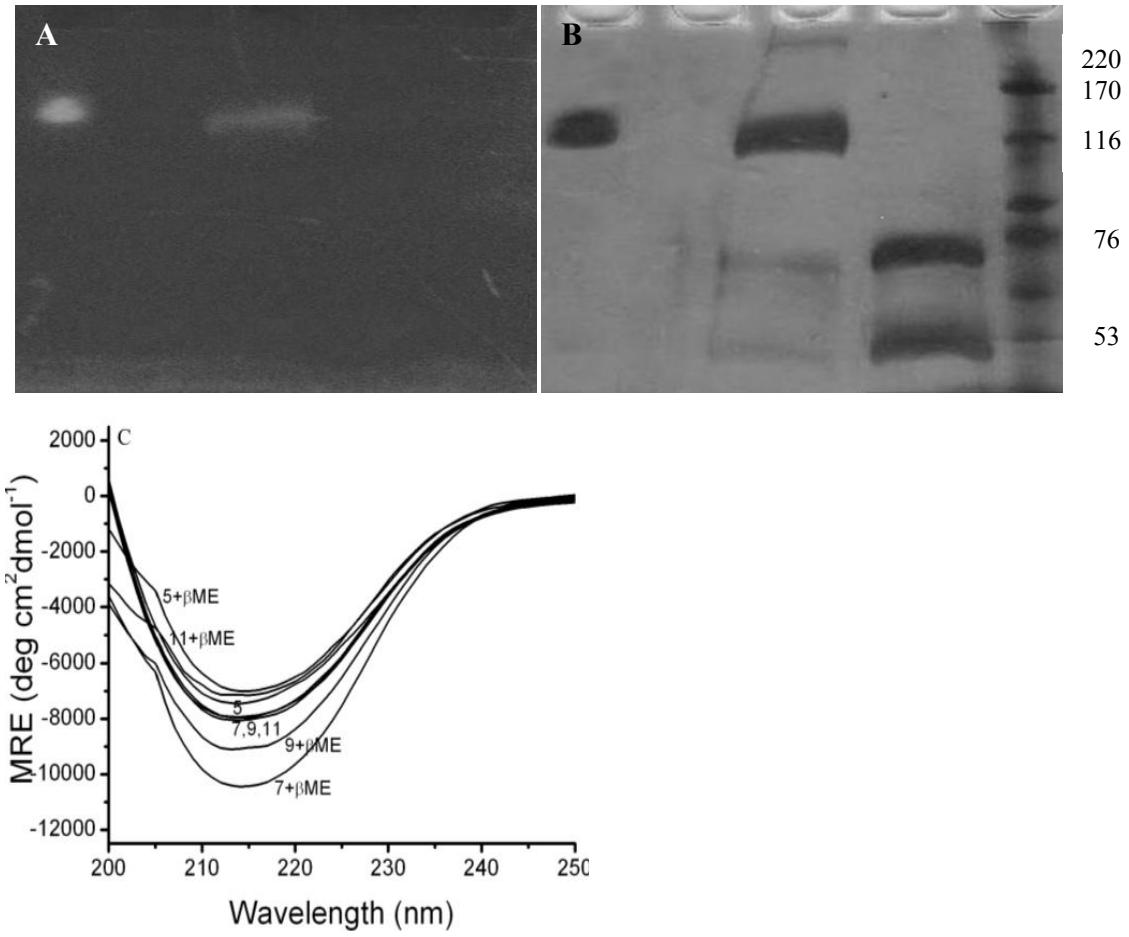

***Fig. 2.5**: **SDS-PAGE of Jbα-man.** (A) Activity staining and (B) silver staining : The protein (20 µg) incubated at room temperature in absence (lane 1) and presence of β-ME (lane 3), boiled in presence of β-ME (lane 4) and molecular weight markers (lane 5). The numbers indicate the molecular weight of the marker bands. (C) Far UV CD spectra of Jbα-man (125 µg/ml) at pH 5.0, 7.0, 9.0 and 11.0 in absence and in presence of 5 mM β-ME. The numbers on the lines indicate pH.*

The effect of β-ME on the conformation and activity of the enzyme was also investigated in the pH range of 5.0 – 11.0. The treatment led to some alteration in the secondary structure (Fig. 2.5C), still retaining the activity of the enzyme. The positive

ellipticity of Jbα-man at 200 nm was decreased in the pH range of 7.0 – 11.0 in presence of β-ME, indicating some rearrangement in the secondary structure. Also, increase in the negative ellipticity observed in the range of 210 – 225 nm at pH 7.0 – 9.0 indicated more compact secondary structure of Jbα-man after the treatment with β-ME.

As mentioned above, the interchain disulfide bonds between 66 and 49 kDa subunits are reduced only after boiling. Probably the reduction of intrachain disulfide bonds at 28 °C could be leading to the rearrangement in the secondary structure.

Substrate kinetics

The K_m and V_{max} of Jbα-man were determined at different temperatures with pNPαman or 4-MeUmbαman. The K_m and V_{max} values were calculated from Michaelis- Menten plots for each substrate at each temperature. The K_m of the enzyme for 4- MeUmbαman (10.52 μM) (Fig. 2.6A) was found to be 200 times lower than that for pNPαman (2.1 mM) (Fig. 2.6B), indicating stronger affinity of the enzyme for 4- MeUmbαman. The specificity constant, K_{cat}/K_m values of pNPαman and 4-MeUmbαman at 45 °C were 41,285 and 485,266 M-1min-1, respectively, indicating higher reaction rate of the enzyme for the substrate 4-MeUmbαman (Table 2.2).

From the slope of the plot of ln Vmax versus 1000/T (Fig. 2.6C), energy of activation (E_a) was calculated as 31.9 kJ mol-1 for pNPαman and 26.7 kJ mol^{-1} for 4-MeUmbαman (Table 2.2).

E_a of Jbα-man using 4-MeUmbαman is three times more as compared to that of the fungal α-mannosidase from *Aspergillus fischeri* (10). This could be due to some constraints of Jbα-man for the substrate to access the active site and also due to slightly hydrophobic surface of the protein.

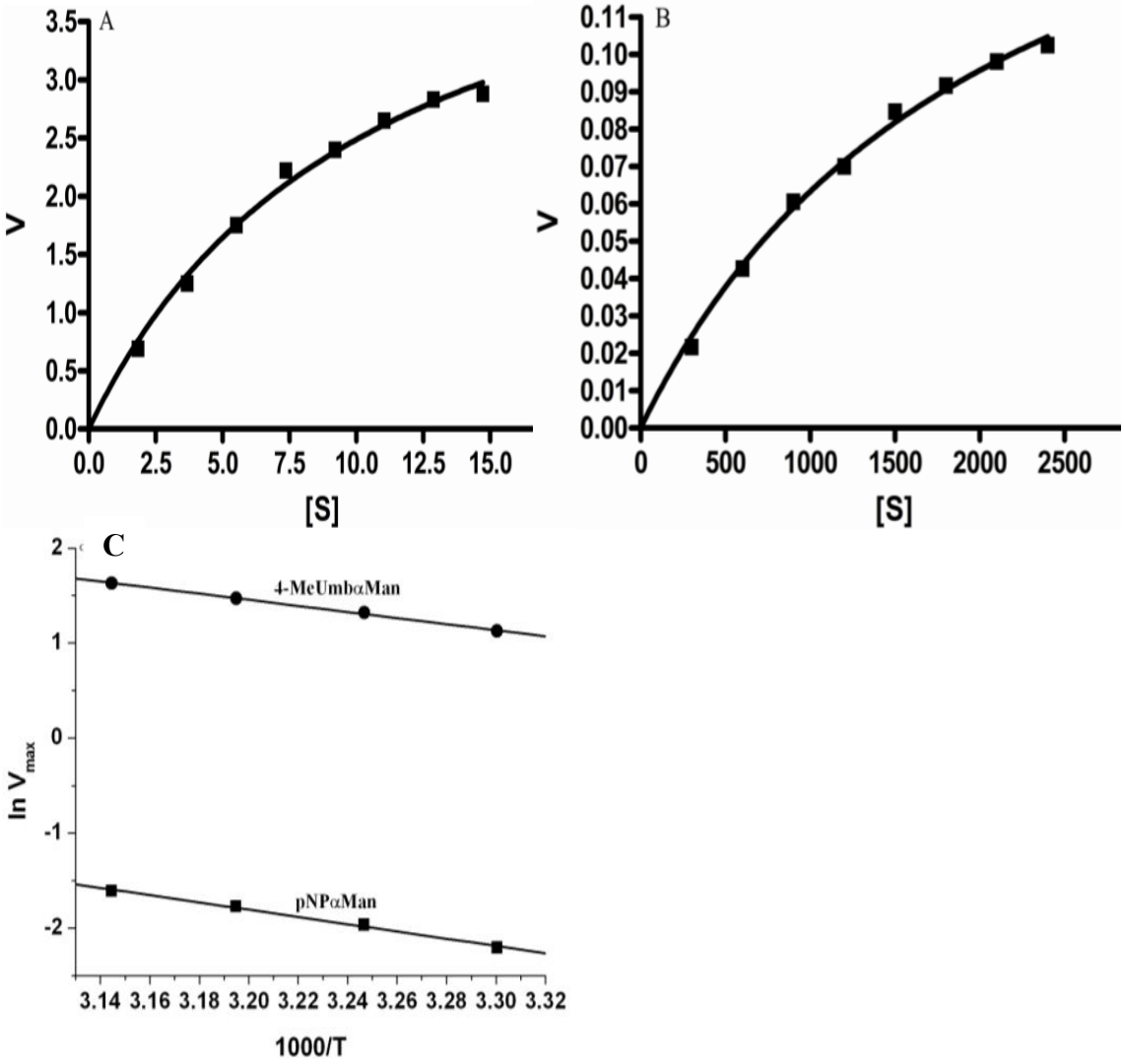

Fig. 2.6: Determination of K_m, V_{max} and Activation Energy (E_a) of Jbα-man. *Determination of K_m and V_{max} of Jbα-man with (A) 4-MeUmbαMan and (B) pNPαMan. V is expressed as U/mg/min and (S) is expressed as µM. (C) Activation energy (E_a) of Jbα-man with 4-MeUmbαman and pNpαman. The protein used was 3 µg for pNpαman and 30 ng for 4-MeUmbαman.*

Inhibition kinetics

Swainsonine is a potential anticancer molecule and known inhibitor of class II α-mannosidases. Inhibition kinetics indicated strong inhibition of Jbα-man with swainsonine (K_i = 53.0 nM) (Fig. 2.7A), which could be due to the close analogy with the substrate.

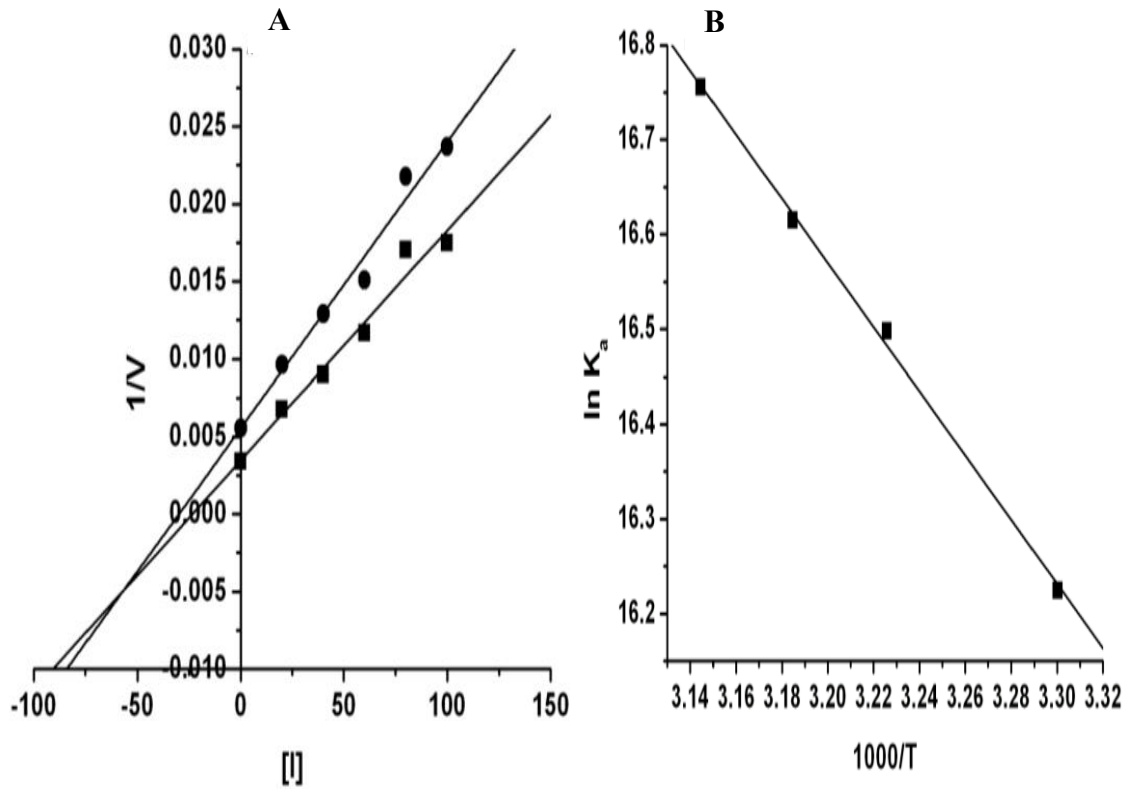

Fig. 2.7: Determination of Ki and thermodynamic parameters of swainsonine binding to Jbα-man. *(A) Determination of Ki of Jbα-man (3 µg) with swainsonine. Substrate used was 250 µM (●) and 500 µM (■) pNpαman. (I) is expressed as nM. (B) Determination of ΔG, ΔH and ΔS of swainsonine binding to Jbα-man (3 µg).*

To determine the thermodynamic parameters, the inhibition kinetics was carried out at different temperatures ranging from 30-45 °C. The decrease in the value of K_i with increase in temperature from 30 to 45 °C (Table 2.2) indicated strong binding of the inhibitor at the optimum temperature i.e., in the most reactive state of the enzyme.

1-deoxymannojirimycin, inhibitor of class I α-mannosidase did not inhibit Jbα-man activity even up to 800 µM concentration. α-mannosidase from *Aspergillus fischeri* showed much higher K_i for swainsonine, 101 µM and lower K_i for 1-deoxymannojirimycin, 284 µM indicating different geometry of the active site although it is a class II α-mannosidase (10).

The positive value of ΔH, 28.14 kJ mol^{-1} (Fig. 2.7B), indicated endothermic reaction. Also, positive value of ΔS (Table 2.2), 228 J mol^{-1} K^{-1} could be due to the increase in entropy caused by release of water molecules from active site of the enzyme as well as from the inhibitor, after binding of swainsonine to the enzyme. The decrease in entropy due to binding could be less than the effective increase in entropy, indicating that the binding of inhibitor to the enzyme is entropy driven process.

***Table 2.2**: Energetics of catalysis and inhibition of Jbα-man.*

Substrate	**K_{cat}/K_m ($M^{-1}min^{-1}$)**				**E_a (kJ mol^{-1})**	**K_m**	**ΔG (kJ mol^{-1})**
pNPαman	41285				31.9	2.10 mM	-16.30
4-MeUmbαman	485266				26.7	10.52 µM	-30.31
Inhibitor	**K_a x 10^7 (M^{-1})[a]**				**ΔG (kJ mol^{-1})**	**ΔH (kJ mol^{-1})**	**ΔS (J mol^{-1})**
	30°C	**35°C**	**40°C**	**45°C**			
Swainsonine	1.11	1.46	1.64	1.89	-44.30	28.14	228

[a] K_a values were expressed as $1/K_i$.

The difference in the characteristics like pH optimum, stability at extreme alkaline pH, bound metal ion, quaternary structure with unidentical subunits, presence of disulfide linkages and activation energy of the present enzyme from the plant source do differentiate it from the same class II enzyme from a fungal source (13).

References

1. Henrissat, B. and Davies, G. 1997. *Curr Opin Struct Biol* **7**: 637-644.
2. Daniel, P.F., Winchester, B. and Warren, C.D. 1995. *Glycobiology* **4**: 551-556.
3. Goss, P.E., Reid, C.L., Bailey, D. and Dennis, J.W. 1997. *Clin Cancer Res* **3**: 1077–1086.
4. Dennis, J.W., Granovsky, M. and Warren, C.E. 1999. *Biochem Biophys Acta* **1473**: 21–34.
5. Snaith, S.M. 1975. *Biochem J* **147**: 83-90.
6. Snaith, S.M. and Levvy, G.A. 1968. *Biochem J* **110**: 663-670.
7. Kang, M.S. and Elbein, A.D. 1983. *Plant Physiol* **71**: 551-554.
8. Howard, S., He, S. and Withers, S.G. 1998. *J Biol Chem* **273**: 2067- 2072.
9. Kumar, A. and Gaikwad, S.M. 2010. *Biochem Biophys Res Commun* **403**: 391-397.
10. Shashidhara, K.S. and Gaikwad, S.M. (2009) *Int J Biol Macromol* **44**: 112-115.
11. Shashidhara, K.S. and Gaikwad, S.M. (2010) *J Fluoresc* **20**: 827-836.
12. Shashidhara, K.S. and Gaikwad, S.M. (2007) *J Fluoresc* **7**: 559-605.
13. Gaikwad, S.M., Keskar, S.S. and Khan, M.I. 1995. *Biochem Biophys Acta* **1250**: 144-148.
14. Habeeb, A.F.S.A. 1972. *Methods Enzymol* **25**: 457-464.
15. Dixon, M. 1953. *Biochem J* **55**: 170-171.

CHAPTER 3

UNFOLDING STUDIES OF A CLASS II α-MANNOSIDASE FROM *CANAVALIA ENSIFORMIS* (JACK BEAN)

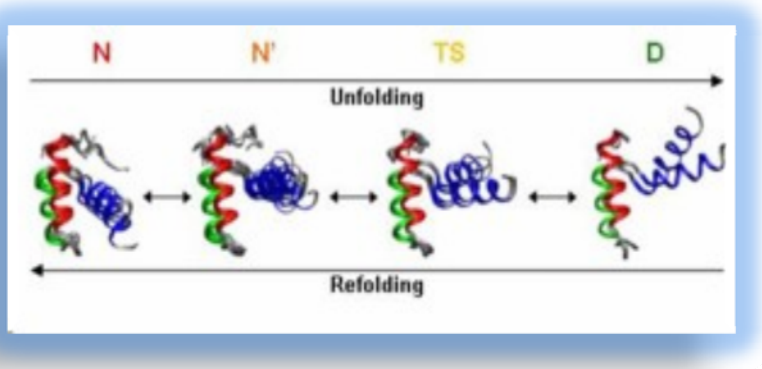

Avinash Kumar and Sushama M. Gaikwad (2010) Multistate unfolding of α-mannosidase from Canavalia ensiformis (Jack Bean): Evidence for the thermostable molten globule. Biochem Biophys Res Commun 403: 391-397

Summary

The relevance of partially ordered states of proteins (such as the molten globule state) in cellular processes is beginning to be understood. We examined the conformational transitions in a multimeric and high molecular weight class II α-mannosidase from *Canavalia ensiformis* (Jack Bean) (Jbα-man) utilizing intrinsic fluorescence, solute quenching, hydrophobic dye binding, size exclusion chromatography and circular dichroism (CD) spectroscopy for the protein in presence of Guanidine hydrochloride (GdnHCl). The decomposition analysis of the protein spectra obtained during unfolding showed progressive appearance of class S, I, II and III trp. The parameter A and spectral center of mass showed multi state unfolding of the protein and phase diagram analysis revealed formation of an intermediate of Jbα-man in the vicinity of 1 M GdnHCl. The intermediate exhibited compact secondary and distorted tertiary structure with exposed hydrophobic amino acids on the surface, indicating the molten-globule nature. The dissociation, partial unfolding and aggregation of Jbα-man occurred simultaneously during chemical denaturation. The molten-globule possessed slightly higher hydrodynamic radius, perturbance in the structure up to 60 °C and stability of the structure up to 80 °C unlike the native jack bean α-mannosidase. The modes of chemical and thermal denaturation of the native protein were different. The solute quenching parameters confirmed the altered confirmation of the intermediate. Time resolved fluorescence studies showed two different lifetimes for both native and denatured protein. Quenching of the fluorescence of the denatured protein by acrylamide involved both static (K_s=7.39 M^{-1}) and collisional (K_{sv}=3.12 M^{-1}) components. Taken together, our results constitute one of the early reports of formation of GdnHCl induced molten globule in a class II α-mannosidase.

Introduction

An important enzyme of the N-linked glycosylation pathway which catalyzes the hydrolysis of terminal non-reducing mannose residues in mannans is an exoglycosidase, known as α-mannosidase (α-mannoside mannohydrolase, E.C. 3.2.1.24. The distribution of the N-linked sugars on the cell surface is altered in many

tumor cell lines like those from breast, skin and colon cancer (1) and therefore the enzymes of this glycosylation pathway are potential targets for development of inhibitors as anticancer agents. A well known inhibitor of α-mannosidase, swainsonine, in early clinical trials was found to reduce the growth of tumors and metastasis (2). The deficiency of this enzyme also causes a fatal disease, mannosidosis in humans and cattle (3).

Study of the partly folded conformations is important to understand the principles governing the protein folding process (4, 5). Misfolded proteins sometimes do lead to aggregation, a phenomenon associated with many neurodegenerative diseases such as amyloidoses, prion disease and cataracts, that are caused by non-specific protein interactions (6). The best way to understand this is to monitor the protein unfolding mediated by a chaotropic agent such as Guanidine hydrochloride (GdnHCl) as it can transform proteins into a more or less completely unfolded state (7). There are reports on existence of GdnHCl induced molten globule like intermediates (8-10) but are very few in comparison to the acid induced molten globules. We have already reported an acid induced molten globule in a class II α-mannosidase from *Aspergillus fischeri* (11).

The Jbα-man has already been purified from Jack Bean meal and characterized (12-15). Although a commercially available enzyme, it has not been characterized structurally, nor has its primary sequence been determined.

In the present chapter, as a step towards its structural characterization, the Jbα-man was subjected to denaturation with GdnHCl and transitions in the structure were monitored by biophysical techniques to understand its conformational stability. We also report the existence and characterization of a molten-globule like intermediate in the vicinity of 1M GdnHCl concentration.

Materials and methods

Materials

α-mannosidase from *Canavalia ensiformis* (Jack Bean) (Jbα-man), N-bromosuccinimide (NBS), Guanidine hydrochloride (GdnHCl) and 1-anilino-8-naphthalenesulfonate (ANS) were obtained from Sigma Aldrich Ltd., USA. All other reagents used were of analytical grade. Solutions prepared for spectroscopic measurements were in MilliQ water.

Preparation of Jbα-man

Jbα-man was reconstituted in 20mM citrate phosphate buffer (CPB), pH 5.0 and dialyzed against the same buffer. Enzyme samples for spectroscopic measurement were spun, filtered through a 0.22 μm filter and the protein concentration was determined by the method of Lowry *et al.* before taking measurement.

Modification of Trp residue with N-bromosuccinimide (NBS)

The modification of Jbα-man with NBS was carried out under native and denaturing (in presence of 6 M GdnHCl) conditions and the number of trp residues modified were determined spectrophotometrically, assuming the molar absorption coefficient of 5,500 $M^{-1}cm^{-1}$ for the modified Trp at 280 nm (16).

Enzyme assay

The α-mannosidase activity was estimated with pNP-α-mannopyranoside (pNPαMan) according to the procedure described in enzyme assay section of Materials and Methods of chapter 2.

Steady state fluorescence measurements

Steady state fluorescence measurements were performed according to the procedure described in steady state fluorescence measurements section of Materials and Methods of chapter 2.

Protein samples (100 µg/ml) were incubated in 0-6 M GdnHCl solution at pH 5.0 for 2 h to attain the equilibrium. Fluorescence spectra were recorded as described above. After taking the scans suitable aliquots were removed from the samples to check for activity.

For refolding studies, the protein sample in 10-fold excess concentration was first denatured to equilibrium in 6 M GdnHCl at 25 °C for 2 h and subsequently diluted with denaturing buffer to the working concentration of the protein in the desired concentration of GdnHCl. Fluorescence spectra were recorded as described above.

Decomposition of fluorescence spectra

The decomposition of trp fluorescence spectra was carried out using PFAST program (http://pfast.phys.uri.edu/pfast/) developed based on the SIMS and PHREQ algorithm as described elsewhere (17, 18).

Spectral center of mass, parameter A and phase diagram analysis

The fluorescence spectra were quantified using spectral center of mass (λ_{av}, average emission wavelength) calculated as

$$\lambda_{av} = \sum \lambda I(\lambda) / \sum I(\lambda), \qquad (1)$$

Where, $I(\lambda)$ is the fluorescence intensity at wavelength λ (19).

Parameter A, the ratio of the intrinsic fluorescence intensity at 320 nm to that at 365 nm (I_{320}/I_{365}), is the characteristic of fluorescence spectral shape and position (20, 21). This analysis is often used to detect protein conformational changes and was used in this research to monitor the structural changes of Jbα-man during GdnHCl induced unfolding and refolding.

The phase diagram analysis was carried out by constructing I_{320} versus I_{365} observed at different GdnHCl concentrations. The I_{320} and I_{365} data were normalized by the corresponding intensity of the spectra recorded in buffer without the addition of GdnHCl (21, 22). In the diagram, a straight line reflects an “all or none” process, while

the non-linearity between I_{320} and I_{365} indicates that the structural transition involves folding intermediate(s). The joint position of two such straight lines indicates existence of an intermediate at the corresponding concentration of GdnHCl (18).

Time resolved fluorescence measurements

Lifetime fluorescence measurements were carried out on an FLS920 spectrometer supplied by Edinburgh Instruments. A picosecond pulsed light emitting diode (model EPLED-295) of pulse width 747.8 ps and band width 10.4 nm was used for excitation and a single photon counting photomultiplier was used for detection of fluorescence. The diluted Ludox solution was used for measuring Instrument Response Function (IRF). Protein sample at a concentration of 0.1 mg/ml was employed for this experiment. The sample was excited at 295 nm and emission was recorded at 338 nm for native and at 356 nm for denatured protein. Slit widths of 15 nm each were used on the excitation and emission monochromators. The resultant decay curve was analyzed by a multiexponential iterative fitting program provided by Edinburgh Instruments. The average life time (τ) was calculated by using the following equation: (23)

$$\tau = \sum \alpha_i \tau_i / \sum \alpha_i \qquad i = 1,2,\ldots. \qquad (2)$$

Circular Dichroism (CD) measurements

The far UV CD spectra of the enzyme were recorded and analyzed (24) according to the procedure described in circular dichroism (CD) measurements section of Materials and Methods of chapter 2.

The tertiary structure of the enzyme (800 μg/ml) was monitored with near UV CD spectra in the wavelength range of 250-300 nm using cell of path length 1 cm.

ANS binding studies

The ANS binding studies were performed according to the procedure described in ANS binding studies section of Materials and Methods of chapter 2 (25).

Size exclusion chromatography

Dissociation of oligomeric Jbα-man in presence of GdnHCl was monitored using WATERS HPLC unit and WATERS gel filtration Protein Pak^{TM} 300SW, 7.5 ×300 mm column. The mobile phase used was 50 mM CPB, pH 5.0 containing respective concentration of GdnHCl. 100 µl protein samples (1 mg/ml) incubated in respective concentration of GdnHCl was injected on to the column. Flow rate kept was 0.5 ml/min and the elution profile was monitored at 280 nm.

Solute quenching studies

Fluorescence quenching experiments were carried out by the addition of a small aliquot of acrylamide, KI or CsCl stock solution (5M) to the protein solution (100 µg/ml) previously incubated in 20 mM CPB, pH 5.0 or 1 M GdnHCl, pH 5.0 at 25 °C for 2 h and the fluorescence intensities were determined.

Iodide stock solution contained 0.2 M sodium thiosulfate to prevent formation of tri-iodide (I^{-3}). For quenching studies with denatured protein, the protein was incubated with 6 M GdnHCl overnight at room temperature. Fluorescence intensities were corrected for volume changes before further analysis of quenching data.

The steady-state fluorescence quenching data obtained with different quenchers were analyzed by Stern–Volmer (Eq. 4) and modified Stern–Volmer (Eq. 5) equations in order to obtain quantitative quenching parameters (26).

$$F_o/F_c = 1+ K_{sv}[Q] \qquad (4)$$

$$F_o/\Delta F = f_a^{-1} + 1/[K_a f_a(Q)] \qquad (5)$$

where, F_o and F_c are the relative fluorescence intensities in the absence and presence of the quencher, respectively, (Q) is the quencher concentration, K_{sv} is Stern–Volmer quenching constant, $\Delta F=F_o-F_c$ is the change in fluorescence intensity at any point in the quenching titration, K_a is the quenching constant and f_a is the fraction of the total fluorophore accessible to the quencher. Eq. 4 shows that the slope of a plot of $F_o/\Delta F$ versus Q^{-1} (modified Stern–Volmer plot) gives the value of $(K_a f_a)^{-1}$ and its Y intercept gives the value of f_a^{-1}.

Time resolved fluorescence measurements for solute quenching of the denatured protein with acrylamide was also performed. The time resolved fluorescence quenching data can be analyzed by Eq. 6 by which the dynamic and the static components can be resolved (27).

$$F_0/F_c = (1+K_{sv}[Q])\,(1+K_s[Q]) \qquad (6)$$

Where Ksv is the Stern–Volmer (dynamic) quenching constant, Ks is the static quenching constant and [Q] is the quencher concentration. The dynamic quenching constant reflects the degree to which the quencher achieves the encounter distance of the fluorophore and can be determined by the fluorescence lifetime measurements according to the equation (27)

$$\tau_0/\tau = (1+K_{sv}[Q]) \qquad (7)$$

Where τ_0 is the average lifetime in absence of the quencher and τ is the lifetime in presence of a quencher at a concentration [Q].

Results and Discussion

Native as well as denatured α-mannosidase from Jack Bean (Jbα-man) yielded 1 trp/mole of the protein upon NBS modification.

Fluorescence measurements

The native Jbα-man, a single trp protein showed fluorescence spectrum with λ_{max} at 338 nm indicating trp residue in the hydrophobic environment. Decomposition analysis of the tryptophan fluorescence spectra of the native protein by PFAST (http://pfast.phys.uri.edu/pfast/) (17) indicated two classes of trp conformers; 24.8 % class S which includes buried tryptophan residue or a conformer with slight flexibility of the microenvironment and 75.2 % class II containing structured water molecules near to the indole ring of trp residue in the protein (Fig. 3.1A). For Jbα-man treated with 0.1-0.5 M GdnHCl, the analysis yielded 100 % class I trp indicating that the residue becomes slightly buried in the hydrophobic core of the protein due to minor change in the microenvironment of the trp. In presence of 1-2 M GdnHCl, 100 % class II trp was detected due to partial unfolding of the protein. The spectra of protein samples treated with 2.5-6 M GdnHCl were resolved into 100 % class III revealing the

complete exposure of trp residues to the solvent indicating maximal unfolding of the protein. The progressive appearance of class I, II, and III trp in Jbα-man in the vicinity of increasing concentration of GdnHCl indicated the unfolding of the protein.

The Jbα-man showed inactivation (20-40 %) in presence of low concentration (0.2-0.4 M) of GdnHCl. The activity was partially recovered (up to 90 %) after dilution of the GdnHCl treated Jbα-man. The inactivation could be due to the presence of carboxylate residues at the active site as shown by Kenoth *et al* and Nath *et al* (23, 28). The positively charged guanidinium group electrostatically interacts with the carboxylate group causing inactivation.

The spectral centre of mass (Fig. 3.1B) shows initial blue shift in the λ_{av} in presence of low concentration of GdnHCl which can be correlated to the appearance of class I trp in the decomposition analysis. The gradual red shift in the λ_{av} indicates multistate unfolding. The red shift of 9 nm in the λ_{max} of native Jbα-man after calculation of λ_{av} (347nm) was observed.

Parameter A, which is the ratio of the intensity at 320 nm to that at 365 nm, is regularly used to analyze the shape and position of the trp fluorescence spectra (20, 21). The parameter A data of Jbα-man confirmed the multi step unfolding process with the intermediates lying between 0.5 M and 2.5 M (Fig. 3.1C). The protein slowly denatures to partially unfolded state upto 2 M and gets almost unfolded in presence of 2.5 M GdnHCl. The denatured protein showed reversible folding upto 0.5 M GdnHCl after renaturation.

Furthermore, the phase diagram, a sensitive tool to characterize the folding intermediate(s) (21, 22) was constructed by monitoring the change of the intensity at 365 nm as a function of that at 320 nm. Two linear parts, corresponding to GdnHCl concentrations of about 0-1.0 M and 3.0-6.0 M, respectively, could be identified for the unfolding transition, again indicating the unfolding to be a multi step process, the intermediates lying in the vicinity of 1.0 M and 3.0 M GdnHCl (Fig. 3.1D).

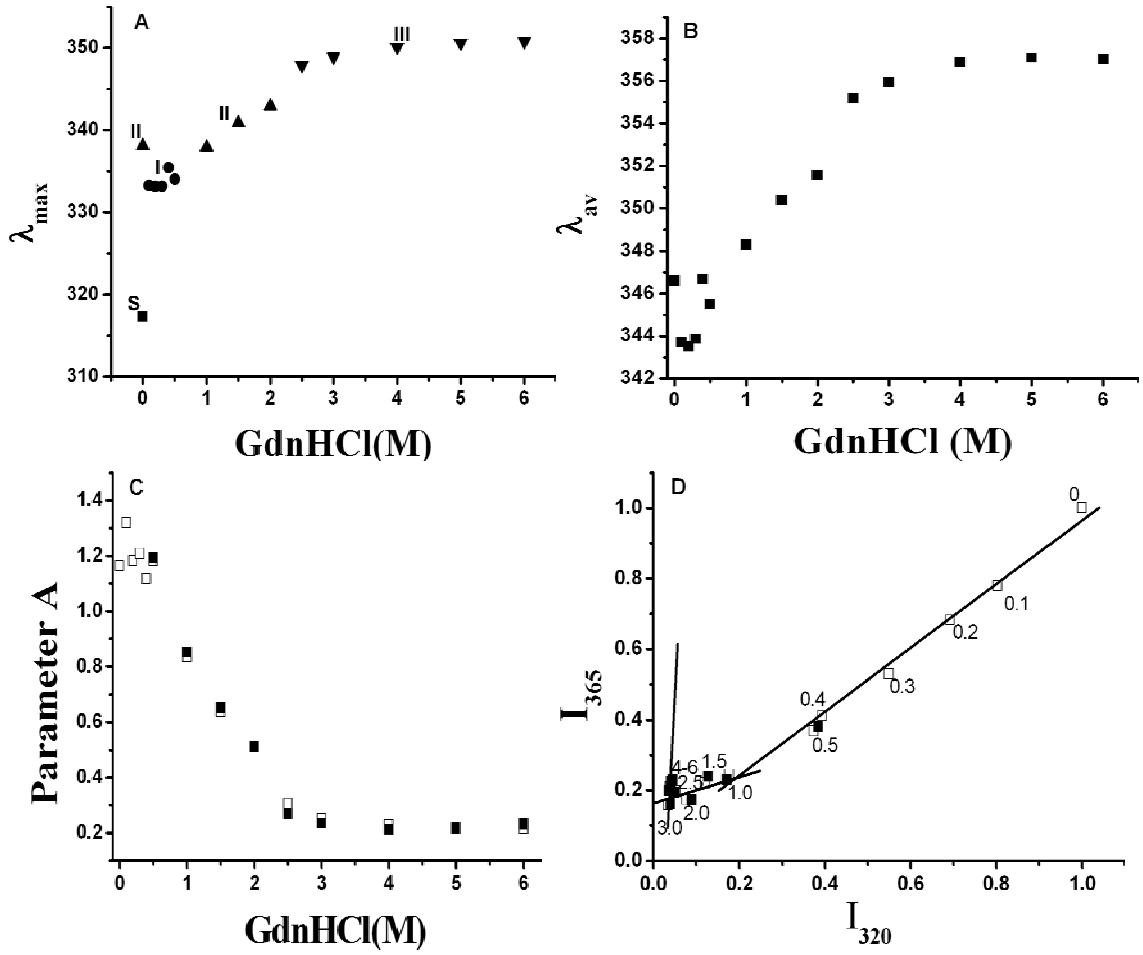

Fig. 3.1: Steady state fluorescence of Jbα-man in presence of GdnHCl. *(A) Decomposition of trp fluorescence spectra of GdnHCl treated Jbα-man (100 µg/ml) incubated in presence of different concentrations of GdnHCl at 25 °C for 2 h. The letters indicate the classes of trp obtained after PFAST analysis of the data. (B) Spectral center of mass of GdnHCl treated Jbα-man (100 µg/ml) incubated in presence of different concentrations of GdnHCl at 25 °C for 2 h. (C) Parameter A of GdnHCl treated Jbα-man (100 µg/ml) incubated in presence of different concentrations of GdnHCl at 25 °C for 2 h. (D) Phase diagram of GdnHCl treated Jbα-man (100 µg/ml) incubated in presence of different concentrations of GdnHCl at 25 °C for 2 h.*

Circular Dichroism (CD) measurements

CD pro analysis of the far UV CD spectrum of native Jbα-man (Fig. 3.2A) yielded the values of the secondary structure elements as: α-helix-8.0 %, β-sheet-35.5 %, turns-

21.1 % and unordered-34.6 %. The negative MRE of the native protein at 219 nm increased in presence of GdnHCl from 0.2-1.0 M indicating formation of more pronounced secondary structure and remained unaltered in the vicinity of 1.0-1.2 M GdnHCl indicating the formation of a stable intermediate. Increasing distortion in the secondary structure of the protein occurred in presence of GdnHCl from 2.0-4.0 M (Inset Fig. 3.2A). The non-coincidence of the fluorescence and CD data of Jbα-man in presence of various concentrations of GdnHCl confirmed the multistep unfolding.

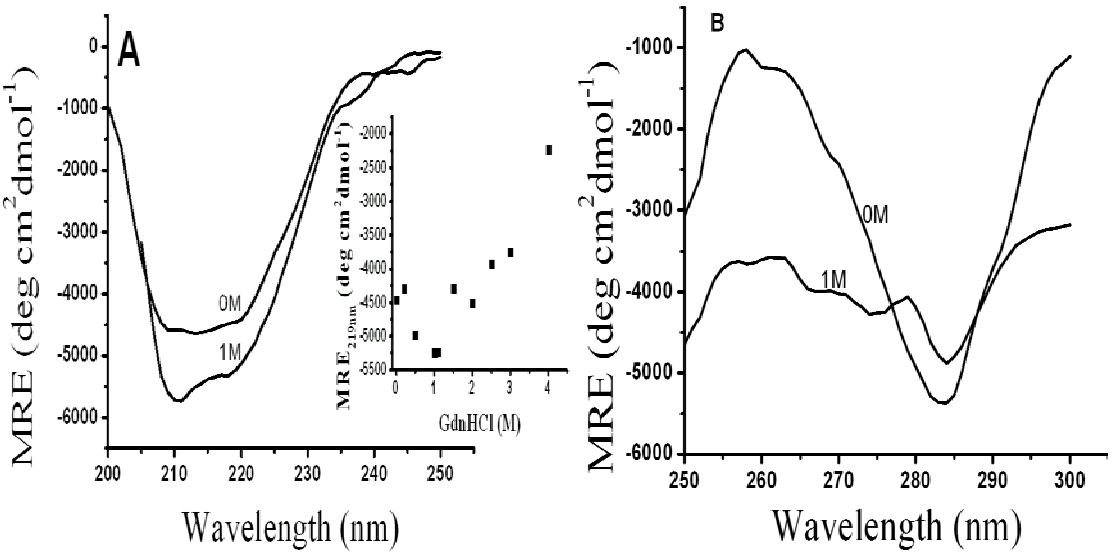

Fig. 3.2: Circular Dichroism measurements of Jbα-man in presence of GdnHCl. *(A) Far UV CD spectra of native and 1M GdnHCl treated protein (125 µg/ml), Inset: MRE at 219 nm. (B) Near UV CD spectra of native and 1M GdnHCl treated protein (800 µg/ml).*

The near UV CD spectrum of the native enzyme showed a negative minimum at 284 nm and maxima at 255 nm and 295 nm, indicating ordered tertiary structure of Jbα-man. The enzyme in the vicinity of 1 M GdnHCl showed significant reduction in the intensity of the signal (Fig. 3.2B) indicating disorganization of the tertiary structure during conversion of native to intermediate state.

ANS binding studies

ANS is a dye which has been shown to bind to hydrophobic regions in a protein and shows increased fluorescence intensity (25). The Jbα-man in different concentrations of

GdnHCl was checked for ANS binding. The protein treated with 1M GdnHCl, showed about 3 times increase in fluorescence intensity (Fig. 3.3) with blue shift of λ_{max} to 480 nm in presence of ANS, indicating exposure of hydrophobic patches on the surface of the protein. The intermediate seemed to possess a molten globule like structure.

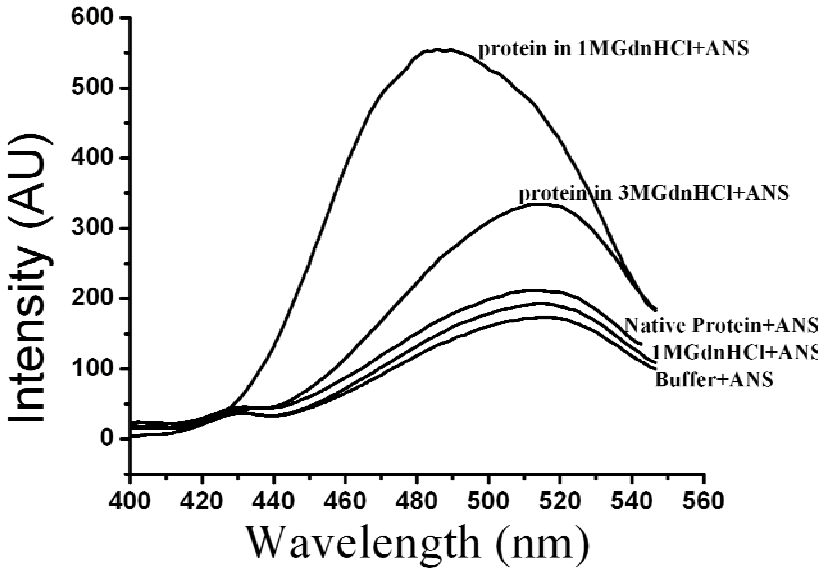

Fig. 3.3*: ANS binding of the protein samples (100 µg/ml) incubated at different concentrations of GdnHCl at 25 °C for 2 h.*

Size exclusion chromatography

The dissociation of oligomeric Jbα-man treated with GdnHCl was monitored using size exclusion chromatography (SEC) in presence of different concentrations of the denaturant. The typical SEC profiles are presented in Fig. 3.4. The native Jbα-man is a protein with molecular mass of 230 kDa (11). It eluted as a single peak centered at 15.13 min. and in the vicinity of 0.5 M GdnHCl, the retention time decreased slightly (14.7 min). The retention time of the protein in presence of 1.0 M GdnHCl decreased further (14.5 min) and a new peak appeared at about 9.17 min. In presence of 2.0 M Gdn-HCl, the peak observed above (14.5 min) totally disappeared and absorbance was detected after 18 min; not in the peak form, which could be due to the retardation of the dissociated subunits. A single peak appearing at 9.17 min; the retention time corresponding to that of void volume of the column could be due to the formation of soluble aggregate of the unfolded protein. The protein seems to undergo simultaneous

dissociation, partial unfolding and aggregation. In presence of 3.0 M GdnHCl, the peak of only aggregate was observed.

***Fig. 3.4**: HPLC Profile of Jbα-man (100µg) incubated at different concentrations of GdnHCl at 25 °C for 2 h.*

The SEC data was used to determine the Stokes' radii of the native and intermediate state. The elution volumes were 7.56 ml for the native and 7.25 ml for the protein in presence of 1 M GdnHCl. The corresponding Stokes' radii were 44.4 Å and 47.5 Å (Table 3.1) indicating a slightly expanded molecular state of the intermediate of the protein.

The Jbα-man, treated with and eluted in presence of different concentrations of GdnHCl by SEC was checked for ANS binding. Only the species eluted with retention time of 14.5 min. in presence of 1.0 M GdnHCl showed 3 times increase in fluorescence intensity with blue shift of λ_{max} to 480 nm suggesting a significant hydrophobic exposure of amino acids on the surface of Jbα-man.

The CD and fluorescence measurements, ANS binding studies and SEC data (Table 3.1) describe the existence of a molten globule like intermediate of Jbα-man in the vicinity of 1 M GdnHCl. The intermediate possessed compact secondary structure,

disrupted tertiary structure, exposed hydrophobic amino acids on the surface of the protein and increased hydrodynamic radius. The structure is similar to the one reported for β-lactamase (10). We found only a single molten globule like intermediate during equilibrium unfolding whereas there are reports of two molten globule like intermediate species (one dimeric and one momomeric) in the unfolding of Yeast glutathione reductase (8). There are also reports of active molten globule like intermediate of peanut lectin (9) in presence of 1-2 M Gdn-HCl. Thus, the present studies exhibit one of the early reports of existence of GdnHCl induced molten globule in a class II α-mannosidase.

Table 3.1: *Summary of the results of different analyses of Jbα-man.*

Protein state	**λ_{max} (nm)**	**FI (AU)**	**MRE_{219nm} (deg cm^2 $dmol^{-1}$)**	**MRE_{280nm} (deg cm^2 $dmol^{-1}$)**	**MRE_{295nm} (deg cm^2 $dmol^{-1}$)**	**ANS binding**	**Retention time in SEC(min)**	**Stokes' radius (Å)**
Native	338	938	-4459	-4923	-2018	-	15.13	44.4
Molten Globule (in the vicinity of 1M GdnHCl)	341.5	162	-5240	-4189	-3325	+++	14.50	47.5
Denatured	357	111	-2238	-	-	-	09.17	-

Characterization of Molten Globule

Temperature Stability studies

The native Jbα-man showed no shift in the λ_{max} up to 70 °C and 3 nm red shift at 75 °C indicating slight unfolding (Fig. 3.5A) of the protein. At and above 80 °C, the trp was

almost exposed to the solvent indicating significant unfolding of the protein. The molten globule structure was stable up to 90 °C.

Similarly, the MRE of the native enzyme at 219 nm was unaltered up to 70 °C, while the molten globule like intermediate formed in presence of 1.0 M GdnHCl showed about 30 % loss in the structure. This could be due to the slightly higher hydrodynamic radius of the molten globule, making it more prone to undergo structural changes (Fig. 3.5B). Interestingly, at 80 °C, the native protein underwent a substantial loss in the secondary structure while the intermediate attained a stable structure. The intermediate showed greater thermo stability than the native protein retaining 70 % of the secondary structure at 80 °C whereas the native protein retained only 34 % of the secondary structure (Fig. 3.5B).

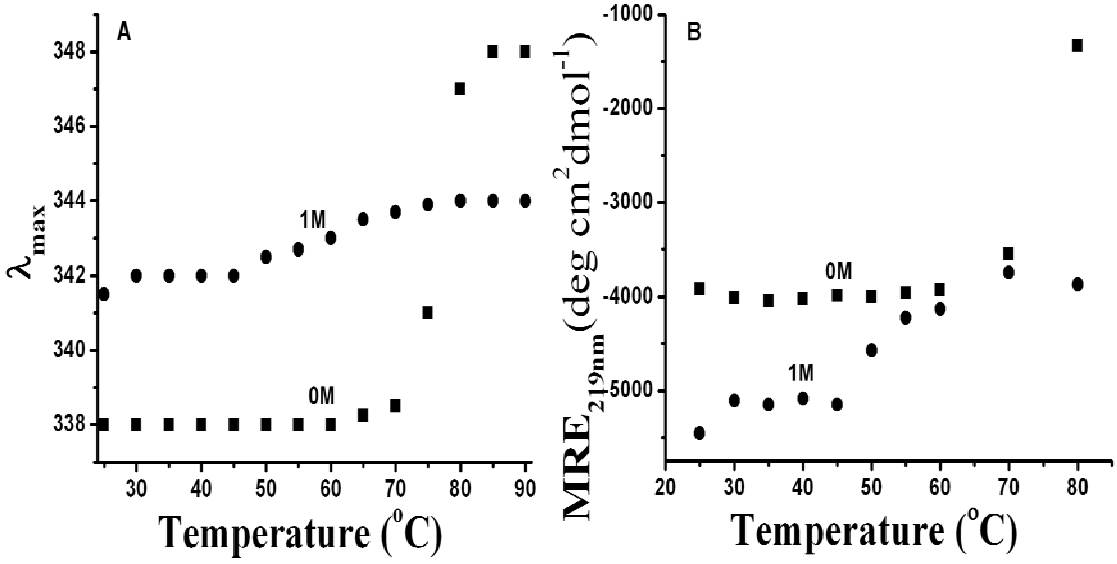

Fig. 3.5: Thermal stability studies of the native and 1M GdnHCl treated Jbα-man. *Effect of temperature on (A) λ_{max} of intrinsic fluorescence and (B) MRE at 219 nm of Jbα-man; native (filled square) and 1M GdnHCl treated (filled circle), incubated at temperatures from 25°C to 80°C for 10 min. Protein concentration used was 100 and 125µg/ml, respectively.*

The fluorescence and CD data does coincide in case of thermal unfolding of native protein unlike GdnHCl induced unfolding indicating differential modes of thermal and chemical denaturation of Jbα-man.

Solute Quenching studies

Quenching of the fluorescence of Jbα-man with acrylamide gave a linear Stern-Volmer plot with K_{sv} values as 3.93 and 5.79 M^{-1} in absence (Fig. 3.6A) and presence of 1 M GdnHCl, (Fig. 3.6B), respectively, indicating higher rate of quenching as the protein undergoes a conformational change. For the denatured protein (6 M GdnHCl treated), the Stern-Volmer plot (Fig. 3.6C) showed upward curvature indicating collisional and static mechanisms of quenching of the fluorescence due to the altered conformation. Among the three quenchers used, acrylamide was the most efficient one as it could penetrate into the interior of the protein. The total fluorescence of Jbα-man was accessible to acrylamide under native as well as denatured condition while 91 % was accessible to the protein in 1 M GdnHCl (Table 3.2) as deduced from the modified Stern-Volmer plot.

The Stern-Volmer plots obtained for quenching of the protein fluorescence with cesium and iodide ions under native conditions (Fig. 3.6A) were linear giving K_{sv} values as 0.58 and 1.34 M^{-1}, respectively. The 1M (Fig. 3.6B) and 6 M GdnHCl (Fig. 3.6C) treated protein samples showed linear Stern-Volmer plots and the K_{sv} values obtained (Table 3.2) were higher for both the ions. However, the K_{sv} values (Table 3.2) for molten globule lie between those of native and denatured protein indicating different rearrangement in its structure. As the charged quenchers can access only surface trp, the higher quenching by iodide ions indicates more density of positive charge around the surface trp conformer.

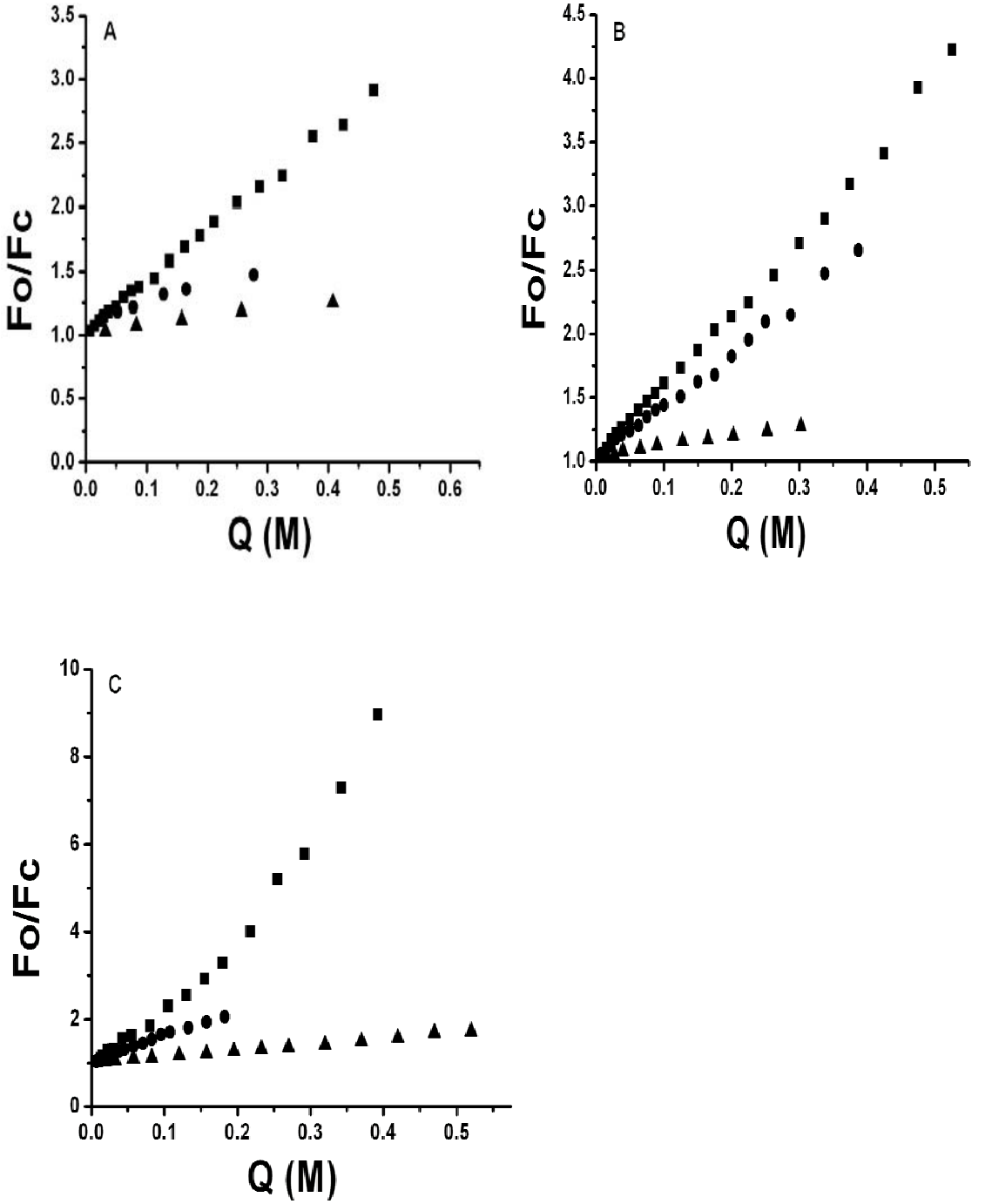

Fig. 3.6: Solute quenching studies of Jbα-man. *Stern–Volmer plots for the quenching of (A) native protein; protein treated with (B) 1M GdnHCl and (C) 6 M GdnHCl. Acrylamide (filled square), cesium (filled triangle) and iodide (filled circle) were used as the quenchers. After fitting the data the R value in each case was 0.99. Protein concentration used was 100 μg/ml.*

***Table 3.2**: Summary of parameters obtained from Stern-Volmer and modified Stern-Volmer analysis of the solute quenching studies of Jbα-man.*

Quencher and condition	K_{sv} (M^{-1})	f_a
Acrylamide		
Native	03.93	1.05
Native + 1M GdnHCl	05.79	0.91
Native + 6M GdnHCl	-----	1.18
KI		
Native	1.34	0.32
Native + 1M GdnHCl	4.13	0.68
Native + 6M GdnHCl	5.90	0.96
CsCl		
Native	0.58	0.37
Native + 1M GdnHCl	0.78	0.42
Native + 6M GdnHCl	1.37	0.65

The lifetime measurement of the intrinsic fluorescence from the decay curve of native (Fig. 3.7A) and denatured (Fig. 3.7B) Jbα-man was done by fitting it to a biexponential function with $\chi 2<1.058$ for the native and $\chi 2<1.116$ for the denatured enzyme. From this fit two decay times τ_1 and τ_2 with their corresponding weight factors α_1 and α_2 were obtained (Table 3.3). The native protein showed two lifetimes, τ_1 (1.47 ns) and τ_2 (4.81 ns) indicating presence of two conformers of the single tryptophan (29). The denatured protein also showed two lifetimes, τ_1 (1.21 ns) and τ_2 (3.34 ns).

From the life time measurements of the quenching of the intrinsic fluorescence of denatured Jbα-man by acrylamide, the decay curve (Fig. 3.7C) could be fitted to a bi-exponential function ($\chi 2<1.188$) Both τ_1 and τ_2 decreased and the average lifetime (τ)

calculated using Eq. 2 decreased from 1.56 to 0.61 ns, which could be due to low collisional frequency.

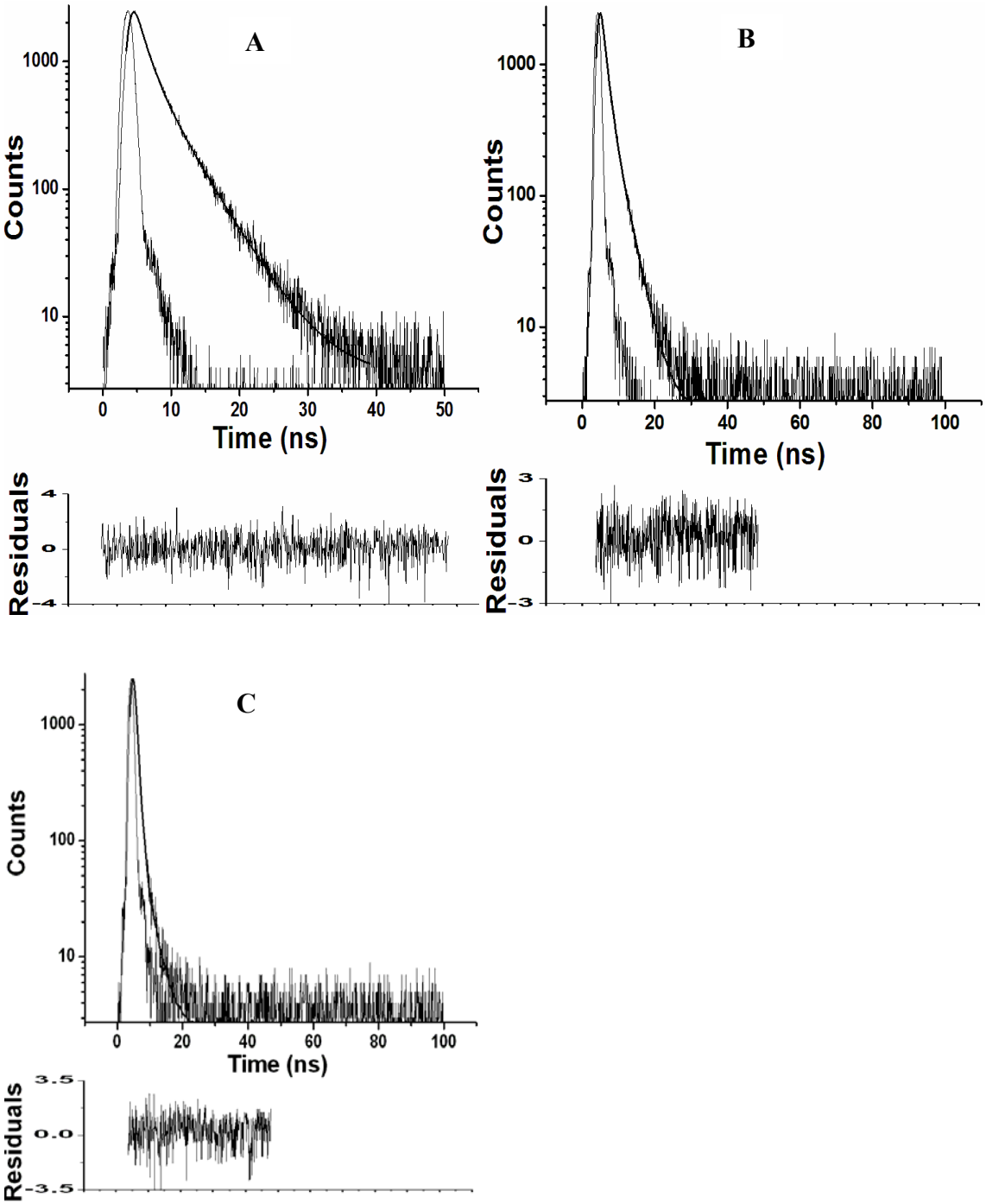

Fig. 3.7: The fluorescence lifetime decay curves *for (A) native, (B) denatured Jbα-man and (C) denatured Jbα-man quenched with 0.5 M acrylamide. The lower panels represent the residuals.*

***Table 3.3**: The lifetimes of fluorescence decay of denatured Jbα-man and the corresponding pre-exponential factors along with calculated average lifetimes for acrylamide quenching.*

[Q]	τ_1	α_1	τ_2	α_2	τ	χ^2
0	1.21	0.097	3.34	0.019	1.55888	1.116
0.01	1.16	0.099	3.17	0.022	1.52545	1.105
0.025	1.18	0.102	3.07	0.016	1.43627	1.036
0.04	1.06	0.109	2.67	0.02	1.30961	1.136
0.065	1.10	0.11	2.8	0.014	1.29194	1.056
0.09	1.02	0.112	2.56	0.016	1.2125	1.106
0.115	0.97	0.13	2.56	0.01	1.08357	1.111
0.14	0.89	0.131	2.24	0.013	1.01187	1.088
0.175	0.89	0.144	2.44	0.008	0.97158	1.188
0.21	0.79	0.146	2.08	0.01	0.87269	1.066
0.245	0.79	0.158	2.59	0.004	0.83444	1.06
0.28	0.73	0.16	2.39	0.006	0.79	1.071
0.315	0.71	0.17	2.8	0.004	0.75805	1.142
0.35	0.69	0.175	3.29	0.002	0.71938	1.095
0.40	0.64	0.180	2.20	0.005	0.68216	1.109
0.45	0.63	0.183	2.59	0.003	0.66161	1.076
0.5	0.59	0.192	2.71	0.002	0.61186	1.201

The plot of τ_0/τ for the quenching data of denatured Jbα-man with acrylamide in native condition is shown in Fig. 3.8A, from which K_{sv} was calculated as 3.12 M^{-1}. Low value of K_{sv} suggested low collision frequency. Putting this value in Eq. 6 and plotting a graph of $(F_0/F_C)/(1+K_{sv}[Q])$ against [Q], the value of the static quenching constant (K_s) was obtained as 7.39 M^{-1} (Fig. 3.8B). Incorporating the values of K_{sv} and K_s in the expression $(1+K_{sv}[Q])(1+K_s[Q])$, the values obtained were plotted against [Q]. It was observed that the values of F_0/F_C and $(1+K_{sv}[Q])(1+K_s[Q])$ match very well (Fig. 3.8C).

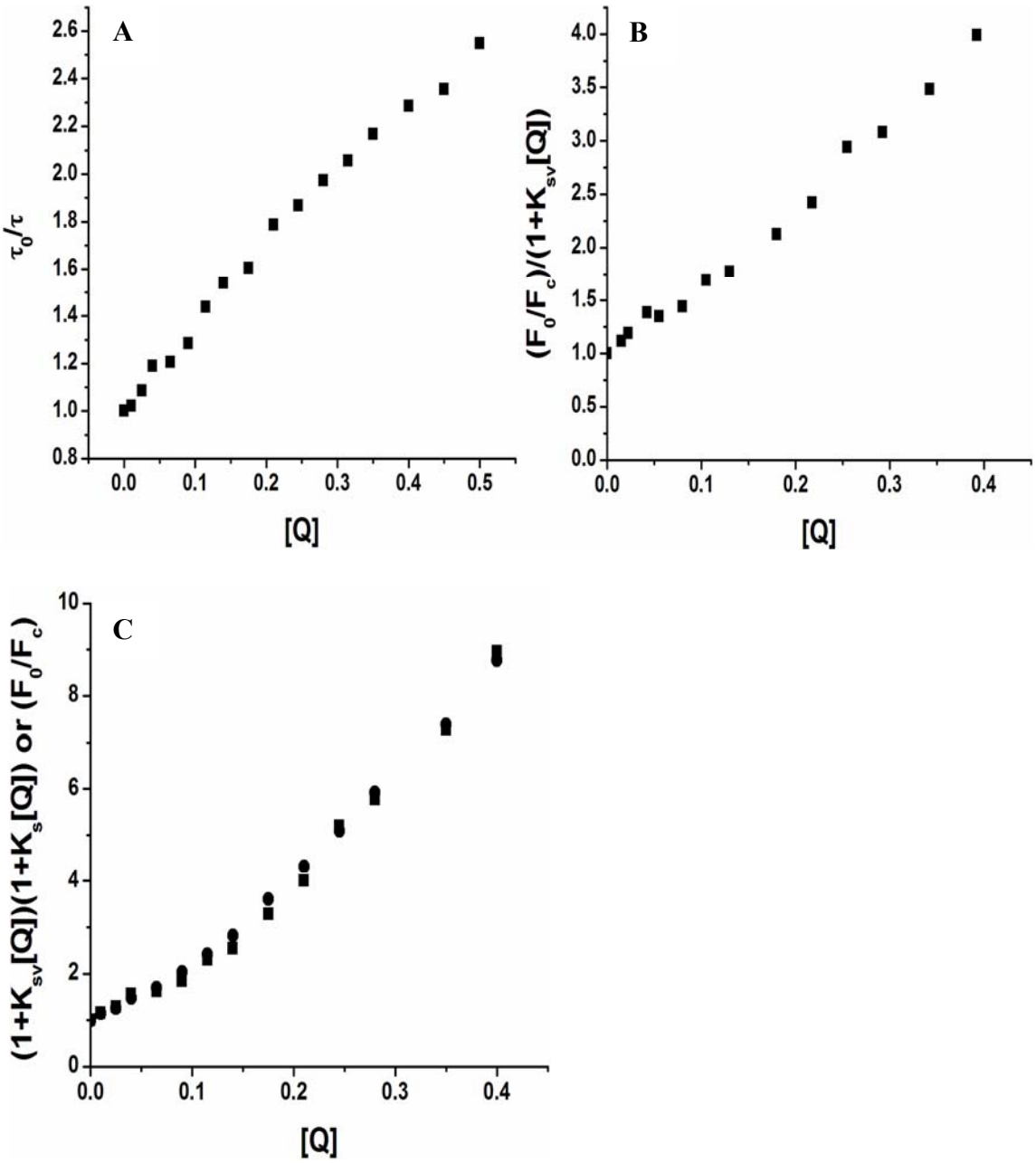

Fig. 3.8: Time resolved fluorescence quenching of denatured Jbα-man with acrylamide. *(A) Plot of τ_0/τ vs [Q] for calculation of K_{sv}. (B) Plot of $(F_0/F_c)/(1+K_{sv}[Q])$ vs [Q] for calculation of K_s and (C) plot of F_0/F_c and $(1+K_{sv}[Q])(1+K_s[Q])$.*

The thermostable molten globule like intermediate and the different modes of chemical and thermal denaturation of a class II α-mannosidase from plant source were observed.

References

1. Dennis, J.W., Granovsky, M. and Warren, C.E. (1999) *Biochem Biophys Acta* **1473**: 21–34.
2. Goss, P.E., Reid, C.L., Bailey, D. and Dennis, J.W. (1997) *Clin Cancer Res* **3**: 1077–1086.
3. Daniel, P.F., Winchester, B. and Warren, C.D. (1995) *Glycobiology* **4**: 551-556.
4. Kobata, A. (1993) *Acc Chem Res* **26**: 319–324.
5. Kuwajima, K. (1989) *Proteins* **6**: 87–103.
6. Dobson, C.M. (2006) *Protein Pept Lett* **13**: 219-227.
7. Baldwin, R.L. (1991) *Chemtracts –Biochem Mol Biol* **2**: 379–389.
8. Louzada, P.R., Sebollela, A., Scaramello, M.E. and Ferreira, S.T. (2003) *Biophys J* **85:** 3255-3261.
9. Reddy, B., Srinivas, V.R., Ahmad, N. and Surolia, A. (1999) *J Biol Chem* **274**: 4500-4503.
10. Sarkar, D. and Dasgupta, C. (1996) *Biochim Biophys Acta* **1296**: 85-94.
11. Shashidhara, K.S. and Gaikwad, S.M. (2010) *J Fluoresc* **20**: 827-836.
12. Snaith, S.M. and Levvy, G.A. (1968) *Biochem J* **110**: 663-670.
13. Snaith, S.M. (1975) *Biochem J* **147**: 83-90.
14. Kang, M.S. and Elbein, A.D. (1983) *Plant Physiol* **71**: 551-554.
15. Howard, S., He, S. and Withers, S.G. (1998) *J Biol Chem* **273**: 2067-2072.
16. Spande, T.F. and Witkop**,** B. (1967) *Methods Enzymol* **11**: 498-506.
17. Burstein, E.A., Abornev, S.M. and Reshetnyak, Y.K. (2001) *Biophys J* **81**: 1699-1709.
18. Wang, S., Liu, W.F., He, Y.Z., Zhang, A., Huang, L., Dong, Z.Y. and Yan, Y.B. (2008) *Biochim Biophys Acta* **1784**: 445-454.

19. Lima, L.M.T.R., Zingali, R.B., Foguel, D. and Monteiro, R.Q. (2004) *Eur J Biochem* **271**: 3580-3587.

20. Turoverov, K.K., Haitlina, S.Y. and Pinaev, G.P. (1976) *FEBS Lett* **62**: 4-6.

21. Su, J.T., Kim, S.H. and Yan, Y.B. (2007) *Biophys J* **92**: 578-587.

22. Bushmarina, N.A., Kuznetsova, I.M., Biktashev, A.G., Turoverov, K.K. and Uversky, V.N. (2001) *Chembiochem* **2**.

23. Kenoth, R. and Swami, M.J. (2003) *J Photochem Photobiol B Biol* **69**: 193–201.

24. Sreerama, N., Venyaminov, S.Y. and Woody, R.W. (1999) *Protein Sci* **8**: 370-380.

25. Semisotnov, G.V., Rodionova, N.A., Razgulyaev, O.I., Uversky, V.N., Gripas, A.F. and Gilmanshin, R.I. (1991) *Biopolymers* **31**: 119–128.

26. Lehrer, S.S. (1971) *Biochemistry* **10**: 3254–3263.

27. Lakowicz, E.M. and Weber, G. (1973) *Biochemistry* **12**: 4171–4179

28. Nath, D. and Rao, M. (2001) *Enzyme Microb Technol* **28**: 397-403.

29. Martinho, J.M.G., Santos, A.M., Fedorov, A., Baptista, R.P., Taipa, M.A. and Cabral, .JM.S. (2003) *Photochem Photobiol* **78**: 15–22.

CHAPTER 4

PURIFICATION AND CHARACTERIZATION OF TWO CLASS II α-MANNOSIDASES FROM *LENS CULINARIS* (LENTIL)

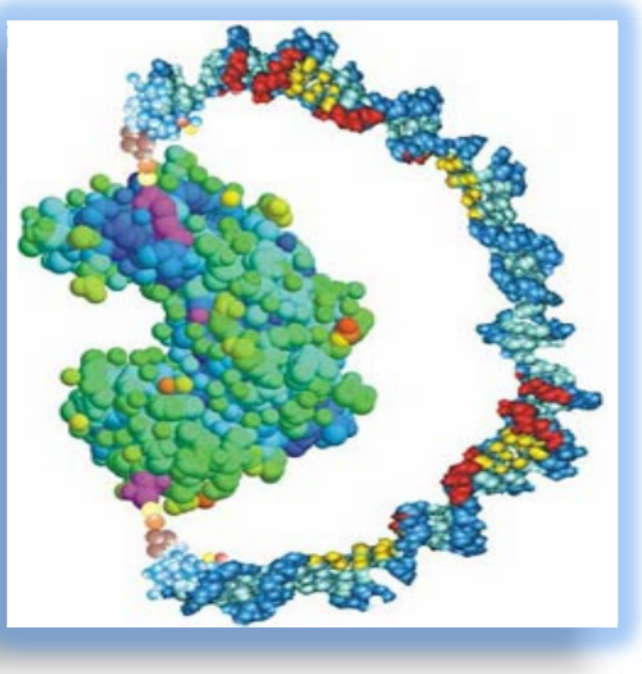

Avinash Kumar and Sushama M. Gaikwad. Purification and biochemical characterization of two class II α-mannosidases from Lens culinaris (Lentil) (Manuscript under preparation)

Summary

Two class II α-mannosidases from *Lens culinaris* (Lentil), slightly differing in the electrophoretic mobility, were purified to homogeneity by alkaline native polyacrylamide gel electrophoresis (PAGE). Both the enzymes are glycoproteins with a carbohydrate content of about 10 %. The pH and temperature optima of the enzymes were 5.0 and 55 °C, respectively. At pH 5.0 the enzyme was stable for 30 min at 55 °C. The K_m and V_{max} of p-nitrophenyl-α-D-mannopyranoside for both the enzymes was about 4 mM and of 4-methylumbelliferryl-α-D-mannopyranoside was 15 μM. The K_i of Swainsonine for both the enzymes was about 5 nM. The enzyme was strongly inhibited by 2 mM Hg^{2+}, Cu^{2+}, Co^{2+} and 1 % SDS and partially inhibited by 100 mM mannose. The steady state fluorescence spectra of both the enzymes showed λ_{max} as 341 nm indicating trp to be in slightly hydrophobic environment and the far UV CD spectra with mimima around 212 nm showed that both the enzymes are predominantly β-sheet proteins. Owing to the similarity in properties and structure of both the enzymes, our results constitute one of the reports of existence of class II α-mannosidases as isozymes.

Introduction

The vital cellular processes such as intercellular communication, immune response and malignancy are mediated by the branching sugar molecules on the cell surface. Glycosidases have proved to be useful tools for probing structural features of cell surface glycoconjugates (1).

α-mannosidase (α-D-mannoside mannohydrolase, EC 3.2.1.24) plays a very important role in the mannose-trimming reaction during the biosynthesis of glycoproteins of higher eukaryotes and a deficiency of this enzyme leads to mannosidosis, a lethal disease in humans (2) and cattle (3,4). During mannose trimmimng, hydrolysis of α1,2-linked mannose residues gives rise to hybrid and high mannose N-glycans, whereas removal of α1,3- and α1,6-linked mannoses leads to formation of complex N-glycans (5,6). Based on the amino acid sequence analysis and some biochemical properties, α-

mannosidases are grouped into glycosyl hydrolase families 38 and 47 which include α1,2-, α1,3- and α1,6- mannosidases commonly referred to as Class II α-mannosidases and α1,2-mannosidases commonly referred to as Class I α-mannosidases (6-8). A number of evidences support the intimate involvement of α-mannosidases in the demannosylation of intermediate oligosaccharides during the process of glycoprotein quality control, a process that facilitates proper folding of newly formed polypeptide chains leading to retention or degradation of malfolded proteins in the Endoplasmic Reticulum (ER) (9). α-mannosidases play a key role in the processing of glycoproteins and thus are of considerable pharmaceutical interest and indeed have emerged as targets for the development of anticancer therapies (10). Inhibitors of Class II α-mannosidases are known to show anticancer activity (11). The enzyme is useful as an analytical tool in the structural analysis of glycoproteins and cell-surface glycopeptides and for the elucidation of their biological role (12).

In the present chapter, we report the purification and biochemical characterization of two α-mannosidases, existing as isozymes, from the seeds of *Lens culinaris* (Lentil) plant, a very common pulse crop.

Materials and methods

Materials

Ammonium sulphate, CM-Sepharose, acrylamide, N,N'-methylenebisacrylamide, SDS, p-nitrophenyl-α-D-mannopyranoside (pNPαMan), 4-methylumbelliferryl-α-D-mannopyranoside (4-MeUmbαMan) and Swainsonine were purchased from Sigma, USA. Molecular weight markers were purchased from GE Life Sciences, USA. All other reagents used were of analytical grade. For spectroscopic measurements, solutions were prepared in MilliQ water.

Enzyme Assay

The α-mannosidase activity was estimated with pNP-α-mannopyranoside (pNPαMan) and 4-methylumbelliferyl-α-mannopyranoside (4-MeUmbαMan) according to the procedure described in enzyme assay section of Materials and Methods of chapter 2.

Optimization of germination and extraction conditions

70 gm of dry lentil seeds were soaked in double distilled water, and kept for germination.10 gm of seeds were removed at different intervals of time for 7 days and crushed to make a paste with 10 mM buffers of pH 5.0, 6.5, 7.2 and 8.8. The buffers used were citrate phosphate buffer for pH 5.0, phosphate buffer for pH 6.5 and 7.2 and tris-HCl buffer for pH 8.8. This mixture was kept on magnetic stirrer for extraction. Samples were removed after 1 h, 3 h, 5 h and 24 h and centrifuged at 10,000 rpm for 5 mins. 50 µl of the supernatant was used for α-mannosidase and protease assay.

Purification of α-mannosidase

The protein was determined by the method of Lowry et al. using bovine serum albumin as a standard.

The prepared seed extract was subjected to fractionation with $(NH_4)_2SO_4$ in the saturation range of 30 – 60 %. The precipitate was pelleted by centrifugation, dissolved and dialyzed against 20 mM citrate phosphate buffer (CPB), pH 5.0 with three changes for 24 h. 30 mg of the dialyzed protein was loaded on a CM-Sepharose column equilibriated with the same buffer. Almost all the activity was obtained in the flow-through fractions. The active fractions were pooled, concentrated and dialyzed against 20 mM CPB, pH 5.0. 200 µg of this active protein was loaded on a 7.5% w/v alkaline native PAGE. The two lentil α-mannosidases (LAM 1 and LAM 2) were obtained as two separate bands which were manually cut from polyacrylamide gel and eluted with 20 mM CPB, pH 5.0.

Determination of Optimum pH and pH stability

For determination of optimum pH, 15 µg enzyme was assayed at different pH, ranging from 2.0 to 9.0 for α-mannosidase activity.

For pH stability determination, 150 µg enzyme was incubated in buffers of different pH, ranging from 2.0 to 9.0. Aliquots were taken out after every 15 mins and assayed for α-mannosidase activity.

Determination of Optimum temperature and temperature stability

For determination of optimum temperature, 15 µg enzyme was assayed at different temperatures (30-70 °C) for α-mannosidase activity.

For temperature stability determination, 150 µg enzyme was incubated at different temperatures (30-70 °C). Aliquots were taken out after every 15min and assayed for α-mannosidase activity.

Determination of K_m and V_{max}

For determination of K_m and V_{max}, 15 µg/5 µg enzyme was assayed for α-mannosidase activity at optimum pH and temperature but with varying substrate (pNP-α-mannopyranoside / 4-methylumbelliferyl-α-mannopyranoside) concentrations. Michaelis Menten (MM) plot was drawn to determine K_m and V_{max}.

Determination of Carbohydrate content

The total neutral sugar content of the enzyme was determined by the phenol-sulfuric acid method of Dubois et al. (13). To 30 µg enzyme 400 µl of 5 % Phenol was added and incubated for 10 mins at room temperature. To this 2 ml of Conc. H_2SO_4 was added and incubated for 20 mins at room temperature. Then the absorbance was taken at 490 nm. This absorbance was used to calculate the amount of sugar per ml of enzyme. It was then divided by the amount of protein per ml of enzyme to yield the carbohydrate content.

Determination of pK_a of amino acids at the active site

Determination of K_m and V_{max} for 15 µg enzyme was performed at different pH ranging from 2.0 to 9.0. Ln (V_{max}/ K_m) Vs pH was plotted to determine pK_a value.

Determination of activation energy

Determination of activation energy for LAM 1 and 2 were performed according to the procedure described in the substrate kinetics section of Materials and Methods of chapter 2.

Determination of IC_{50} and K_i of Swainsonine

For determination of IC_{50} 5 µg enzyme was incubated with varying concentrations of Swainsonine for 10 mins and then assayed at a constant substrate (4-methylumbelliferyl-α-mannopyranoside) concentration for α-mannosidase activity. Percent Inhibition Vs [I] was plotted to yield the IC_{50} value.

For K_i determination 5 µg enzyme was incubated with varying concentrations of Swainsonine for 10 mins and then assayed at two different substrate (4-methylumbelliferyl-α-mannopyranoside) concentrations for α-mannosidase activity. The reciprocal of activity (1/V) Vs [I] (14) was plotted to yield the K_i value.

Effect of metal ions and detergents

The enzyme (5 µg) was incubated with either metal ions (2 mM) or detergents (1 %) in 20 mM CPB, pH 5.0 (volume 0.5 ml), for 10 min at 30 °C and the α-mannosidase activity was assayed as described above.

Steady state fluorescence measurements

Steady state fluorescence measurements for LAM 1 and 2 were performed according to the procedure described in steady state fluorescence measurements section of Materials and Methods of chapter 2.

Circular Dichroism (CD) Measurements

The CD measurements for LAM 1 and 2 were performed according to the procedure described in circular dichroism (CD) section of materials and methods of chapter 2.

Solute Quenching studies

The solute quenching for LAM 1 and 2 were performed using the ionic quenchers, I^- and Cs^+ according to the procedure described in solute quenching studies section of Materials and Methods of chapter 3.

Results and Discussion

Optimization of germination and extraction conditions

The lentil seeds soaked for 21 h and extracted with 10 mM tris-HCl buffer, pH 8.8 for 3 h (Fig. 4.1A) were found to have optimal α-mannosidase activity (97.2 U/100 gm of dry lentil seeds) and negligible protease activity.

Purification of α-mannosidase

An array of purification techniques involving ammonium sulphate fractionation, different chromatographic techniques such as ion exchange, gel filtration, hydrophobic interaction, affinity, hydroxyapatite, chromatofocussing, isoelectric focussing and preparative gel electrophoresis was applied to purify α-mannosidase from *Lens culinaris* (Lentil). Finally separation of the protein bands on analytical PAGE, cutting and eluting them led to purification of these enzymes to electrophoretic homogeneity.

Both LAM 1 and LAM 2 were purified to about 70 fold purification with 15 % recovery using the following steps: (i) ammonium sulphate fractionation in the range of 30-60% saturation, (ii) CM-sepharose cation exchange chromatography and (iii) 7.5% alkaline native PAGE (Table 4.1). The specific activity of the purified α-mannosidases was found to be 2.59 and 2.25 U/mg, respectively. The activity staining of the α-mannosidase from crude lentil extract on 7.5% alkaline native PAGE showed a single but very diffused fluorescent band (Fig. 4.1A) whereas the α-mannosidase activity staining of the CM-sepharose flow through fractions which showed positive activity towards pNPαMan showed two close fluorescent bands (Fig. 4.1B). The homogeneity of the purified enzymes was checked on a 7.5 % w/v alkaline native PAGE (Fig. 4.2) which was both activity (Fig. 4.2A) as well as protein stained (Fig. 4.2B). The purified enzymes showed a single band with activity indicating a homogeneous active protein.

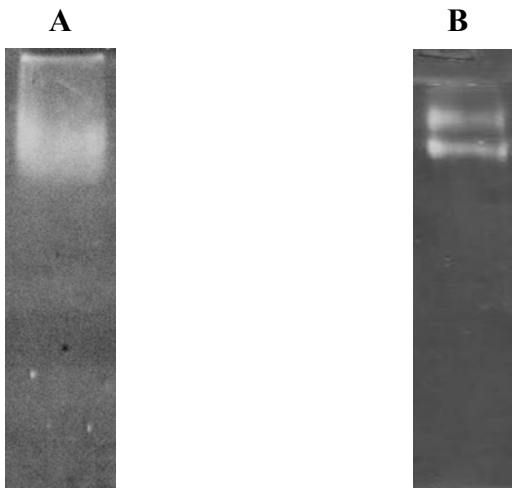

Fig. 4.1: Activity staining of LAM 1 and 2. *7.5% alkaline native PAGE activity stained for class II α-mannosidases in (A) crude lentil extract and (B) CM-sepharose flow through active fractions. 25 µg protein was loaded on the gel.*

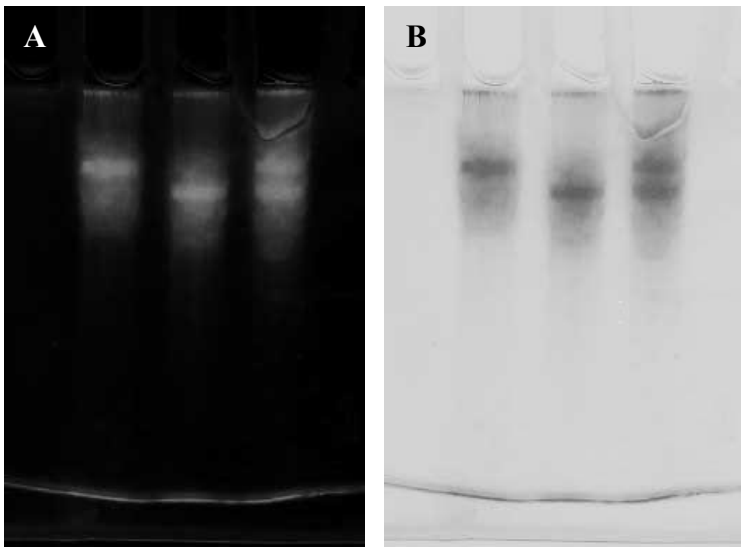

Fig. 4.2: Alkaline native PAGE of purified LAM 1 and LAM 2. *(A) Activity staining and (B) Silver staining. Lane1 is blank, Lane 2: 20 µg of purified LAM 1, Lane 3: 20 µg of purified LAM 2 and Lane 4: 20 µg of purified LAM 1 mixed with 20 µg of purified LAM 2.*

***Table 4.1**: Purification chart.*

S.No	Purification table		Volume (ml)	Activity (U)	Protein (mg)	Specific activity (U/mg)	Fold purification	Recovery (%)
1.	Crude extract (200 gms. of lentil seeds)		400	194.40	6000	0.0324	1	100
2.	Ammonium sulphate precipitated (30-60% saturation)		100	165.24	800	0.2066	6.38	85
3.	CM-Sepharose		60	139.96	300	0.4665	14.40	71.99
4.	7.5%PAGE pH(8.8)	I	50	27.22	10.5	2.5924	80.01	14
		II	50	29.26	13.0	2.2508	69.47	15

Characterization of LAM 1 and 2

Both LAM 1 and LAM 2 show maximum activity at pH 5.0 (Fig. 4.3) and was stable at this pH at 30 °C for 75 min (Fig. 4.3).

Fig. 4.4 shows the optimum temperature of both α-mannosidases to be 55 °C. Both the enzymes were also found to be stable for 30 min at 55 °C, however, at 60 °C, 30 % loss in activity was observed (Fig. 4.4).

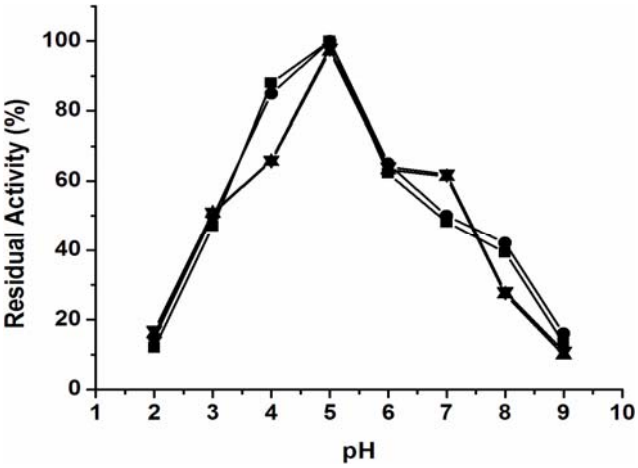

Fig. 4.3: Effect of pH on activity and stability of LAM 1 and LAM 2. *For the effect on activity, 15 µg each of LAM 1 (■) and LAM 2 (●) was assayed for α-mannosidase activity at 55 °C in 50 mM buffer. The buffers used were Glycine-HCl for pH 1-3, acetate for pH 4-5, phosphate for pH 6-7, Tris-HCl for pH 8-9. For the effect on stability, aliquots of both LAM 1 (▲) and LAM 2 (▼) were incubated for 75 min in the pH range 2 – 9 and the enzyme activity was measured at 55 °C as described in Materials and methods.*

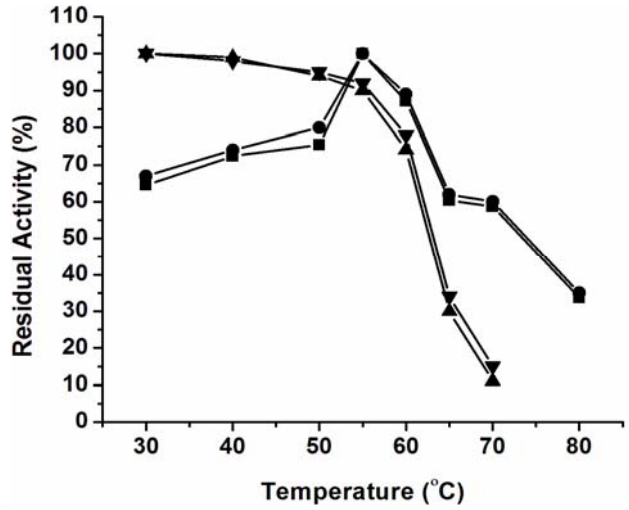

Fig. 4.4: Effect of temperature on activity and stability of LAM 1 and LAM 2. *For the effect on activity, 15 µg each of LAM 1 (■) and LAM 2 (●) was assayed for α-mannosidase activity at different temperature (30 - 80 °C). For the effect on stability, aliquots of both LAM 1 (▲) and LAM 2 (▼) were incubated for 30 min at different temperatures (30 – 70 °C) and the enzyme activity was measured at 55 °C as described in Materials and methods.*

The optimum pH for the lentil α-mannosidases was similar to the one reported for another plant α-mannosidase, Jbα-man (15) but different from the one reported for *Aspergillus fischeri* α-mannosidase (pH 6.5) (16) whereas the optimum temperature was found to be close to the *Aspergillus fischeri* α-mannosidase (50 °C) (16).

K_m and V_{max} was determined for LAM 1 and LAM 2 with the substrates, pNPαMan and 4-MeUmbαMan. Table 4.2 shows the values of K_m and V_{max} for both the enzymes with both the substrates.

***Table 4.2**: K_m and V_{max} values for LAM 1 and LAM 2.*

Enzyme	Substrate	K_m	V_{max} (U/mg/min)
LAM 1	pNPαMan	3.72mM	0.2316
LAM 2	pNPαMan	3.91mM	0.1685
LAM 1	4-MeUmbαMan	14.95μM	10.67
LAM 2	4-MeUmbαMan	15.09 μM	10.47

Both LAM 1 and LAM 2 showed similar values of K_m and V_{max} for each substrate but the K_m for 4-MeUmbαMan was about 250 times lower than that for pNPαMan (Table 4.2) indicating much greater affinity for 4-MeUmbαMan than pNPαMan due to the more hydrophobic nature of 4-MeUmbαMan.

Both LAM 1 and LAM 2 were found to be glycoproteins with a neutral sugar content of 09.84 and 09.87 % respectively. The neutral sugar content of the two lentil α-mannosidases was found to be very close to the *Erythrina indica* α-mannosidase (8.6%) (17) which is also a plant α-mannosidase but different from the *Aspergillus fischeri* α-mannosidase.

The pK_a values of the amino acids probably involved at the active site of the enzyme were deduced to be 4.19 and 5.00 for LAM 1 and 4.21 and 4.95 for LAM 2, respectively (Fig. 4.5). The pK_a value of 4.2 indicated the involvement of the carboxylate (COO^-) ion at the active site of the enzymes. The other pK_a of 5.0 indicated probable involvent of histidine at the active site, the pK_a of which would have changed due to change in the microenvironment. COO^- ion has been reported to be involved at the active site in many class II α-mannosidases earlier also. The involvement of histidine at the active site of LAM 1 and 2 could not be investigated further due to low yield, low stability and presence of spectroscopic impurities.

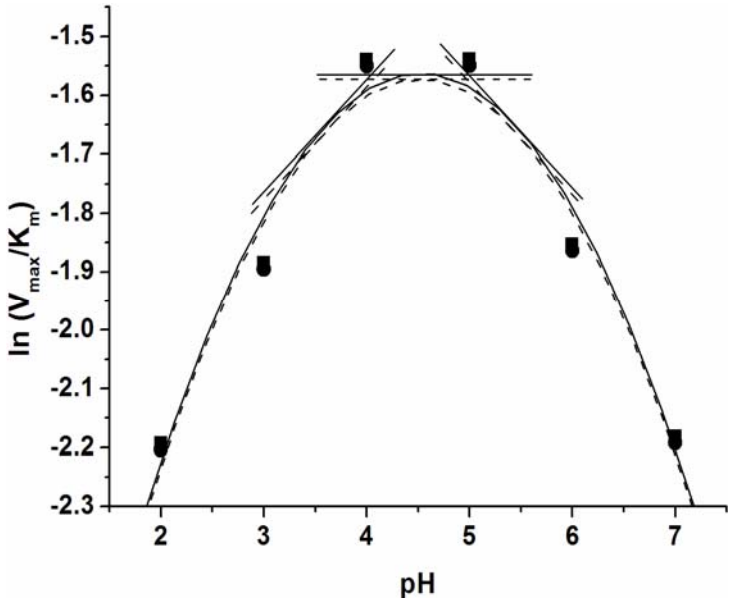

Fig. 4.5: Determination of pK_a value for LAM 1 and LAM 2. *K_m and V_{max} of pNPαMan for 15 μg of both the enzymes was determined in the pH range 2 – 7. Ln (K_m/V_{max}) of both LAM 1 (■) and LAM 2 (●) was plotted against pH. The values were subjected to polynomial fitting procedure for both LAM 1 (——) and LAM 2 (– – –) to yield the pK_a values.*

Activation energy (E_a) for both the enzymes with pNPαman was found to be 40.33 kJ mol^{-1} (Fig. 4.6). This was found to be close to both, the *Aspergillus fischeri* α-mannosidase (38.70 kJ mol^{-1}) as well as Jbα-man (31.90 kJ mol^{-1}).

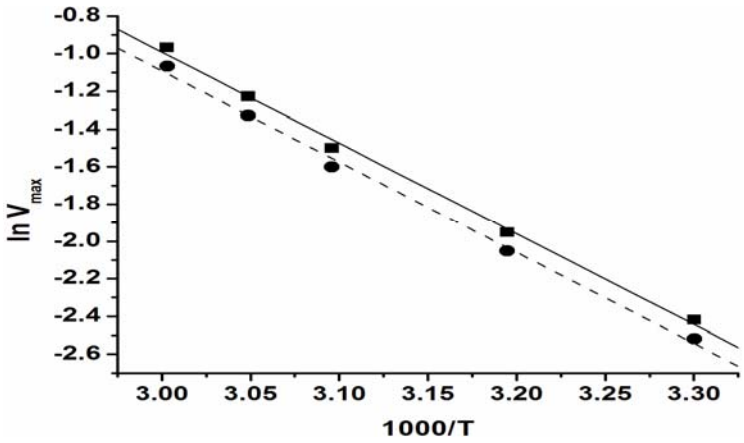

Fig. 4.6: Determination of activation energy (E_a) for LAM 1 and LAM 2. *K_m and V_{max} of pNPαMan for 15 µg of both the enzymes was determined in the temperature range of 30 – 60 °C. Ln V_{max} of both LAM 1 (■) and LAM 2 (●) was plotted against temperature. The values were subjected to linear fitting procedure for both LAM 1 (——) and LAM 2 (– – –) to yield the E_a values.*

K_i of both LAM 1 and LAM 2 for the inhibition with class II α-mannosidase specific inhibitor, Swainsonine was found to be 5.12 and 5.29 nM respectively (Fig. 4.7).

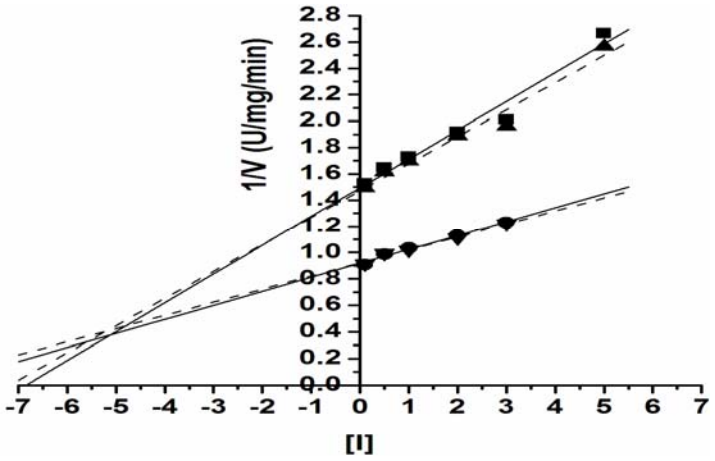

Fig. 4.7: Dixon plot of Swainsonine for LAM 1 and LAM 2. *15 µg of LAM 1 with 250 µM (■) and 500 µM (●) pNPαMan and 15 µg of LAM 2 with 250 µM (▲) and 500 µM (▼) pNPαMan were assayed for enzyme activity at pH 5.0, 55 °C and at different concentrations of Swainsonine. The values were subjected to linear fitting procedure for both LAM 1 (——) and LAM 2 (– – –) to yield the K_i values.*

The K_i value of both LAM 1 and LAM 2 for Swainsonine was found to be 10 times less than that for Jbα-man (53.9 nM) (15) but 20000 times less than that for *Aspergillus fischeri* α-mannosidase (101 μM) (18).

Effect of metal ions and detergents

The enzymes were strongly inhibited by Hg^{2+}, Cu^{2+} and Co^{2+} and partially by Mg^{2+} and Ca^{2+}. The enzymes when treated with 10 mM EDTA showed about 80 % inhibition (Table 4.3). The present enzyme differs in this aspect from the *Aspergillus fischeri* α-mannosidase (16) but resembles the other plant α-mannosidase from Jack bean (15). Table 4.3 shows that the enzyme is inhibited by anionic detergent, SDS but activated by cationic detergents, Triton X-100 and Tween 20.

***Table 4.3**: Effect of metal ions and other reagents on enzyme activity.*

Reagent	Residual Activity (%) of LAM 1	Residual Activity (%) of LAM 2
10 mM EDTA	78	79
Metal ions (2 mM)		
Mg^{2+}	71	74
Ca^{2+}	50	51
Co^{2+}	05	07
Cu^{2+}	03	04
Hg^{2+}	00	00
Detergents (1 %)		
SDS	03	04
TritonX-100	147	148
Tween 20	150	152

Steady state fluorescence and Circular Dichroism (CD) spectra

The native LAM 1 and LAM 2 showed fluorescence spectrum (Fig. 4.8) with λ_{max} at 341 nm indicating trp residue to be in slightly hydrophobic environment.

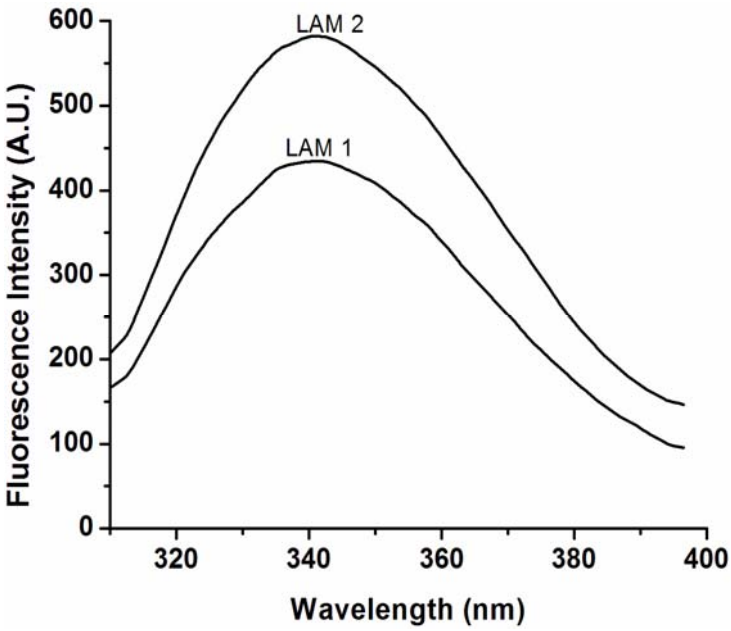

Fig. 4.8: Steady state fluorescence spectra of LAM 1 and LAM 2. *Intensity of fluorescence emission of 50 µg/ml of both LAM 1 and LAM 2 in the wavelength range of 310 – 400 nm, when excited at 295 nm.*

Decomposition analysis of the steady state tryptophan fluorescence spectra of both LAM 1 and LAM 2 by PFAST (http://pfast.phys.uri.edu/pfast/) (19) indicated two classes of trp; 12.5% class S which includes buried tryptophan residue or a conformer with slight flexibility of the microenvironment and 87.5% class II containing structured water molecules near to the indole ring of trp residue in the protein for LAM 1 and 17.8% class S and 82.2% class II for LAM 2.

CD pro analysis of the far UV CD spectra of both LAM 1 and LAM 2 (Fig. 4.9) yielded the values of the secondary structure elements as: α-helix: 3.0-3.3%, β-sheet: 35-36%, turns: 22-21.8% and unordered: 40-35.7%.

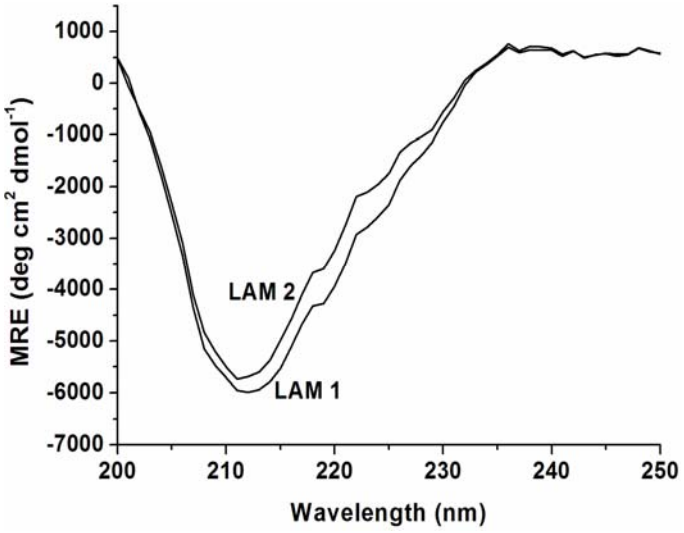

Fig. 4.9: Far UV CD spectra of LAM 1 and LAM 2. *Circular Dichroism (CD) in Mean Residue Ellipticity (MRE) of 80 µg/ml of both LAM 1 and LAM 2 in the wavelength range of 250 – 200 nm.*

Solute quenching studies

LAM 1 and 2 do not differ much in any of the properties studied above but still they run as two separate bands on 7.5% alkaline native PAGE. The slight difference in the overall charge on the surface of LAM 1 and 2 probably due to amino acid substitutions could be responsible for this differential mobility. To investigate this difference in overall charge density on the surface, solute quenching studies of both LAM 1 and 2 with the ionic quenchers, I^- and Cs^+ were carried out.

Quenching of the fluorescence of LAM 1 and 2 with iodide ions under native conditions gave a linear Stern-Volmer plot (Fig. 4.10A) with K_{sv} values as 16.9 and 17.1 M^{-1}, respectively, indicating efficient quenching. Cs^+ ions failed to quench the fluorescence of proteins. The total fluorescence of LAM 1 and 2 with f_a values as 1.23 and 1.41 was accessible to iodide ions under native condition as deduced from the modified Stern-Volmer plot (Fig. 4.10B). As the ionic quenchers can access only surface trp, the extensive quenching of fluorescence by iodide ions and failure in quenching of fluorescence by cesium ions indicates high density of positive charge around the surface trp conformer.

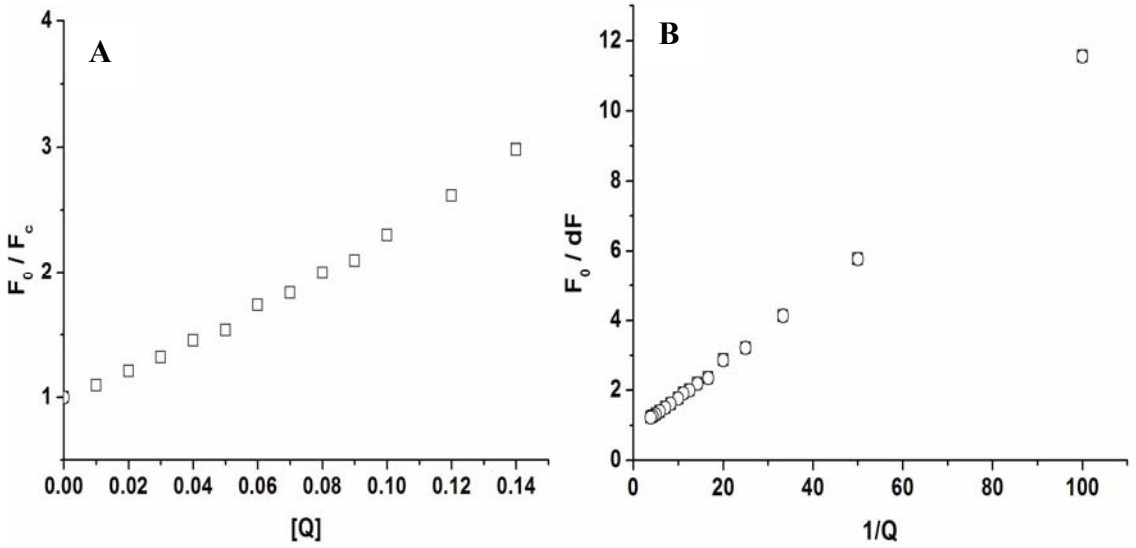

Fig. 4.10: Solute quenching studies of LAM 1 and 2. *(A) Stern-Volmer and (B) modified Stern-Volmer plot for solute quenching of LAM 1 and 2 by iodide ions. Protein concentration used was 75 µg/ml.*

The basis of slight difference in the electrophoretic mobility of LAM 1 and 2 could not be deduced from these results, as K_{sv} values for both the enzymes were similar and I^- ions had full accessibility towards surface trp.

Isozymes (also known as isoenzymes) were first described by R. L. Hunter and Clement Markert (1957) who defined them as "different variants of the same enzyme having identical functions and present in the same individual". This definition encompasses:

(1) Enzyme variants that are the products of different genes and thus represent different loci (described as *isozymes*) and

(2) Enzymes that are the products of different alleles of the same gene (described as *allozymes*).

The existence of isozymes permits the fine-tuning of metabolism to meet the particular needs of a given tissue or developmental stage.

Isozymes (and allozymes) are variants of the same enzyme. Unless they are identical in terms of their biochemical properties, for example their substrates and enzyme kinetics,

they may be distinguished by a biochemical assay. However, such differences are usually subtle (particularly between allozymes which are often neutral variants). This subtlety is to be expected, because two enzymes that differ significantly in their function are unlikely to have been identified as isozymes. While isozymes may be almost identical in function, they may differ in other ways. In particular, amino acid substitutions that change the electric charge of the enzyme (such as replacing aspartic acid with glutamic acid) are the most common differences found in isozymes (allozymes).

There are already reports on class II α-mannosidases existing as isozymes in Tomato (20) and *Phaseolus vulgaris* (21).

The two class II α-mannosidases from lentil seeds, LAM 1 and LAM 2 were found to be pretty similar in their overall properties and secondary structure content but differ in the overall charge density on the surface of the protein, indicating that they may be isozymes.

As the finally standardized method of purification had the limitations of producing the proteins in low yield and with presence of spectroscopic impurities, the structure-function relationship of the enzymes could not be investigated further.

References

1. Olden, K., Bernard, B.A, Humphries, M.J. *et al.* (1985) *Trends Biochem Sci* **10**: 78-82.
2. Ockerman, P.A. (1967) *Lancet* **290**: 239-241.
3. Philips, N.C., Robinson, D., Winchester, B.G. and Jolly, R.D. (1974) *Biochem J* **137**: 363-371.
4. Burditt, L.J., Philips, N.C., Robinson, D., Winchester, B.G., Van De Water, N.S. and Jolly, R.D. (1978) *Biochem J* **175**: 1013-1022.
5. Kornfeld, R. and Kornfeld, S. (1985) *Annu Rev Biochem* **54**: 631-664.
6. Henrissat, B. and Davies, G. (1997) *Curr Opin Struct Biol* **7**: 637-644.
7. Herscovics, A. (1999) *Biochim Biophys Acta* **1473**: 96-107.
8. Bourne, Y. and Herscovics, A. (2001) *Curr Opin Struct Biol* **11**: 593-600.
9. Mora-Montes, H.M., López-Romero, E., Zinker, S., Ponce-Noyola, P. and Flores-Carreón, A. (2006) *FEMS Microbiol Lett* **256**: 50-56.
10. Howard, S., He, S. and Withers, S.G. (1998) *J Biol Chem* **273**: 2067–2072.
11. Daniel, P.F., Winchester, B. and Warren, C.D. (1995) *Glycobiology* **4**: 551–556.
12. Li, Y.T. (1967) *J Biol Chem* **242**: 5474-5480.
13. Dubois, M., Gilles, K.A., Hamilton, J.K., Rebers, P.A. and Smith, F. (1956) *Anal Chem* **28**: 350-356.
14. Dixon, M. (1953) *Biochem J* **55**: 170-171.
15. Kumar, A. and Gaikwad, S.M. (2011) *Int J Biol Macromol* (Under Review).
16. Gaikwad, S.M., Keskar. S.S. and Khan, M.I. (1995) *Biochim Biophys Acta* **1250**: 144-148.
17. Kestwal, R.M., Konozy, E.H., Hsiao, C.D., Roque-Barreira, M.C. and Bhide, S.V. (2007) *Biochim Biophys Acta* **1770**: 24-28.

18. Shashidhara, K.S. and Gaikwad, S.M. (2009) *Int J Biol Macromol* **44**: 112-115.

19. Burstein, E.A., Abornev, S.M. and Reshetnyak, Y.K. (2001) *Biophys J* **81**: 1699–1709.

20. Suvarnalatha G. and Prabha T.N. (1999) *Phytochemistry* **50**, 1111-1115.

21. Paus E. and Christensen T.B. (1972) *Eur. J. Biochem.* **25**, 308-314.

CHAPTER 5

DISCUSSION & CONCLUSION

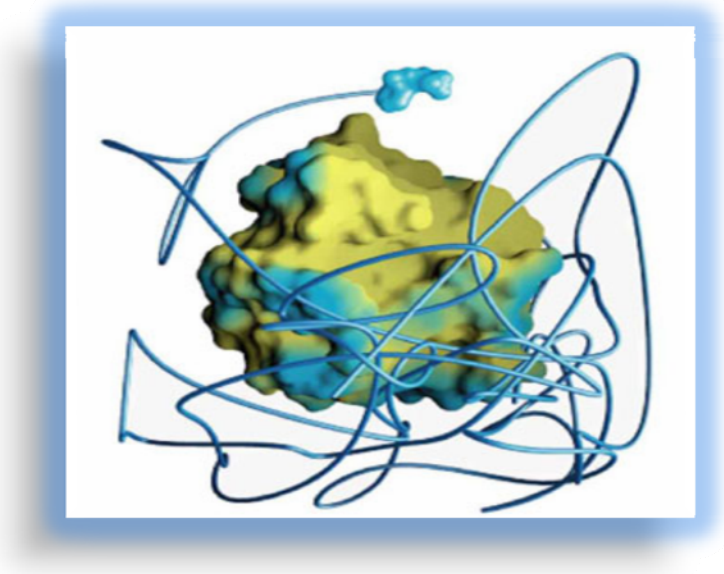

α-mannosidases are involved in both glycoprotein biosynthesis (Golgi mannosidases) and degradation (lysosomal mannosidases) from yeast to human beings (1, 2). The absence of this enzyme causes the genetic lysosomal storage disease α-mannosidosis in humans and cattle (3). The enzymes are categorized as class I and class II mannosidases and based on the sequence alignments; they belong to family 47 and family 38 glycosidase, respectively in Henrissat's glycosidase classification (1, 4). A number of these enzymes have been cloned and sequenced; also some success has been achieved in their high level expression. There has been widespread interest in α-mannosidase in recent years, in particular, mammalian Golgi mannosidase-II involved in glycoprotein biosynthesis and is currently an important therapeutic target for the development of anticancer agents (5).

α-mannosidases have been studied widely (6) and categorized into two Classes. In Class I, the enzymes hydrolyze specifically linked α-D-mannosidic bonds (α1–2). These enzymes have strict stereo-chemical requirements. Class I enzymes cannot hydrolyze aryl substrates like para-nitro phenyl α-D-mannopyranoside (pNPαMan) and 4-methylumbelliferylα-mannopyranoside (4-MeUmbαMan). In Class II, the enzyme hydrolyzes nonreducing terminal α-mannosidic linkages regardless of the aglycon moiety. It includes those enzymes which act on para-nitro phenyl α-D-mannopyranoside (pNPαMan) and do not have strict linkage specificity i.e. they act on α(1–2), α(1–3), α(1–4) and α(1–6) linkages although with different rates (4). During past many years, several reports on plant class II α-mannosidases have been published (7-26).

The Class II α-mannosidases from different plant species studied so far are from Jack bean, *Erythrina indica*, Mung bean, Tomato, *Capsicum annum*, Rice, *Phaseolus vulgaris*, *Gingko biloba*, Almond and Babaco (7-26) but there are hardly any detailed reports on the studies of the active site, conformational and functional transitions under the effect of particular conditions, energetics of catalysis and energetics and thermodynamics of inhibition of these or any other plant Class II α-mannosidases but there are reports on the denaturation studies of glycosidases such as xylanases,

xylosidases etc. We have also reported an acid induced molten globule in a class II α-mannosidase from *Aspergillus fischeri* (27)

In the present study, the Class II α-mannosidase from *Canavalia ensiformis*, Jack bean was procured commercially from Sigma Ltd., USA and characterized for the conformational and functional transitions under the effect of particular denaturing conditions. The enzyme was also used to study the energetics of catalysis and energetics and thermodynamics of inhibition. Also, two Class II α-mannosidases from *Lens culinaris*, Lentil were purified and characterized for its various biochemical and biophysical properties.

Discussion

The pseudo first order kinetics of the modification of Jbα-man with citraconic anhydride at pH 11.0, reactivation at pH 5.0, protection by substrate and favourable changes in the K_m and V_{max} values of the modified enzyme do indicate the presence of free amino group at or near the active site. This could be conferring the stability to the active site geometry of the enzyme. Drastic loss in the secondary structure of Jbα-man, incubated in the pH range of 1.0 to 3.0 was observed. The total loss of activity in this pH range can be correlated with the collapse of the secondary structure. The secondary structure of Jbα-man was almost intact in the alkaline conditions (pH 8-12). The hydrophobic amino acids were also exposed to the surface in the pH range of 1.0-3.0 as the protein did bind ANS with increase in fluorescence intensity and blue shift in emission maximum, the effect being more pronounced at pH 1.0.

The enzyme retained almost 50% activity after 2 h at 55 °C. The far UV CD spectra indicated that it could be the perturbance in the active site and not the distortion of the β-sheet region which leads to inactivation of the enzyme at and above 55 °C. The ratio of calorimetric enthalpy and vant hoff enthalpy at pH 11.0 indicated that the monomers start to unfold first followed by the unfolding of the complete oligomer. The study of effect of EDTA on the enzyme indicated that the metal ion is important for properly folded structure of the enzyme.

Jbα-man consists of three free cysteine residues in the native condition and showed eleven after reduction of the denatured protein as determined by DTNB modification. Four disulfide linkages could be deduced from the data, which can be inter subunit or some of them can be intra subunit linkages. Either all or few of these disulfide linkages along with non-covalent interactions bring about the association of the unidentical subunits to constitute the active site of the enzyme. The reduction in mean hydrodynamic diameter of the enzyme upon treatment with β-ME at 28 °C and further reduction in mean hydrodynamic diameter up on boiling suggested that the native enzyme exists as a dimer of active dimers formed with disulfide linked monomers and the disulfide bonds are reduced and subunits separated only after boiling. The positive ellipticity of Jbα-man at 200 nm was decreased in the pH range of 7.0 – 11.0 in presence of β-ME, indicating some rearrangement in the secondary structure. Also, increase in the negative ellipticity observed in the range of 210 – 225 nm at pH 7.0 – 9.0 indicated more compact secondary structure of Jbα-man after the treatment with β-ME. Probably, the reduction of intrachain disulfide bonds at 28 °C could be leading to the rearrangement in the secondary structure.

The K_m of the enzyme for 4- MeUmbαman was found to be 200 times lower than that for pNPαman, indicating stronger affinity of the enzyme for 4- MeUmbαman. The specificity constant, K_{cat}/K_m values of pNPαman and 4-MeUmbαman at 45 °C indicated higher reaction rate of the enzyme for the substrate 4-MeUmbαman. E_a of Jbα-man using 4-MeUmbαman is three times more as compared to that of the fungal α-mannosidase from *Aspergillus fischeri* (28). This could be due to some constraints of Jbα-man for the substrate to access the active site and also due to slightly hydrophobic surface of the protein. Inhibition kinetics indicated strong inhibition of Jbα-man with swainsonine. The binding of inhibitor to the enzyme is an endothermic and entropy driven process.

The difference in the characteristics like pH optimum, stability at extreme alkaline pH, bound metal ion, quaternary structure with unidentical subunits, presence of disulfide

linkages and activation energy of the present enzyme from the plant source do differentiate it from the same class II enzyme from a fungal source (28).

Native α-mannosidase from Jack Bean (Jbα-man) is a single trp protein with the trp residue in the hydrophobic environment. Decomposition analysis of the tryptophan fluorescence spectra of the native protein by PFAST showed the progressive appearance of class I, II, and III trp in Jbα-man in the vicinity of increasing concentration of GdnHCl, indicating the unfolding of the protein. The Jbα-man showed inactivation in presence of low concentration (0.2-0.4 M) of GdnHCl which could be due to the presence of carboxylate residues at the active site as shown by Kenoth *et al* and Nath *et al* (29, 30). The positively charged guanidinium group electrostatically interacts with the carboxylate group causing inactivation. The gradual red shift in the λ_{av} and parameter A data indicated multistate unfolding. Phase diagram analysis revealed the intermediates in the vicinity of 1.0 M and 3.0 M GdnHCl.

The negative MRE of the native protein at 219 nm remained unaltered in the vicinity of 1.0-1.2 M GdnHCl indicating the formation of a stable intermediate. The non-coincidence of the fluorescence and CD data of Jbα-man in presence of various concentrations of GdnHCl confirmed the multistep unfolding. The near UV CD spectrum showed significant reduction in the intensity of the signal in the vicinity of 1 M GdnHCl indicating disorganization of the tertiary structure during conversion of native to intermediate state.

The protein treated with 1M GdnHCl, showed positive ANS binding, indicating exposure of hydrophobic patches on the surface of the protein. The intermediate seemed to possess a molten globule like structure. Size exclusion chromatography studies showed that the protein seems to undergo simultaneous dissociation, partial unfolding and aggregation. Stokes' radii indicated a slightly expanded molecular state of the intermediate of the protein.

The CD and fluorescence measurements, ANS binding studies and SEC data describe the existence of a molten globule like intermediate of Jbα-man in the vicinity of 1 M GdnHCl. The intermediate possessed compact secondary structure, disrupted tertiary structure, exposed hydrophobic amino acids on the surface of the protein and increased hydrodynamic radius. The structure is similar to the one reported for β-lactamase (31). We found only a single molten globule like intermediate during equilibrium unfolding whereas there are reports of two molten globules (one dimeric and one momomeric) in the unfolding of Yeast glutathione reductase (32). There are also reports of active molten globule like intermediate of peanut lectin (33) in presence of 1-2 M GdnHCl. Thus, the present studies exhibit one of the early reports of existence of GdnHCl induced molten globule in a class II α-mannosidase.

The intermediate showed greater thermo stability than the native protein. The fluorescence and CD data does coincide in case of thermal unfolding of native protein unlike GdnHCl induced unfolding indicating differential modes of thermal and chemical denaturation of Jbα-man. Steady state and time resolved fluorescence quenching studies confirmed the altered conformation of the molten globule state as compared to the native and denatured enzyme.

During the past ten years, apart from the GdnHCl induced molten globule of Jbα-man reported by us, the reports on denaturation studies of glycosidases include - acid induced molten globule of β-xylosidase from *Geobacillus stearothermophilus* (34), conformational and catalytic stability of xylanase II from *Trichoderma reesei* (35), characterization of a partially unfolded state of β-momorcharin (36), effect of calcium depletion on the structure and thermal stability of d-galactose/d-glucose–binding protein (GGBP) from *Escherichia coli* (37), effects induced by mono- and divalent cations on protein regions responsible for thermal adaptation in ß-glycosidase from *Sulfolobus solfataricus* (38), acid-induced partly folded conformation resembling a molten globule state of xylanase II from an alkalothermophilic *Bacillus* sp. (39), fluorescence study on interactions of α–Crystallin with the Molten Globule State of 1, 4–β–D–Glucan Glucanohydrolase from *Thermomonospora* sp. induced by guanidine

hydrochloride (40), conformational and functional transitions in Class II α-mannosidase from *Aspergillus fischeri* (27) and many more which are beyond the purview of this thesis.

The active β-xylosidase from *Geobacillus stearothermophilus* (34) was a highly hydrated dimer, whose active site was formed by the two protomers, and it probably involved aromatic residues. At low pH, the protein was not active and it populated a monomeric molten globule like species, which had a conformational transition with a pK_a of ~ 4.0. The protein at physiological pH was formed by α-helix (30%) and β-sheet (30%), as shown by CD and FTIR. Comparison with other xylosidases of the same family indicated that the percentages of secondary structure seem to be conserved among the members of the family.

Xylanase II from *Trichoderma reesei* QM 9414 (35) treated with increasing guanidinium hydrochloride concentrations was denatured in a cooperative way regarding secondary and tertiary structures with midpoint transitions 5.6 and 3.7 M, respectively, whereas the enzymatic activity showed an intermediate state at 2–4 M denaturant. Treatment with urea showed that xylanase secondary structure had a transition midpoint of 5.7 M, but the ellipticity at 220 nm was greater than control in the presence of urea up to 6 M. Tertiary structure in the presence of urea also showed intermediate states with partial cooperative transitions with a midpoint of 2.7 and 6.7 M, respectively, whereas the enzymatic activity was enhanced about 40% at 2 M and inhibited above 4 M urea. Assays with the fluorescent probe 4,40-bis-1-phenylamine-8-naphftalene sulfonate (bis-ANS) proved that the intermediate states had the characteristics of molten globule structures. The change of free energy for xylanase in absence of denaturants obtained from the spectral centre of mass (SCM) data at 298 K was 17 kJ mol^{-1}. In the presence of increasing trifluoroethanol (TFE), the enzyme gained α-helix content and lost tertiary structure and catalytic activity. Changes in pH (2–9) had practically no effect on the secondary structure of the enzyme, whereas the SCM values indicated that tertiary structure is maintained above pH 4. Bis-ANS bound

to xylanase at pH 2 and 2.5 and in the presence of 30–40% TFE (v/v) characterizing molten globule states in these environmental conditions.

The specific conformation of partially unfolded state of β-momorcharin (36) was characterized through the steady-state and time-resolved fluorescence spectroscopic studies on a single Trp-190 which was located adjacently to the active site. The content of secondary structure was retained, the binding of ANS was remarkably enhanced, and the correlation time of entire protein rotation was prolonged at the partially unfolded state formed by being equilibrated with the mild concentration of guanidine hydrochloride. The time-resolved fluorescence depolarization and excitation energy transfer analysis suggest that Trp-190 approached 2 Å closer to Tyr-70 and was hidden from the exposure to the protein surface, while the rotational correlation time and freedom of its segmental motion were shortened and enhanced, respectively. These results suggested that the transient folding/unfolding intermediate state of β-momorcharin adopted the specific conformation at the vicinity of the active site, although it exhibited very similar properties with those of the generally known molten globule state.

The effect of the depletion of calcium on the structure and thermal stability of the D-galactose/D-glucose–binding protein (GGBP) from *Escherichia coli* (37) was studied by fluorescence spectroscopy and Fourier-transform infrared spectroscopy. The calcium-depleted protein (GGBP-Ca) was also studied in the presence of glucose (GGBP-Ca/Glc). The results showed that calcium depletion has a small effect on the secondary structure of GGBP and in particular it affected a population of α-helices with a low exposure to solvent. Alternatively, glucose-binding to GGBP-Ca eliminated the effect induced by calcium depletion by restoring a secondary structure similar to that of the native protein. In addition, the infrared and fluorescence data obtained revealed that calcium depletion markedly reduced the thermal stability of GGBP. In particular, the spectroscopic experiments showed that the depletion of calcium mainly affected the stability of the C-terminal domain of the protein. However, the binding of glucose restored the thermal stability of GGBP-Ca.

The perturbation induced by mono- and divalent cations on the thermophilicity and thermostability of *Solfolobus solfataricus* β-glycosidase (38), a hyperthermophilic tetrameric enzyme, was investigated. Mono- and divalent cations inhibited the β-glycosidase activity to a different extent, whose kinetic constants showed an apparent competitive inhibition of the catalytic process. The thermostability was also affected by the nature and charge of the cations, reaching maximal effects for the case of Mg^{2+}. Fourier transform infrared spectroscopy revealed very small changes in the protein secondary structure in the presence of the investigated cations at 20 °C, while large effects on the protein melting temperatures were observed.

The conformation and stability of Xyl II (39) at acidic pH was investigated by equilibrium unfolding methods. Using intrinsic fluorescence and CD spectroscopic studies, the researchers established that Xyl II at pH 1.8 (A-state) retained the helical secondary structure of the native protein at pH 7.0, while the tertiary interactions were much weaker. At variance, from the native species (N-state), Xyl II in the A-state bound 1-anilino-8-sulfonic acid (ANS) indicating a considerable exposure of aromatic side chains. Lower concentration of GdnHCl was required to unfold the A-state. For denaturation by GdnHCl, the midpoint of the cooperative unfolding transition measured by fluorescence for the N-state was 3.5 M, which was higher than 2.2 M, observed for the A-state at pH 1.8. This alternatively folded state exhibited certain characteristics of the molten globule but differed distinctly from it by its structural stability that was characteristic for native proteins.

The interaction between α- crystallin and molten globule structure of 1,4–β–D–Glucan Glucohydrolase (TSC) from an alkalothermophilic *Thermomonospora* sp. (40) was investigated. Denaturation studies using GdnHCl indicated that TSC folds through a partially folded state that resembles molten globule at 1.8 M GdnHCl. The chaperone activity of α- crystallin was employed to study refolding of TSC. Intrinsic tryptophan fluorescence and ANS binding studies suggested that α-crystallin formed a complex with a putative intermediate molten globule like intermediate (TSC -m complex) in the refolding pathway of TSC. Reconstitution of the active TSC was observed on cooling

the α-crystallin TSC -m complex to 4°C. Addition of α-crystallin to the molten globule like intermediate of TSC (TSC-m complex) complex initiated the refolding of TSC with 69 % recovery of the biological activity of the enzyme.

The conformational transitions in an oligomeric and high molecular weight class II α-mannosidase from *Aspergillus fischeri* (27) were examined. The enzyme lost the activity first and then the overall folded conformation and secondary structure. The midpoint values of GdnHCl mediated changes measured by inactivation; fluorescence and negative ellipticity were 0.48 M, 1.5 M and 1.9 M, respectively. The protein almost completely unfolded in 4.0 M GdnHCl but not at 90 °C. The inactivation and unfolding were irreversible. At pH 2.0, the protein exhibited molten globule like intermediate with rearranged secondary and tertiary structures and exposed hydrophobic amino acids on the surface. This species showed increased accessibility of trp to the quenchers and got denatured with GdnHCl in a different manner. The insoluble aggregates of a thermally denatured protein could be detected only in the presence of 0.25–0.75 M GdnHCl.

In the last part of the thesis, we have studied two α-mannosidases from *Lens culinaris* (Lentil) seeds.

The lentil seeds soaked for 21 h and extracted with 10 mM tris-HCl buffer, pH 8.8 for 3 h were found to have optimal α-mannosidase activity. The partially purified extract showed two α-mannosidases, LAM 1 and LAM 2, which were purified to homogeneity and the purified enzymes showed a single band with activity indicating a homogeneous active protein.

The biochemical parameters were identical for both the enzymes and were similar to the one reported for another plant α-mannosidase, Jbα-man (41) but different from the one reported for *Aspergillus fischeri* α-mannosidase (42). Both LAM 1 and LAM 2 showed similar values of K_m and V_{max} for each substrate but the K_m for 4-MeUmbαMan was about 250 times lower than that for pNPαMan indicating much

greater affinity for 4-MeUmbαMan than pNPαMan due to the more hydrophobic nature of 4-MeUmbαMan. The neutral sugar content of the two lentil α-mannosidases was found to be very close to the *Erythrina indica* α-mannosidase (43) which is also a plant class II α-mannosidase but different from the fungal *Aspergillus fischeri* α-mannosidase (42). The pH-activity profile indicated the involvement of the carboxylate (COO^-) ion and histidine at the active site of the enzymes. COO^- ion has been reported to be involved at the active site in many class II α-mannosidases earlier also (6). Activation energy (E_a) for both the enzymes with pNPαman was found to be close to both, the *Aspergillus fischeri* α-mannosidase (28) as well as Jbα-man (41). The K_i value of both LAM 1 and LAM 2 for swainsonine was found to be 10 times less than that for Jbα-man (41) but 20000 times less than that for *Aspergillus fischeri* α-mannosidase (28).

The enzymes when treated with 10 mM EDTA showed about 80 % inhibition. The present enzyme differs in this aspect from the *Aspergillus fischeri* α-mannosidase (42) but resembles the other plant α-mannosidase from Jack bean (41).

The fluorescence spectrum of both the enzymes indicated trp residue to be in slightly hydrophobic environment. CD pro analysis of the far UV CD spectra indicated that both the enzymes were predominantly β-sheet proteins. The extensive quenching of fluorescence by iodide ions and failure in quenching of fluorescence by cesium ions indicated high density of positive charge around the surface trp conformer. The basis of slight difference in the electrophoretic mobility of LAM 1 and 2 could not be deduced from these results, as K_{sv} values for both the enzymes were similar and I^- ions had full accessibility towards surface trp.

The two class II α-mannosidases from lentil seeds, LAM 1 and LAM 2 were found to be pretty similar in their overall properties and secondary structure content but differ in the overall charge density on the surface of the protein, indicating that they may be isozymes.

Conclusions

1. Jbα-man, a Class II α-mannosidase, showed maximum activity at pH 5.0 and 45 °C and in the pH range of 1.0 to 10.0, the enzyme was maximally stable at pH 5.0. The stability declined fast in the pH range of 1.0-3.0 and 8.0-10.0, however, the enzyme incubated in the pH range of 11.0-12.0, showed 1.3 times higher activity which was also more stable as compared to that at pH 5.0.
2. The free amino group was found to be present at or near the active site which probably was involved in the stability and activation mechanism in the extreme alkaline pH range.
3. The active site is constituted by the association of two unidentical (66 and 49 kDa) subunits which are connected by disulfide linkages.
4. Jbα-man, the metalloenzyme, has Zn^{2+} ions tightly bound to it and chelation of the metal ion reduces the thermal stability of the protein.
5. E_a of Jbα-man with pNPαman as a substrate was 31.9 kJ mol^{-1} and with 4-MeUmbαman was 26.7 kJ mol^{-1}.
6. The strong binding of the class II α-mannosidase inhibitor, Swainsonine (K_i = 52.9 nM), to the enzyme was found to be entropy driven.
7. The native Jbα-man, showed λ_{max} at 338 nm indicating trp residue in the hydrophobic environment. Decomposition analysis revealed the progressive appearance of class S, I, II and III trp in Jbα-man in the vicinity of increasing concentration of GdnHCl indicated the unfolding of the protein.
8. The gradual red shift in the λ_{av} and parameter A data indicates multistate unfolding of Jbα-man. The phase diagram analysis also indicated the unfolding to be a multistep process, the intermediates lying in the vicinity of 1.0 M and 3.0 M GdnHCl.
9. CD pro analysis yielded the values of the secondarys tructure elements as: α-helix-8.0%, β-sheet-35.5%, turns-21.1% and unordered-34.6%. The MRE at 219 nm remained unaltered in the vicinity of 1.0-1.2 M GdnHCl indicating the

formation of a stable intermediate. The near UV CD spectrum indicated ordered tertiary structure of Jbα-man and disorganization of the tertiary structure during conversion of native to intermediate state.

10. The intermediate with exposed hydrophobic patches seemed to possess a molten-globule like structure, which showed greater thermo stability than the native protein.
11. The solute quenching parameters confirmed the altered conformation of the intermediate. There is more density of positive charge around the surface trp conformer.
12. Two isozymes of Class II α-mannosidase from *Lens culinaris* (Lentil), slightly differing in the electrophoretic mobility were purified to homogeneity by alkaline native polyacrylamide gel electrophoresis (PAGE).
13. The temperature and pH optima, temperature and pH stability, K_m and V_{max} values for pNPαMan and 4-MeUmbαMan, carbohydrate content and K_i for swainsonine were found to be almost similar for LAM 1 and 2.
14. The enzymes were strongly inhibited by 2 mM Hg^{2+}, Cu^{2+}, Co^{2+} and 1 % SDS.
15. The biophysical properties like environment of trp with high density of positive charge around it and composition of the secondary structure were also almost identical for both the enzymes.
16. The extensive quenching of fluorescence of LAM 1 and 2 by iodide ions and failure in quenching of fluorescence by cesium ions indicated high density of positive charge around the surface trp conformer of the proteins.

References

1. Moremen, K.W., Trimble, R.B. and Herscovics, A. (1994) *Glycobiology* **4**, 113-125.
2. Liao, Y.F., Lal, A. and Moremen, K.W. (1996) *J Biol Chem* **271**, 28348-58.
3. Neufeld, E.F. (1991) *Annu Rev Biochem* **60**, 257-280.
4. Henrissat, B., , and Bairoch, A. (1991) *Biochem J.* **316**, 695-696.
5. Goss, P.E., Baker, M.A., Carver, J.P., Dennis, J.W. (1995) *Clinical Cancer Res* **1**, 935-944.
6. Keskar, S.S., Gaikwad, S.M., Khan, M.I. . (1996) *Enz Micro Tech* **18**, 602-60.
7. Li, Y.T. (1967) *J Biol Chem* **242**, 5474-80.
8. Snaith, S.M. and Levvy, G.A. (1968) *Biochem J* **110**, 663-70.
9. Snaith, S.M. (1975) *Biochem J* **147**, 83-90.
10. Hara, K., Fujita, K., Nakano, H., Kuwahara, N., Tanimoto, T., Hashimoto, H., Koizumi, K. and Kitahata, S. (1994) *Biosci Biotechnol Biochem* **58**, 60-3.
11. Howard, S., Braun, C., McCarter, J., Moremen, K.W., Liao, Y.F. and Withers, S.G. (1997) *Biochem Biophys Res Commun* **238**, 896-8.
12. Howard, S., He, S. and Withers, S.G. (1998) *J Biol Chem* **273**, 2067-72.
13. Kang, M.S. and Elbein, A.D. (1983) *Plant Physiol* **71**, 551-554.
14. Kestwal, R.M. and Bhide, S.V. (2005) *Indian J Biochem Biophys* **42**, 159-160.
15. Kestwal, R.M., Konozy, E.H., Hsiao, C.D., Roque-Barreira, M.C. and Bhide, S.V. (2007) *Biochim Biophys Acta* **1770**, 24-8.
16. Kaushal, G.P., Szumilo, T., Pastuszak, I. and Elbein, A.D. (1990) *Biochemistry* **29**, 2168-2176.
17. Suvarnalatha G. and Prabha T.N. (1999) *Phytochemistry* **50**, 1111-1115.
18. Priya Sethu K.M. and Prabha T.N. (1997) *Phytochemistry* **44**, 383-387.

19. Kishimoto T., Hori H., Takano D., Nakano Y. Watanabe M. and Mitsui T. (2001) *Physiol. Plant.* **112**, 15-24.

20. Woo K.K., Miyazaki M., Hara S., Kimura M. and Kimura Y. (2004) *Biosci. Biotechnol. Biochem.* **68**, 2547-2556.

21. Woo K.K. and Kimura Y. (2005) *Biosci. Biotechnol. Biochem.* **69**, 1111-1119.

22. Paus E. and Christensen T.B. (1972) *Eur. J. Biochem.* **25**, 308-314.

23. Paus E. (1976) *FEBS Lett.* **72**, 39-42.

24. Paus E. (1977) *Eur. J. Biochem.* **73**, 155-161.

25. Misaki R., Fujiyama K., Yokoyama H., Ido Y., Miyauchi K., Yoshida T. and Seki T. (2003) *J. Biosci. Bioengg.* **96**, 187-192.

26. Blom H., Reyes F. and Carlsson J. (2008) *J. Agric. Food Chem.* **56**, 10872-10878.

27. Shashidhara K.S. and Gaikwad S.M. (2010) *J Fluoresc* **20**: 827-836.

28. Shashidhara, K.S. and Gaikwad, S.M. (2009) *Int J Biol Macromol* **44**: 112-115.

29. Kenoth, R. and Swami, M.J. (2003) *J Photochem Photobiol B Biol* **69**: 193–201.

30. Nath, D. and Rao, M. (2001) *Enzyme Microb Technol* **28**: 397-403.

31. Sarkar, D. and Dasgupta, C. (1996) *Biochim Biophys Acta* **1296**: 85-94.

32. Louzada, P.R., Sebollela, A., Scaramello, M.E. and Ferreira, S.T. (2003) *Biophys J* **85:** 3255-3261.

33. Reddy, B., Srinivas, V.R., Ahmad, N. and Surolia, A. (1999) *J Biol Chem* **274**: 4500-4503.

34. Contreras, L.M., Gomez J., Prieto, J., Clemente-Jiménez, J.M., Heras-Vázquez, F.J.L., Rodríguez-Vico, F., Blanco, F.J. and Neirs J.L. (2008) *Biochim Biophys Acta* **1784**: 1924-1934.

35. Lopez, G., Banares-Hidalgo, A. and Estrada, P. (2011) *J Ind Microbiol Biotechnol* **38**: 113-125.

36. Fukunaga, Y., Nishimoto, E., Yamashita, K., Otosu, T. and Yamashita, S. (2007) *J Biochem* **141**: 9-18.

37. D'Auria, S., Ausili, A., Marabotti, A., Varriale, A., Scognamiglio, V., Staiano, M., Bertoli, E., Rossi, M. and Tanfani, F. (2006) *J Biochem* **139**: 213-221.

38. Bismuto E., Nucci, R., Febraio, F., Tanfani, F., Gentile, F., Briante, R., Scire, A., Bertoli, E. and Amodeo, P. (2004) *Eur Biophys J* **33**: 38-49.

39. Nath D. and Rao M. (2001) *Biochem Biophys Res Commun* **288**: 1218-1222.

40. Jagtap S. and Rao M. (2009) *J Fluoresc* **19**: 967-973.

41. Kumar, A. and Gaikwad, S.M. (2011) *Int J Biol Macromol* (Under Review).

42. Gaikwad, S.M., Keskar. S.S. and Khan, M.I. (1995) *Biochim Biophys Acta* **1250**: 144-148.

43. Kestwal, R.M., Konozy, E.H., Hsiao, C.D., Roque-Barreira, M.C. and Bhide, S.V. (2007) *Biochim Biophys Acta* **1770**: 24-28.